

**CFD SIMULATION OF FIRE AND VENTILATION
IN THE STATIONS OF UNDERGROUND TRANSPORTATION SYSTEMS**

**A THESIS SUBMITTED TO
THE GRADUATE SCHOOL OF NATURAL AND APPLIED SCIENCES
OF
MIDDLE EAST TECHNICAL UNIVERSITY**

BY

SERKAN KAYILI

**IN PARTIAL FULFILLMENT OF THE REQUIREMENTS FOR
THE DEGREE OF MASTER OF SCIENCE
IN
MECHANICAL ENGINEERING**

JUNE 2005

Approval of the Graduate School of Natural and Applied Sciences

Prof. Dr. Canan Özgen
Director

I certify that this thesis satisfies all the requirements as a thesis for the degree of
Master of Science

Prof. Dr. Kemal İder
Head of Department

This is to certify that we have read this thesis and that in our opinion it is fully
adequate, in scope and quality, as a thesis for the degree of Master of Science

Prof. Dr. O. Cahit Eralp
Supervisor

Examining Committee Members:

Prof. Dr. Kahraman ALBAYRAK	(METU,ME)	_____
Prof. Dr. O. Cahit Eralp	(METU,ME)	_____
Assoc. Prof. Dr. Cemil YAMALI	(METU,ME)	_____
Asst. Prof. Dr. Cüneyt SERT	(METU,ME)	_____
Mahmut Arsava (M.S.Civil Engineer)	(ARI PROJE)	_____

I hereby declare that all information in this document has been obtained and presented in accordance with academic rules and ethical conduct. I also declare that, as required by these rules and conduct, I have fully cited and referenced all material and results that are not original to this work.

Serkan KAYILI

ABSTRACT

CFD SIMULATION OF FIRE AND VENTILATION IN THE STATIONS OF UNDERGROUND TRANSPORTATION SYSTEMS

Kayılı, Serkan

M.S., Department of Mechanical Engineering

Supervisor: Prof. Dr. O. Cahit Eralp

June 2005, 136 pages

The direct exposure to fire is not the most immediate threat to passengers' life in case of fire in an underground transportation system. Most of the casualties in fire are the results of smoke-inhalation. Numerical simulation of fire and smoke propagation provides a useful tool when assessing the consequence and deciding the best evacuation strategy in case of a train fire inside the underground transportation system. In a station fire the emergency ventilation system must be capable of removing the heat, smoke and toxic products of combustion from the evacuation routes to ensure safe egress from the underground transportation system station to a safe location. In recent years Computational Fluid Dynamics has been used as a tool to evaluate the performance of emergency ventilation systems. In this thesis, Computational Fluid Dynamics technique is used to simulate a fire incidence in underground transportation systems station. Several case studies are performed in

two different stations in order to determine the safest evacuation scenario in CFDesign 7.0. CFD simulations utilize three dimensional models of the station in order to achieve a more realistic representation of the flow physics within the complex geometry. The steady state and transient analyses are performed within a simulation of a train fire in the subway station. A fire is represented as a source of smoke and energy. In transient analyses, a fast t^2 growth curve is used for the heat release rate and smoke release rate. The results of the studies are given as contour plots of temperature, velocity and smoke concentration distributions. One of the case studies is compared with a code well known in the discipline, the Fire Dynamics Simulator, specifically developed for fire simulation. In selection of the preferred direction of evacuation, fundamental principles taken into consideration are stated.

Keywords: Fire safety, Computational Fluid Dynamics, Fire Simulation, Station Fire, Emergency Ventilation, Underground Transportation Systems, FDS, CFDesign

ÖZ

YERALTI TAŞIMA SİSTEMLERİ İSTASYONLARINDA HESAPLAMALI AKIŞKANLAR DİNAMIĞI YÖNTEMİYLE YANGIN VE HAVALANDIRMA SİMÜLASYONU

Kayılı, Serkan

Yüksek Lisans, Makina Mühendisliği Bölümü

Tez Yöneticisi: Prof. Dr. O. Cahit Eralp

Haziran 2005, 136 sayfa

Yeraltı toplu taşıma sistemlerinde oluşan yangınlarda insan hayatını esas tehdit eden yangına direkt maruz kalmak değildir. Yangınlarda ölümlerin büyük bölümü duman solunması sonucudur. Yeraltı toplu taşıma sisteminde oluşan bir tren yangınında yangın ve duman yayılımının sayısal simülasyonu, sonuçların değerlendirilmesi ve en iyi kaçış stratejisinin belirlenmesinde faydalı bir araç olarak kullanılmaktadır. Bir istasyon yangınında acil durum havalandırma sistemi ısıyı, dumanı ve yanmadan oluşan zehirli atıkları kaçış yönünden uzaklaştırarak istasyondan tehlikesiz bir bölgeye güvenli bir kaçışı garanti edecek yeterlilikte olmalıdır. Son yıllarda, acil havalandırma sistemlerinin performansının değerlendirilmesinde araç olarak Hesaplamalı Akışkanlar Dinamiği kullanılmaktadır. Bu tezde yeraltı toplu taşıma sistemindeki bir istasyonda, Hesaplamalı Akışkanlar Dinamiği kullanılarak yangın

simülasyonu yapılmıştır. En güvenli kaçış senaryosunun belirlenmesi amacıyla iki farklı istasyonda çeşitli örnek çalışmalar CFDesign 7.0 ile yapılmıştır. Hesaplamalı Akışkanlar Dinamiği simülasyonlarında karmaşık geometrilerdeki akış dağılımını gerçeğe daha yakın tasvir edebilmek için üç boyutlu istasyon modelleri kullanılmıştır. Metro istasyonunda çıkan bir tren yangını simülasyonu için zamandan bağımsız ve zamana bağımlı analizler yapılmıştır. Yangın, duman ve enerji kaynağı olarak ifade edilmiştir. Zamana bağımlı analizlerde ısı ve duman yayılım hızları için hızlı t^2 büyüme eğrisi kullanılmıştır. Bu çalışmalardan elde edilen sonuçlar sıcaklık, hız ve duman yoğunluk dağılımları kontur grafikleri ile verilmiştir. Çalışmalardan biri, yangın güvenliği için özel olarak geliştirilmiş, Fire Dynamics Simulator programı ile karşılaştırılmıştır. Tercih edilen kaçış yolu seçiminde göz önünde bulundurulacak temel unsurlar belirtilmiştir.

Anahtar Kelimeler: Yangın Güvenliği, Hesaplamalı Akışkanlar Dinamiği, Yangın Simülasyonu, İstasyon Yangını, Acil Durum Havalandırması, Yeraltı Toplu Taşımacılık Sistemi, FDS, CFDesign.

To My Family

ACKNOWLEDGMENTS

I wish to express my sincere gratitude to my advisor Professor Dr. O. Cahit Eralp for his excellent guidance, valuable advice and innovative ideas during the course of M.S. study. Working with him has been an enjoyable, unique and valuable learning experience which I will treasure throughout my life.

Special thanks go to my colleagues, Tolga KÖKTÜRK, Eren MUSLUOĞLU, Ekin ÖZGİRGİN, Ertuğrul ŞENCAN, Cihan KAYHAN, F. Ceyhun ŞAHİN and Gençer KOÇ for many simulating discussions, coffee, lunch and dinner breaks. I also wish to thank Dr. Ertuğrul BAŞEŞME for permitting me to use CFDesign software and his support.

2.2.2 Turbulent Fire Plume Characteristic.....	21
2.2.2.1 The Ideal Plume.....	23
2.2.2.2 Plume Equations Based on Experiments.....	25
2.2.2.2.1 The Zukowski Plume.....	25
2.2.2.2.2 The Heskestad Plume	25
2.2.2.2.3 The McCaffrey Plume.....	27
2.2.2.2.4The Thomas Plume.....	28
2.2.2.3 Walls and Corner Interactions with Plume.....	29
3. FIRE MODELING.....	31
3.1.1 Fire Modeling.....	31
3.1.2 Zone Models.....	32
3.1.2.1 Limitations of Zone Modeling.....	34
3.1.3 Field Models (CFD).....	35
3.1.3.1 CFD Modeling of Fire in Underground Transportation Systems.....	37
3.1.3.2 CFD Fire Modeling Approach in Thesis.....	49
4. CFDESIGN 7.0.....	52
4.1 Introduction.....	52
4.2 Physical Boundaries.....	53
4.2.1 Surface Boundary Condition Details.....	56
4.2.2 Volume Boundary Condition Details.....	58
4.2.3 Transient Conditions.....	58
4.3 Installed Database Materials.....	58
4.3.1 Fluid Properties.....	59
4.4 Turbulence.....	60
4.5 Scalar.....	61
5. CASE STUDIES.....	62
5.1 Introduction.....	62
5.2 Case Study-1 KCK Station Fire.....	64
5.2.1 Results of KCK Station Train Fire.....	82
5.2.1.1 Scenario-1.....	82

5.2.1.2 Scenario-2.....	83
5.2.1.3 Evaluation.....	84
5.2.2. Comparison of Scenario-1 of KCK Station Fire with Fire Dynamics Simulator (FDS).....	85
5.3 Case Study-2 Polytechnika Station Fire.....	87
5.3.1 Results of Polytechnika Station Train Fire.....	104
5.3.1.1 Scenario-1.....	104
5.3.1.2 Scenario-2.....	105
5.3.1.3 Scenario-3.....	106
5.3.1.4 Evaluation.....	107
6. DISCUSSION AND CONCLUSION.....	108
6.1 Comments on the Results.....	108
6.2 Recommendations for Future Work.....	110
REFERENCES.....	112
APPENDICES	
A. STEADY STATE EMERGENCY VENTILATION SCENARIOS IN KCK STATION.....	116
B. DESCRIPTION OF THE FIRE DYNAMICS SIMULATOR& KCK STATION FIRE SIMULATION RESULTS WITH FDS....	123

LIST OF TABLES

TABLE

2.1 Values of α for different growth rates.....	18
2.2 Constants in McCaffrey's plume equations.....	28
4.1 List of materials in CFdesign 7.0 database.....	59
4.2 List of properties and variational method.....	60
5.1 Commentary on Scenario 1 in KCK Station.....	82
5.2 Commentary on Scenario 2 in KCK Station.....	83
5.3 Commentary on Scenario 1 in Polytechnika Station.....	105
5.4 Commentary on Scenario 2 in Polytechnika Station.....	106

LIST OF FIGURES

FIGURE

2.1 Generic temperature time history in the fire.....	11
2.2 Diagram showing the energy balance for the hot layer in an enclosure fire.....	14
2.3 Heat release rate variation with time.....	19
2.4 The three zones of the axisymmetric buoyant plume.....	22
2.5 Some of the characteristics of a buoyant axisymmetric plume.....	23
2.6 Some plume characteristics.....	26
2.7 Fire sources near walls and corners.....	29
3.1 Illustration of the zone model concept.....	33
3.2 CFD analysis basic steps.....	36
3.3 Fire modeling in the CFD analysis.....	50
4.1 CFD design solution procedure.....	55
5.1 Heat release rate versus time.....	63
5.2 Smoke generation rate versus time.....	63
5.3 3-D representation of KCK Station in Krakow Fast Tram.....	65
5.4 Schematic drawing of fire and ventilation scenarios in KCK Station..	67
5.5 Boundary conditions applied in the CFD analysis for KCK Station...	68
5.6 Section 1 (Horizontal plane 2.5 m above floor level).....	69
5.7 Section 2 and Section 3 (Vertical planes passing through fire axis)....	69
5.8 Temperature distribution at Section-1 (KCK Scenario-1).....	70
5.9 Scalar distribution at Section-1 (KCK Scenario-1).....	71

5.10 Velocity distribution at Section-1 (KCK Scenario-1).....	72
5.11 Velocity distribution at fire axis (KCK Scenario-1).....	73
5.12 Temperature distribution at fire axis (KCK Scenario-1).....	74
5.13 Scalar (S) distribution at fire axis (KCK Scenario-1).....	75
5.14 Temperature distribution at Section-1 (KCK Scenario-2).....	76
5.15 Scalar distribution at Section-1 (KCK Scenario-2).....	77
5.16 Velocity distribution at Section-1 (KCK Scenario-2).....	78
5.17 Velocity distribution at fire axis (KCK Scenario-2).....	79
5.18 Scalar distribution at fire axis (KCK Scenario-2).....	80
5.19 Temperature distribution at fire axis (KCK Scenario-2).....	81
5.20 3D representation of POLYTECHNIKA Station In Krakow Fast Tram.....	89
5.21 Schematic drawing of ventilation scenarios in Polytechnika.....	90
5.22 Boundary conditions applied in the unsteady CFD analyses for Polytechnika Station.....	91
5.23 Temperature distribution at 2.5 m above the platform in Polytechnika Scenario-1.....	92
5.24 Scalar distribution at 2.5 m above the platform in Polytechnika Scenario-1.....	93
5.25 Velocity distribution at 2.5 m above platform level in Polytechnika Scenario-1.....	94
5.26 Temperature distribution along the evacuation direction in Polytechnika Scenario-1.....	95
5.27 Scalar distribution along the evacuation direction in Polytechnika Scenario-1.....	96
5.28 Velocity distribution at 2.5 m above platform level in Polytechnika Scenario-2.....	97
5.29 Temperature distribution at 2.5 m above platform level in Polytechnika Scenario-2.....	98
5.30 Scalar distribution at 2.5 m above platform level in Polytechnika Scenario-2.....	99

5.31 Temperature distribution along the evacuation direction in Polytechnika Scenario-2.....	100
5.32 Scalar distribution along the evacuation direction in Polytechnika Scenario-2.....	101
5.33 Velocity distribution at 2.5 m above platform level in Polytechnika Scenario-3.....	102
5.34 Temperature distribution at 2.5 m above platform level in Polytechnika Scenario-3.....	102
5.35 Scalar distribution at 2.5 m above platform level in Polytechnika Scenario-3.....	103
5.36 Temperature distribution along the evacuation direction in Polytechnika Scenario-3.....	103
5.37 Scalar Distribution along the evacuation direction in Polytechnika Scenario-3.....	104

LIST OF SYMBOLS

A_o	Area of the opening [m^2]
A_T	Boundary surface area for heat transfer considerations [m^2]
c	Specific heat [kJ/kg.K]
c_p	Specific heat at constant pressure [kJ/kg.K]
c_v	Specific heat at constant volume [kJ/kg.K]
C_d	Discharge coefficient. [-]
D	Base diameter of fire [m]
E	Total energy of combustion [kJ]
E_d	Energy released during decay [kJ]
g	Gravitational acceleration [m/s^2]
h_k	Effective heat conduction term for the solid boundaries [kW/kg.K]
H_N	Height of neutral layer in an enclosed space [m]
H_o	Height of opening of an enclosed space [m]
k	Thermal conductivity [W/m.K]
	Turbulence Kinetic Energy [m^2/s^2]
L	Mean flame height [m]
\dot{m}_g	Mass flow rate out through the opening [kg/s]
\dot{m}_p	Plume mass flow rate [kg/s]
P	Pressure; [kPa]
	Perimeter of fire [m]
S	Scalar [-]
\dot{Q}	Heat release rate [kW]

\dot{Q}_c	Convective energy release rate [kW]
t	Time [s]
t_{FC}	Time for full fire development phase of a fire [s]
T	Temperature [$^{\circ}$ C or K]
T_a	Ambient temperature [$^{\circ}$ C or K]
U	Velocity in x direction [m/s]
V	Velocity in y direction [m/s]
W	Width of opening of an enclosed space[m]; Velocity in z direction [m/s]
z	Height above the fire source [m]

Greek Letters

α	Growth factor of fire; [kW/s ²] Thermal diffusivity [m ² /s]
ε	Turbulence dissipation rate
δ	Thickness of boundary of an enclosed space [m]
η	Constant
κ	Constant
Δ	Difference
ρ	Density [kg/m ³]

Abbreviations

CFD	Computational Fluid Dynamics
SES	Subway Environment Simulation
FDS	Fire Dynamics Simulator

Subscripts

a	Air
c	Ceiling
g	Gas
F	Floor
o	Virtual origin
T	Total area
w	Wall
0.005	0.5 % of
p	Thermal penetration
FO	Flashover of a fire
FD	Fully developed fire phase
decay	Decay period of a fire

CHAPTER 1

INTRODUCTION

1.1 General

It was during the 1850's that the cities of the world proved that mass transportation and individual transportation could not mix in urban areas. However, when railways offered separate mass transportation systems, the cities' commuters were reluctant to use them. Many municipalities insisted on railway stations being kept beyond their city boundaries. The first urban railway system and the world's first underground line (Metropolitan) opened on January 10, 1883, in London. Up to now, many rapid transit systems involving subway facilities have been constructed. The rate of population growth and increasing traffic congestion in the major cities of the world are the main reasons for requirement of more rapid ways of transportation. Improved facilities and operations result in higher train speeds, shorter headways and heavier passenger loads. As these transportation lines become more frequent, the environmental control in vehicles, in subway stations and tunnels become more crucial for the life safety and the comfort of the passengers.

Paramount among the problems of subway environment is that of heat buildup and disposal. Removal of excess heat often may be as important to subway patrons as the speed of their ride, and subway operating agencies are discovering that the

environmental conditions of subway waiting areas and transit vehicles significantly affect the level of utilization of the facility.

The temperature, humidity and air movement of the subway are important for the comfort level, but the environment also includes the pressure variations, noise, dust and odors. Controlling of the design of major construction features and installations of environmental control equipment regulate the temperature and air velocities in the subway environment.

To control the environment in subway provides an appropriate place not only for the passengers but also for operating and maintenance personnel. Also, it helps to remove a sufficient amount of the heat generated together with haze and odors throughout the system operations. In the event of a fire or a similar emergency case, smoke must be exhausted from the subway system and fresh air must be supplied to the patrons, operating personnel and the firefighters.

The train piston effect, air movement in front of a train through the tunnel of the subway system due to the pressure wave generated by the movement of the train, was the primary source of ventilation in older subway systems. However; today, mechanical or forced ventilation supplements the piston effect in order to provide a sufficient ventilation rate. A reasonable environment within the stations and tunnels must be maintained due to usage of air-conditioned vehicles in the recent systems. The Subway Environmental Design Handbook [28] is a valuable guide and reference for the planning, design, construction and operation of underground rapid transit systems, covering broad range of parameters, including temperature, humidity, air quality and rapid pressure change.

Three types of operation modes can be classified according to the population density in a subway system. They are normal, congested and emergency modes. In the normal operations, trains are moving through the system according to the schedule and passengers are traveling smoothly through the stations. Congested operations

occur due to operational problems or delays leading to a blockage of train operations. In such cases, trains may wait in the stations, or stop at a predetermined location in the tunnel, but in any case passengers are not exposed to any danger or are not evacuated from train. The environment controlling equipment should supply the required ventilation to support the continuous operation of air-conditioning units in the trains, therefore maintaining comfort of the passengers during congested operations. Lastly, emergency operations occur when there is a malfunction of the transit vehicle generally leading to the disrupted traffic in the subway. The most serious emergency case is a train on fire stopped in a tunnel. As a result, it is required to evacuate the passengers immediately. In this case, ventilation is necessary for maintaining a safe evacuation path from train clear of smoke and hot gases. In the design stage, the required ventilation rates for all these three operations in a subway environment must be taken into account.

The types of the ventilation in subway environment can be classified as natural ventilation, mechanical ventilation, and emergency ventilation.

1.1.1 Natural Ventilation

Natural ventilation in subway systems is primarily the result of train operation in the tunnel. The air flows created by the movement of the trains through tunnels and stations are similar to the types of flows caused by the movement of a piston within a cylinder. Hence, the ventilation of a subway which is created by the movements of the train is also termed “piston action” ventilation. The moving train pushes air ahead of it through the subway system and some of the air travels to the outside atmosphere via vent shafts. As the train moves past a shaft or station, fresh air is drawn into the system behind it. Therefore, some cooling is accomplished by exchanging hotter inside air with cooler outside air.

The effective exchange of stale air for fresh air will obviously depend on such factors as the proportion of tunnel cross-section occupied by the train, the area and length of

shafts or other openings and their sitting, the frequency of the train service and to a major extent on whether twin single track tunnels or double track two-way tunnels are used. When two trains traveling in opposite directions pass each other, considerable short-circuiting in subway structures especially in stations or in tunnels with perforated or non-dividing walls occurs. Such short-circuiting causes excess air velocities on station platforms and in station entrances, which can lead to an undesirable amount of heat accumulation during the peak operation and peak ambient temperatures.

To overcome these negative effects, ventilation shafts are usually placed at locations closer to the station beginning and end at the tunnels. Shafts in the approach tunnel are called blast shafts, through which part of the air pushed in front of the train is forced out from the system. Shafts in the departure tunnel are often called relief shafts. Relief shafts relieve the negative pressure created during the departure of the train, and outside air can be taken into the system through these shafts rather than through station entrances. Additional ventilation shafts may be provided between stations depending on the tunnel lengths. The high cost of these ventilation structures requires a design for optimum performance. Internal resistances due to bends and offsets should be kept at minimum, and shaft cross-sectional areas should be approximately equal to the cross-sectional area of a single-track tunnel.

1.1.2 Mechanical Ventilation

If the ventilation induced by the train operation is not adequate during normal scheduled ventilation, it is supplemented by mechanical ventilation (i.e. fans). The air exchange between heated air and the cool outside air is accomplished by the help of mechanical ventilation. Another duty of mechanical ventilation is to provide outside air for passengers in stations or tunnels in an emergency case or during other unscheduled interruptions of traffic. Lastly, extracting smoke from the system for the life safety of the passengers is another function of mechanical ventilation in case of fire.

Especially, in multitrack tunnels, the piston-action-induced ventilation may not be adequate. The air in the tunnel between the vent shafts is pushed one way and then back as trains pass back and forth through the tunnels, and thus there is little net flow of air through the tunnel or vent shafts. Fans in vent shafts help produce a net flow through the tunnel. Also, it sometimes becomes necessary to locate a vent shaft in an area where a suitable grade level site is at a considerable distance from a deep tunnel, and the airflow resistance may be too high to provide adequate ventilation without a fan.

Some vent shafts may serve a dual purpose. During normal operation, they may handle piston-action air flow without the aid of fans, whereas fans would be required for emergency operation. The vent shaft to grade level is over the end with normally open dampers. For emergency operation, the dampers go to the opposite positions to prevent fan air from short circuiting. The fans are reversible to permit either exhaust or intake, as required. The direction of rotation of the fans is predetermined based on the overall ventilation concept except for emergency cases. If the subway stations are not air-conditioned, the heated air should be exchanged with the cool outside air at the maximum rate. The inflow of warmer outside air should be limited and controlled, if the stations are air-conditioned to have temperatures below ambient.

A more direct ventilation concept is the underplatform exhaust system, removes station heat at its primary source, the underside of the train. Experiments have shown that this ventilation system not only decreases the upwelling of the heated air onto platforms, but also it removes important amount of the heat generated from the brakes and from air-conditioning condensers located underneath the train. In ideal cases, in order to provide a positive control over the direction of the airflow, makeup air for exhaust should be introduced at the track level. Underplatform exhaust systems without makeup supply air are least effective and, in some cases, may be harmful since the heated tunnel air may flow into the station.

1.1.3 Emergency Ventilation

An emergency in a subway system is defined as any unusual situation or occurrence that halts movement of the train and makes it necessary for passengers to leave the vehicle and enter the tunnel or that requires evacuation of a station. Furthermore, an emergency may include situations where maintenance of environmental conditions in the tunnel is required to make it necessary for the patrons to leave a stalled train.

Emergency ventilation is the major control strategy in a subway fire. During subway emergencies involving fire or generation of smoke, the products of combustion or electrical arcing will produce gases and aerosols some of which are potentially toxic or incapacitating. All the aerosols in smoke also tend to limit visibility. The emergency ventilation equipment may be used to: (1) move combustion and decomposition products, and heat in a preferred direction; (2) lessen the concentration of combustion and decomposition products; and (3) lessen the heat buildup and air temperatures in the subway.

An increase in air supply decreases the fire progression by lowering the flame temperature. The percent theoretical air required to provide a physiologically acceptable environment for the passengers is much greater than the minimum required to stop the fires from spreading. Therefore, increased air flow will not promote the spread of subway fire.

Emergency ventilation fans should have nearly full reverse flow capacity so that fans on either side of a malfunctioned train operate together to control the direction of airflow and to counteract the progression of smoke. When a train is malfunctioned between two stations and smoke is present, fresh air from outside is supplied to the tunnel and the smoke is extracted from the tunnel via these emergency ventilation fans of which operation modes (supply or exhaust) are specified with respect to the shortest evacuation path of the passengers.

For a subway system, it is necessary that provisions should be made to overcome several possible emergency case scenarios each of which begins with the recognition of any emergency situation till the evacuation of the passengers including the operation modes of the emergency ventilation fans. Midtunnel and station track way ventilation fans may be used to improve the emergency ventilation system; however, these fans must withstand elevated, temperatures for a prolonged period and have reverse flow capacity. The most critical fire location in the tunnel is the tunnel section with the largest cross-sectional area and maximum slope for the single track system. The downhill ventilation is the most critical due to adverse effect of buoyancy forces. In other words, hot gases tend to move upward but ventilation direction is downward. The critical velocity is higher in downward direction than in upward direction. The term “Critical Velocity” means the minimum air velocity past a fire to prevent backlayering which is used to mean the flow reversal of smoke and hot gases from the intended ventilation direction. Ventilation system has to prevent backlayering.

In conclusion, the design objectives are set by NFPA 130 Standard [6] as far as the egress routes are concerned. They are listed as follows:

- A stream of noncontaminated air is provided to evacuees on a path of egress away from fire. As far as carbon monoxide is concerned, it is recommended that air carbon monoxide (CO) content is as follows:
 - Maximum of 2000 ppm for a few seconds
 - Averaging 1500 ppm or less for the first 6 minutes of the exposure
 - Averaging 800 ppm or less for the first 15 minutes of the exposure
 - Averaging 50 ppm or less for the remainder of the exposure
- During emergency, evacuees should not be subjected to air temperatures that exceed 60 °C.
- Longitudinal airflow rates are produced to prevent backlayering of smoke on a path of egress away from fire. High ventilation rates can cause difficulties

in walking. Evacuees under emergency conditions can tolerate velocities as high as 11 m/s.

- It is recommended that smoke obscuration levels should be continuously below the point at which a sign internally illuminated 80 lx is discernible at 30 m and doors and walls are discernible at 10 m.
- The fans should be designed to withstand elevated temperatures in the event of fire (remain operational for a minimum of 1 hour in an air stream temperature of 250 °C)

Emergency ventilation systems should be designed based on a design fire size that is related to the types of vehicles that are expected to use in the tunnel. The fan capacities are to be such that, they can supply enough flow rate to the system to create air velocities above the critical velocity near the fire. For a train on fire in a tunnel, the air flow generated by the tunnel ventilation fans should be large enough to enable the passengers to sense the direction of airflow (minimum of 2.5 m/s) and not result in such a high air speed that passengers would be hindered when walking against it (Maximum of 11 m/s) [7, 28]. An air exchange rate of between 8 and 12 volumes per hour is recommended in the station fire incident [15].

1.2 Aim of The Thesis

When the fire safety is under consideration in the underground transportation system station, the fire occurring on the vehicle is the most critical incidence due to its high heat release rate. There is great difficulty in predicting and modeling the characteristics of a fire in a given situation, particularly the behavior of the rate of heat release and its variation with time. This thesis is investigated how to model a station fire incidence in the underground transportation system and to evaluate emergency ventilation system effectiveness. The complexity of the station geometry is required to analyze the fire by using Computational Fluid Dynamics (CFD)

techniques. CFD analysis is performed in CFDesign7.0. The CFD analysis of station fire is conducted to gain a better understanding of flow patterns and to determine smoke propagation and temperatures on passenger escape routes and to evaluate if emergency fans will function and serve as intended. The emergency ventilation system is satisfied the requirement of the NFPA-130 Standard [6]. Two different stations in Krakow Fast Tram System are modeled and their emergency ventilation systems are evaluated as case studies.

CHAPTER 2

COMPARTMENT FIRE

2.1 Introduction

Fire is a physical and chemical phenomenon. The interactions between the flame, its fuel, and the surroundings can be strongly nonlinear, and quantitative estimation of the processes involved is often complex. The processes of interest in an enclosure fire mainly involve mass fluxes and heat fluxes to and from the fuel and surroundings. The term compartment fire is used to define a fire that is confined in a room or similar enclosure within a building. The overall dimensions are important, but in most cases compartment fire analysis deals with room-like volumes of the order of 100 m³.

When an item burns inside an enclosure, two factors mainly influence the energy released and the burning rate. First, the hot gases will collect at the ceiling level and heat the ceiling and the walls. These surfaces and the hot gas layer will radiate heat toward the fuel surface, thus enhancing the burning rate. Second, the enclosure vents (doors, windows, leakage areas) may restrict the availability of oxygen needed for combustion. This causes a decrease in the amount of fuel burnt, leading to a decrease in energy release rate and an increase in the concentration of unburnt gases.

A fire in the open space releases lower energy than the fire in an enclosure with an opening where the hot surfaces and gases transfer heat to the fuel bed, thus increasing the burning rate. If, however, the opening is relatively small, the limited availability of oxygen will cause incomplete combustion, resulting in a decrease in energy release rate, which in turn causes lower gas temperatures and less heat transfer to the fuel. The fuel will continue to release volatile gases at a similar or somewhat lower rate. Only a part of the gases combust, releasing energy, and unburnt gases will be collected at ceiling level. The unburnt gases can release energy when flowing out through an opening and mixing with oxygen, causing flames to appear at the opening. In summary, compartment heat transfer can increase the mass loss rate of the fuel, while compartment vitiation of the available air near the floor will decrease the mass loss rate. The rate at which energy is released in a fire depends mainly on the type, quantity, and orientation of fuel and on the effects that an enclosure may have on the energy release rate.

2.2 Fire Development in Enclosure

Enclosure fires are divided into different stages according to the temperature development in the compartment. Figure-2.1 displays an idealized variation of temperature with time, along with the growth stages, for the case where there is no attempt to control the fire.

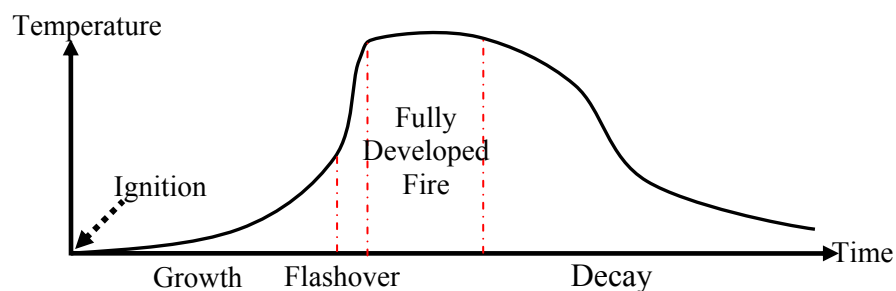


Figure 2.1 Generic temperature time history in the fire [16]

The stages of fire can be classified as follows [7, 16, 17]:

- **Ignition** : Ignition is defined as that process by which rapid, exothermic reaction is initiated, which then develops and causes the material involved to undergo change, producing temperatures greatly in excess of ambient. It is convenient to distinguish two types of ignition. It can occur either by piloted ignition (by flaming match, spark or other pilot source) or by spontaneous ignition (due to accumulation of heat in the fuel). Once the ignition occurs, part of the solid fuel in the compartment is pyrolyzing, releasing gaseous volatiles which burn as they mix with air. The accompanying combustion process can be either flaming combustion or smoldering combustion.
- **Growth** : Following ignition, fire grows at a rate dependent upon the type of fuel, access to oxygen, compartment configuration and the type of combustion. Heat transfer to contiguous and nearby combustible surfaces can raise these to temperatures at which they will begin to burn. During this stage, a hot gas produced by the fire rise due to buoyancy entraining the surrounding air, and a fire plume is formed. Impingement of a fire plume on the ceiling of the compartment gives rise to formation of a hot smoke layer in the upper part of the room. A smoldering fire can produce hazardous amounts of toxic gases while the energy release rate may be relatively low. It has a long growth period, and it may die out before later stages are reached. In the flaming combustion, the growth stage can occur very rapidly. The fuel is flammable enough to allow rapid flame spread over its surface, and heat flux from the first burning package is sufficient to ignite adjacent fuel packages. Lastly, sufficient oxygen and fuel are available for rapid fire growth. After ignition and during initial fire growth stage, the fire is said to be fuel-controlled (with sufficient amount of oxygen).
- **Flashover** : Flashover is a rapid transition from the growth period to a fully developed fire, resulting in the total surface of the combustible material

being involved in fire. Flashover represents a thermal instability caused primarily by strong radiation from the smoke layer to combustible materials within the enclosure.

- **Fully developed fire:** After a flashover has occurred, the exposed surfaces of all combustible items in the room of the origin will be burning and the rate of heat release will develop to a maximum, producing high temperature. The development of the fire is often limited by the availability of oxygen (ventilation-controlled). The average temperatures in the compartment are very high, in the range of 700-1200 °C.
- **Decay :** During this stage, the energy release rate diminishes as the fuel becomes consumed. The fire may go from ventilation-controlled to fuel-controlled in this period.

2.2.1 The Compartment Fire Equations

2.2.1.1 Simplified Energy Balance

Consider a fire in a compartment with an opening of height H_o and area A_o . \dot{Q} represents an energy release rate of fire in a compartment. The mass flow rate out through the opening is \dot{m}_g which consists of air and combustion products. T_g and T_a are the temperatures of the upper layer (hot) and the ambient atmosphere respectively. It is assumed that the layer is well mixed and its temperature is uniform. Simple energy balance in the compartment fire is shown in Figure 2.2. Rate of heat release rate is rate of heat loss from the compartment.

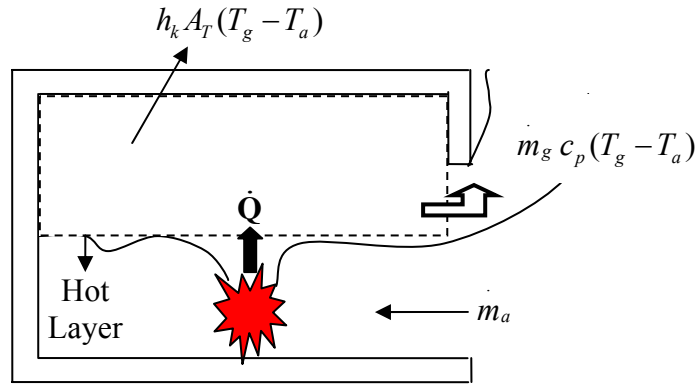


Figure 2.2 Diagram showing the energy balance for the hot layer in an enclosure fire [17]

A number of other terms can be taken into account, the terms given may be considered as the dominant terms. The simple energy balance can be written as

$$\dot{Q} = \dot{m}_g c_p (T_g - T_a) + h_k A_T (T_g - T_a) \quad (2.1)$$

where \dot{Q} is the energy release rate (kW), \dot{m}_g is the mass flow rate out through the opening (kg/s), c_p is the specific heat of the gases (kJ/kgK), T_g and T_a are the upper layer and ambient gas temperatures ($^{\circ}\text{C}$ or K), and h_k be defined as an effective heat conduction term for the solid boundaries (kW/m²K), and A_T as the boundary surface area to be used for heat transfer considerations (m²).

It is assumed that the energy release rate is known. The energy release rate is marked in a design situation. On the contrary in a situation where experiments have been carried out, the energy release rate is either measured or calculated from the mass loss rate of fuel.

Second expression in the right hand side of Equation 2.1 is expressed the heat lost to the boundaries. Radiation and convective heat transfer occurs at the solid boundaries, followed by conduction of heat into the solid. Radiative heat loss also occurs at openings. The dominant term is heat lost by conduction to the solid at the

boundaries. Therefore h_k should be defined as an effective heat conduction term for the solid boundaries.

The flow rate of hot gases out through the opening should be known to find the energy lost due to fluid flow through openings. The mass flow rate of gas leaving the compartment can be approximated by the following equation: [7, 16, 17]

$$\dot{m}_g = \frac{2}{3} C_d W \rho_a \left[2g \frac{T_a}{T_g} \left(1 - \frac{T_a}{T_g} \right) \right]^{1/2} (H_o - H_N)^{3/2} \quad (2.2)$$

where H_o is the height of the opening, H_N is the height of the neutral layer, W is the width of the opening, and C_d is the discharge coefficient.

Since H_N in equation 2.2 is not known, \dot{m}_g should be written as some function of the known variables. Noting that $W.H_o^{3/2}$ can be written as $A_o \sqrt{H_o}$ (often termed the ventilation factor) where A_o is the area of the opening, the following equation can be obtained

$$\dot{m}_g = \rho_a g^{1/2} A_o H^{1/2} \cdot f(T_g, \dot{Q}, A_o, H_o) \quad (2.3)$$

where f stands for “a function of.”

Equation 2.1 can be rearranged in terms of temperature increase ($\Delta T = T_g - T_a$) as

$$\frac{\Delta T}{T_a} = \frac{\dot{Q}}{\dot{m}_g c_p T_a + h_k A_T T_a} = \frac{\dot{Q} / \dot{m}_g c_p T_a}{1 + \frac{h_k A_T}{\dot{m}_g c_p}} \quad (2.4)$$

Substituting the known dimensions from Equation 2.3 into the above expression and rearranging, $\Delta T/T_a$ can be expressed as a function of two dimensionless groups:

$$\frac{\Delta T}{T_a} = f \left(\frac{\dot{Q}}{g^{1/2} \rho_a c_p T_a A_o H_o^{1/2}}, \frac{h_k A_T}{g^{1/2} \rho_a c_p A_o H_o^{1/2}} \right) \quad (2.5)$$

These two dimensionless groups can be designated as X_1 and X_2 and the following relationship can be assumed for the dimensionless temperature rise.

$$\frac{\Delta T}{T_a} = C \cdot X_1^N \cdot X_2^M \quad (2.6)$$

To determine the appropriate numerical values for the coefficients C, N, and M, McCaffrey et al.[17] analyzed data from more than 100 experimental fires in which steady burning rates were achieved, but upper gas layer temperatures did not exceed 600 °C. Through regression analysis of the experimental data, the constants C, N, and M were found, so that Equation 2.5 could be rewritten as

$$\frac{\Delta T}{T_a} = 1.63 \left(\frac{\dot{Q}}{\sqrt{g \rho_a c_p T_a A_o} \sqrt{H_o}} \right)^{2/3} \cdot \left(\frac{h_k A_T}{\sqrt{g \rho_a c_p A_o} \sqrt{H_o}} \right)^{-1/3} \quad (2.7)$$

A more convenient form of Equation 2.7 is achieved by using conventional values for some constant quantities ($g = 9.81 \text{ m/s}^2$, $\rho_a = 1.2 \text{ kg/m}^3$, $T_a = 293 \text{ K}$, and $c_p = 1.05 \text{ kJ/kg K}$). This results in the expression

$$\Delta T = 6.85 \cdot \left(\frac{\dot{Q}^2}{A_o \sqrt{H_o} h_k A_T} \right)^{1/3} \quad (2.8)$$

In the above equation specific units must be used, \dot{Q} in (kW), h_k in (kW/m²K), areas in (m²) and the opening height in (m).

It is necessary to obtain appropriate values for h_k which depend on the duration of the fire and the thermal characteristics of the compartment boundary. The time at which the conduction can be considered to be approaching stationary heat conduction is termed the thermal penetration time, t_p . This time can be given as

$$t_p = \frac{\delta^2}{4\alpha} \quad (2.9)$$

and indicates the time at which $\approx 15\%$ of the temperature increase on the fire-exposed side has reached the outer side of the solid. α used in the above equation represents the thermal diffusivity, also given by relation $\alpha = k/\rho c$, and given in (m²/s) and δ is the boundary thickness (m).

McCaffrey and colleagues analyzed the surface materials used in the experiments, and defined h_k in the following manner:

$$\text{For } t < t_p \quad h_k = \sqrt{\frac{k\rho c}{t}} \quad (2.10)$$

$$\text{and for } t \geq t_p \quad h_k = \frac{k}{\delta} \quad (2.11)$$

For an enclosure bounded by different lining materials, the overall value of h_k must be weighted with respect to areas. For example, if the walls and ceiling (W,C) are of a different material to the floor (F), the value of h_k is calculated as follows

$$\text{For } t < t_p \quad h_k = \frac{A_{W,C}}{A_T} \sqrt{\frac{(k\rho c)_{W,C}}{t}} + \frac{A_F}{A_T} \sqrt{\frac{(k\rho c)_F}{t}} \quad (2.12)$$

$$\text{and for } t \geq t_p \quad h_k = \frac{A_{W,C}}{A_T} \frac{k_{W,C}}{\delta_{W,C}} + \frac{A_F}{A_T} \frac{k_F}{\delta_F} \quad (2.13)$$

If T_a is taken as 295 K, Equation 2.7 can be rewritten as

$$\Delta T = 480 \cdot X_1^{2/3} \cdot X_2^{-1/3} \quad (2.14)$$

Equation 2.14 can be used to estimate the size of fire necessary for flashover to occur. If a temperature rise of 500 K is taken as a conservative criterion for the upper layer gas temperature at the onset of flashover then substitution for X_1 and X_2 in Equation 2.14 gives after rearrangement

$$\dot{Q} = \left[g^{1/2} (c_p \rho_a) T_a^2 \left(\frac{\Delta T}{480} \right)^3 \right]^{1/2} (h_k A_T A_o H_o^{1/2})^{1/2} \quad (2.15)$$

With $\Delta T = 500$ K, and appropriate values for g , c_p , ρ_a etc.,

$$\dot{Q}_{FO} = 610 (h_k A_T A_o \sqrt{H_o})^{1/2} \quad (2.16)$$

where h_k is in (kW/m²K), A_T and A_o are in (m²) and H_o is in (m) where \dot{Q}_{FO} (kW) is the rate of heat output necessary to produce a hot layer at approximately 500 °C beneath the ceiling. The square root dependence indicates that if there is 100% increase in any of the parameters h_k , A_T or A_o , then the fire will have to increase in heat output by only 40% to achieve the flashover criterion as defined.

2.2.1.2 The T-Squared Fire

Over the past decade, those interested in developing generic descriptions of the rate of heat release of fires have used a “t-squared” approximation. The initial growth period is nearly always accelerating in real fires. A t-squared fire is one in which the burning rate varies proportionally to the square of time. By multiplying time squared by a factor α , various growth velocities can be simulated, and the energy release rate as a function of time could be expressed as

$$\dot{Q} = \alpha \cdot t^2 \quad (2.17)$$

where α is a growth factor (often given in kilowatts per second squared (kW/s²)) and t is the time from established ignition, in seconds. This relationship has been found to fit well with the growth rates exhibited by various different items, but only after ignition has been well established and the fire has started to grow.

The t-squared fire has been used extensively in the design of detection systems, and guidance on selecting values for the growth time associated with various materials is available in NFPA 204M [22]. T-squared fires are classified as “ultra fast”, “fast”, “medium”, and “slow” according to growth factor α values. Table 2.1 gives the corresponding values of α and the time it takes to reach 1055 kW.

Table 2.1 Values of α for different growth rates [16]

Growth Rate	α (kW/s²)	Time (s) to reach 1055 kW
Ultra fast	0.19	75
Fast	0.047	150
Medium	0.012	300
Slow	0.003	600
<i>Source: NFPA, Guide for Smoke and Heat Venting, NFPA 204M, [22]</i>		

The contents and the type of enclosure affect the selection of the growth rate. If considerable knowledge about the contents of the enclosure is available, a suitable ignition scenario can be assumed, and experimental data on materials can be used to determine the growth rate factor α . There is very scarce information available about the enclosure, in such cases the designer can decide on the growth rate factor due to the recommendations suggested in the literature.

2.2.1.3 Heat Release Rate Equations in Stages and Duration of Fire

The heat release rate variation with time can be represented as in Figure 2.3.

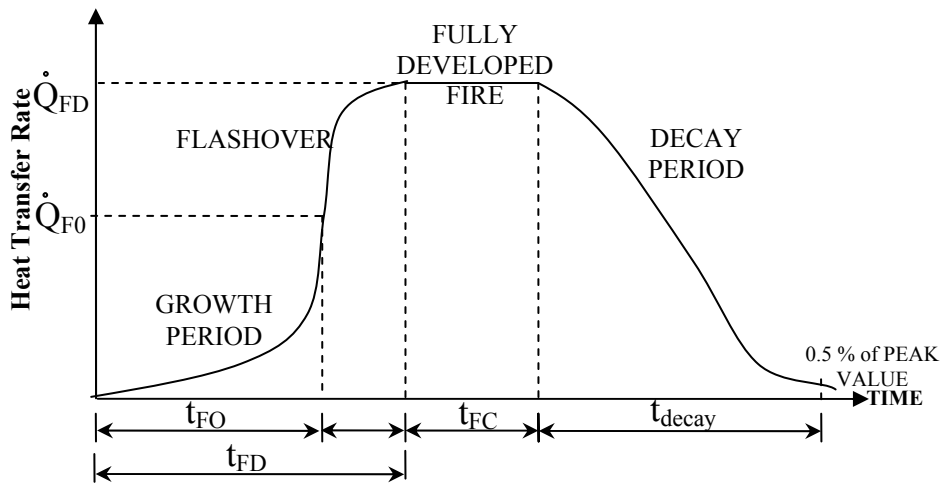


Figure 2.3 Heat release rate variation with time [7, 16, 17, 21]

The rate of the heat release rate at flashover, \dot{Q}_{FO} , is given in Equation 2.16 as

$$\dot{Q}_{FO} = 610(h_k A_T A_o \sqrt{H_o})^{1/2}$$

Initial variation of heat release rate is assumed to be t-squared fire and related equation is given in Equation 2.17 as

$$\dot{Q} = \alpha \cdot t^2$$

where α is taken to be 1 W/s² for Ankara Metro train based on the information given by Mott MacDonald [21]. Therefore estimated time to flashover can be calculated from

$$t_{FO} = \sqrt{\frac{\dot{Q}_{FO}}{\alpha}} \quad (2.18)$$

General values on the burning rates of the combustible materials throughout the various stages of the compartment fire development are as follows. At the point when the fire reaches full fire development, 20% of the combustible items have been burnt. During the period of full fire development when the heat release rate is approximately constant, the amount of combustible material remaining falls from 80% to 30% (Equation (2.21)). In this stage, a state of flaming combustion prevails where all the combustible surfaces within the compartment are involved in the fire. The remaining 30% of combustible material is consumed during the final decay period. Based on this knowledge the heat release rate equations and periods of stages can be summarized as follows

$$t_{FD} = \left[\frac{0.6 \cdot E}{\alpha} \right]^{1/3} \quad (2.19)$$

where t_{FD} is the time to full fire development and E is the total heat of combustion for items in the burning enclosure. Heat release rate at full fire development can be given as

$$\dot{Q}_{FD} = \alpha \cdot t_{FD}^2 \quad (2.20)$$

Time for the full fire development phase is calculated from the equation given below

$$t_{FC} = \frac{0.5 \cdot E}{\dot{Q}_{FD}} \quad (2.21)$$

Taking the decay characteristics to be exponential

$$\dot{Q} = \dot{Q}_{FD} e^{-\beta \cdot t_d} \quad (2.22)$$

The energy released during decay is given by

$$E_d = \int_0^{\infty} \dot{Q}_{FD} e^{-\beta \cdot t_d} dt_d \quad (2.23)$$

Solving

$$E_d = \frac{\dot{Q}_{FD}}{\beta} \quad (2.24)$$

30% of the energy is released during decay. Thus

$$\beta = \frac{\dot{Q}_{FD}}{0.3 \cdot E} \quad (2.25)$$

Then the time corresponding to the stage when heat release rate is 0.5% of the peak heat release rate is

$$t_{decay} = \frac{1}{\beta} \ln \left(\frac{\dot{Q}_{FD}}{\dot{Q}_{0.005}} \right) \quad (2.26)$$

As a result, the summation of t_{FD} , t_{FC} , and t_{decay} is given the total duration of the fire. By knowing all the periods and heat release rates using the equations given, the trend of the heat release rate over the time can be drawn as given in Figure 2.3.

2.2.2 Turbulent Fire Plume Characteristic

When a mass of hot gases is surrounded by colder gases, the hotter and less dense mass will rise upward due to the density difference, or rather, due to buoyancy. This is what happens above a burning fuel source, and the buoyant flow, including any flames, is referred to as a fire plume. As the hot gases rise, cold air will be entrained into the plume, causing a layer of hot gases to be formed. Many applications in fire safety engineering have to do with estimating the properties of the hot layer and the rate of its descent. This depends directly on how much mass and energy is transported by the plume to the upper layer.

Fire plumes can be characterized into various groups depending on the scenario under investigation. In this section we shall concentrate on the plume most commonly used in fire safety engineering, the so-called buoyant axisymmetric plume

caused by a diffusion flame formed above the burning fuel. Diffusion flames refer to the case where fuel and oxygen are initially separated, and mix through the process of diffusion. Burning and flaming occur where the concentration of the mixture is favorable to combustion. Although the fuel and the oxidant may come together through turbulent mixing, the underlying mechanism is molecular diffusion. This is the process in which molecules are transported from a high to low concentration. Flames in accidental fires are nearly always characterized as diffusion flames. An axis of symmetry is assumed to exist along the vertical centerline of the plume. The axisymmetric fire plume is conventionally divided into the three zones, as shown in Figure 2.4. In the continuous flame zone the upward velocity is near zero at the base and increases with height. In the intermittent flame zone the velocity is relatively constant, and in the far field zone the velocity decreases with height. Figure 2.5 shows some of the characteristics of a buoyant axisymmetric plume.

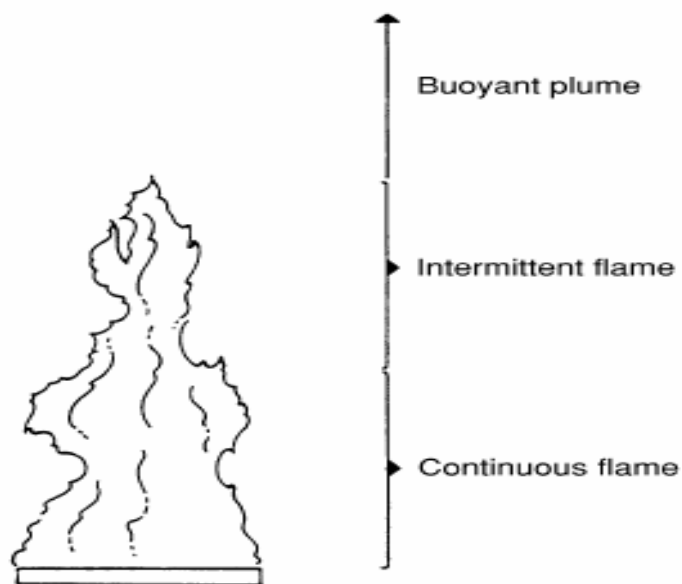


Figure 2.4 The three zones of the axisymmetric buoyant plume [16]

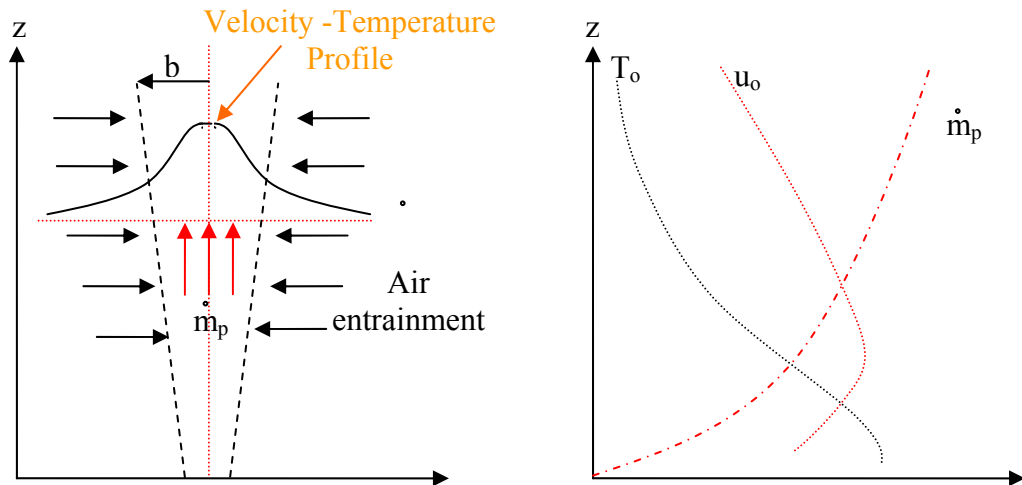


Figure 2.5 Some of the characteristics of a buoyant axisymmetric plume [16]

2.2.2.1 The Ideal Plume

The ideal plume or the point-source plume is a very simple type of fire plume. By using the fundamental equations, derivation of analytical solutions for the mass flow, velocity, and temperature of the gases in the simplified plume is obtained. Assumptions are used in the calculation:

1. All the energy is injected at the point source of origin and that energy remains in the plume, i.e., that there are no heat losses in the system due to radiative losses. In real fire plumes the radiative part is typically 20 to 40% of the total energy released from many common fuel sources.
2. The density variations throughout the plume height are small and only need to be considered when the difference $(\rho_a - \rho)$ appears directly. The ideal plume theory is therefore sometimes referred to as the weak plume theory, where, due to mixing (entrainment) of air, the plume temperature is only slightly higher than the ambient. At certain points in the derivation it shall be assumed that $\rho_a = \rho$. However, when expressing the buoyancy force, which is

caused by the density difference, $(\rho_a - \rho)$, this assumption does not apply. This approximation is sometimes referred to as the Boussinesq approximation.

3. The velocity, temperature, and force profiles are of similar form independent of the height, z . The velocity and temperature are constant over the horizontal section at height z along the radius b , and that the velocity at a certain height above the fuel source $u = 0$, and $T = T_a$ outside the plume radius.
4. The air entrainment at the edge of the plume is proportional to the local gas velocity in the plume, so that the entrainment velocity can be written as $v = \alpha.u$, where α is a constant and is taken to be 0.15. In other words, the horizontal entrainment velocity is assumed to be 15% of the upward plume velocity. This value is difficult to measure but has been found to correspond reasonably with experimentally measured values.

The plume mass flow rate, \dot{m}_p , defined as the total mass flowing upward, at a certain height above the fuel source, within the plume boundaries is calculated at height z

$$\dot{m}_p = 0.2 \left(\frac{\rho_a^2 g}{C_p T_a} \right)^{1/3} \dot{Q}^{1/3} z^{5/3} \quad (2.27)$$

The heat release rate from a fire can be expressed:

$$\dot{Q} = \dot{m}_p c_p \Delta T \quad (2.28)$$

by assuming no radiative heat transfer. As a result, the plume temperature difference at height z difference

$$\Delta T = 5.0 \left(\frac{T_a}{g c_p^2 \rho_a^2} \right)^{1/3} \dot{Q}^{2/3} z^{-5/3} \quad (2.29)$$

where \dot{m}_p is plume mass flow rate (kg/s), \dot{Q} is the energy release rate (kW), c_p is the specific heat of the gases (kJ/kgK), z is the height above the fire source (m); T_a (K) and ρ_a (kg/m³) are temperature and density value of ambient air. [16, 17]

2.2.2.2 Plume Equations Based on Experiments

2.2.2.2.1 The Zukoski Plume

Several experimental measurements on the plume mass flow rate as a function of height and energy release rate were made possible by adjusting the fuel height and energy release rate. Zukoski used the ideal plume theory and adjusted very slightly to get a best fit with the experiments. The resulting plume mass flow equation became

$$\dot{m}_p = 0.21 \left(\frac{\rho_a^2 g}{C_p T_a} \right)^{1/3} \dot{Q}^{1/3} z^{5/3} \quad (2.30)$$

Zukoski equation is also commonly shown in the form

$$\dot{m}_p = 0.071 \dot{Q}^{1/3} z^{5/3} \quad (2.31)$$

where the ambient air properties are assumed to be $T_a=293\text{K}$, $\rho_a= 1.1 \text{ kg/m}^3$ and $c_p=1.0 \text{ kJ/kgK}$. The expressions for plume and plume temperature associated with the Zukoski mass flow equation can be assumed to be ideal when it compares with the ideal plume equation. [16,17]

2.2.2.2.2 The Heskestad Plume

Three of the main assumptions for the ideal plume will be removed or limited:

1. The point source assumption is relaxed by introducing a “virtual origin” at height z_0 (Figure-2.6). Also, account will be taken of the fact that some plume properties depend on the convective energy release rate, \dot{Q}_c .
2. The Boussinesq approximation will be removed so that large density differences can be taken into account. This means that it is not assumed that $\rho_\infty=\rho$ in certain equations. Because of the Boussinesq approximation, the ideal plume theory is said to describe weak plumes; the equations discussed in this section are said to describe strong plumes.

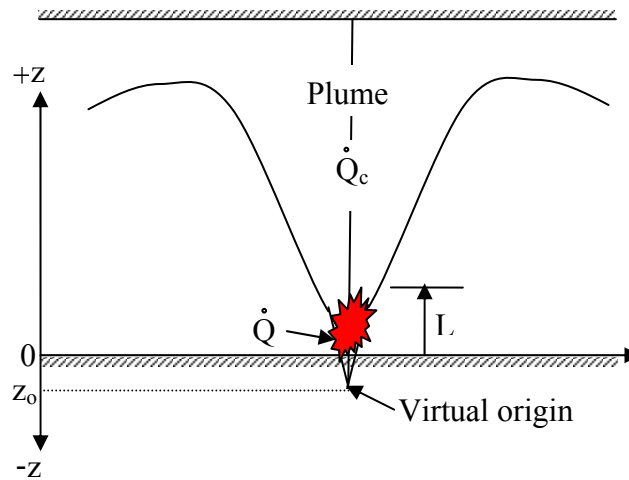


Figure 2.6 Some plume characteristics [16]

The mass flow rate in the plume depends on whether locations above or below the mean flame height are considered. The mean flame height is calculated from

$$L = -1.02D + 0.235 \dot{Q}^{2/5} \quad (2.32)$$

where L is mean flame height (m), D is base diameter of fire (m) and \dot{Q} is the energy release rate (kW).

When the mean flame height, L , is below the interface and z is at or above the flame height but at or below the interface height, the mass flow rate in the fire plume

$$\dot{m}_p = \left[0.071 \dot{Q}_c^{1/3} (z - z_0)^{5/3} \right] \left[1 + 0.027 \dot{Q}_c^{2/3} (z - z_0)^{-5/3} \right] \quad (2.33)$$

where \dot{m}_p is mass flow rate in the plume (kg/sec), \dot{Q}_c is convective heat release rate (approximately $0.7 \dot{Q}$) (kW), z is the height above the base of the fire (m) and z_0 is the height of virtual origin above the base of the fire (below the base of the fire, if negative) (m). [16, 17, 23]

$$\dot{m}_p = \left[0.0056 \dot{Q}_c \right] \frac{z}{L} \quad (2.34)$$

The virtual origin z_o is the effective point source of the fire plume

$$z_o = 0.088Q^{2/5} - 1.02D \quad (2.35)$$

The centerline temperature

$$\Delta T_o = 9.1 \left(\frac{T_a}{g c_p^2 \rho_a^2} \right)^{1/3} \dot{Q}_c^{2/3} z^{-5/3} \quad (2.36)$$

2.2.2.2.3 The McCaffrey Plume

McCaffrey used experimental data and dimensional analysis to arrive at plume relations for upward velocity and temperature. Methane flame is used for experiments. The constants are arrived at by correlations using the total heat release rate.

These relations were of the form

$$\Delta T_o = \left(\frac{\kappa}{0.9 \cdot \sqrt{2g}} \right)^2 \left(\frac{z}{\dot{Q}^{2/5}} \right)^{2\eta-1} \cdot T_a \quad (2.37)$$

$$u_o = \kappa \left(\frac{z}{\dot{Q}^{2/5}} \right)^\eta \dot{Q}^{1/5} \quad (2.38)$$

The constants η and κ vary depending on the three regions. The constants are given in Table 2.2

Table 2.2 Constants in McCaffrey's plume equations [16, 17]

Region	$z/\dot{Q}^{2/5}$	η	κ
Continuous	< 0.08	1/2	6.8
Intermittent	0.08-0.2	0	1.9
Plume	> 0.2	-1/3	1.1

For both plume temperatures and plume velocities, the McCaffrey equations will result in values roughly 10 % higher than those given by the Heskestad equation. [16, 17]

2.2.2.2.4 The Thomas Plume

The experimental data on which the above plume equations are based did not include experiments where the flame height, L, was significantly less than the fuel source diameter, D. Thomas found that in the continuous flame region, or in the near field, the plume mass flow rate was more or less independent of the energy release rate and more a function of the perimeter of fire, P, and the height above the fire source, z⁴. [17] This has been found to be particularly valid for fires where the mean flame height is considerably smaller than the diameter. The Thomas plume mass flow rate equation is written as

$$\dot{m}_p = 0.188 \cdot P \cdot z^{3/2} \quad (2.39)$$

where P is the fire perimeter in [m] and z is the height in [m] at which the mass flow rate in [kg/s]. The equation is especially useful for cases where L/D < 1. [16, 17]

2.2.2.3 Walls and Corner Interactions with Plumes

The equations are discussed in the previous section, the fuel source has been assumed to be circular and the plume has been assumed to be free from the interference of walls and other surfaces. Zukoski discussed studies made where the fire sources are placed near or flush with the walls and corners. Figure-4 shows a characteristic sketch of three cases studied. Experimenters reported that when a circular burner was placed with one edge tangent to a vertical wall (Figure 2.7.a); there was very little influence on plume geometry and plume entrainment up to a height of three times the burner diameter. However, when a semicircular burner was

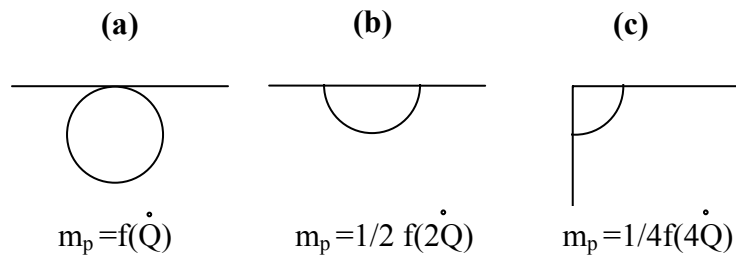


Figure 2.7 Fire sources near walls and corners [17]

placed with its straight edge against a wall (Figure 2.7b), the plume was attached to the wall and developed as a half plume with plume properties closely approximating these for a full circular burner of twice the energy release rate. The plume mass flow can therefore be calculated to be half of the plume mass flow of a fire with twice the energy release rate. We can use the simple Zukoski plume mass flow equation (2.31) to develop a relationship for the case in Figure 2.7b by writing

$$\dot{m}_{p,wall} = 0.045 \dot{Q}^{1/3} z^{5/3} \quad (2.40)$$

Similarly, for the case of the corner (Figure 2.7c), the plume mass flow is roughly one quarter of the flow from an unbounded fire with the four times the energy release rate. It is found that

$$\dot{m}_{p,corner} = 0.028(\dot{Q})^{1/3} z^{5/3} \quad (2.42)$$

CHAPTER 3

FIRE MODELING

3.1.1 Fire Modeling

Mathematical models in fire science concern different ways of describing fire-related phenomena using analytical and numerical techniques. Due to rapidly growing knowledge and understanding of fire-related phenomena and wide spread access to powerful computers at reasonable cost, great progress has been made when predicting event such as smoke spread, presence and concentration of combustible and toxic gases, calculation of pressure and temperature fields in enclosures due to fire, etc. There are two approaches in mathematical fire modeling, non-deterministic and deterministic.

The non-deterministic approach do not make direct use of the physical and chemical principles involved in fires, but make statistical predictions about fire frequencies, barrier failures, fire growth etc. The course of fire is described as a series of discrete stages that summarizes the nature of fire. Different methods are incorporated to take account for uncertainties and in the literature; one sometimes encounters the division into probabilistic and stochastic models.

The deterministic approach is the most widespread one and it clearly dominates all other methods. The deterministic models are based on chemical and physical

relationships, empirical or analytically derived. A specific scenario is studied and outputs are provided as discrete numbers. Unlike the non-deterministic models a limited number of designed fires are considered in order to cover relevant scenarios. Deterministic models are used in fire safety engineering. Design of buildings can be divided into a number of categories depending on the type of problem to be addressed. Some of the main problem categories are smoke and heat transport in enclosures, detector/sprinkler activation, evacuation of humans, and temperature profiles in structural elements. Mathematical models used today, hand-calculation models as well as computer models, are based on this way of thinking. Deterministic models for simulating the transport of smoke and heat in enclosures are normally handled either by zone modeling or field modeling using computational fluid dynamics. [16]

3.1.2 Zone Models

Zone models emerged very early in fire research, as their application does not require substantial computational resources and are based primarily on analytical and semi-analytical considerations. Zone models are the simpler models and can generally be run on personal computers. Zone models usually divide the space into two distinct control volumes, an upper control volume near the ceiling called upper layer, consisting of burnt and entrained hot gases produced by the fire and a lower layer, which is the source of entrainment air. Figure 3.1 illustrates the zone model concept.

The size of the two zones varies during the course of a fire, depending on the rate of flow from the lower to the upper zone, the rate of exhaust of the upper zone and the temperature of the smoke and gases in the upper zone. Because of the small number of zones, zone models use engineering equations for heat and mass transfer to evaluate the transfer of mass and energy from the lower to the upper zone, the heat and mass losses from the upper zone, and other special features. Generally, the equations assume that conditions are uniform in each respective zone. Based on the

principle of the conservation of mass and energy, as well as ideal gas law, a set of ordinary differential equations are derived.

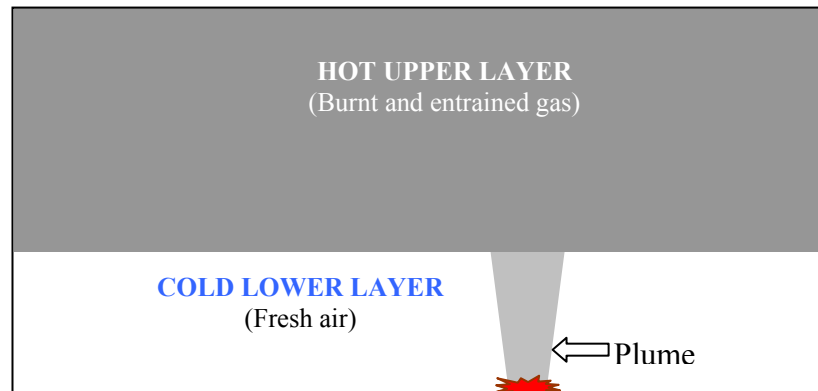


Figure 3.1 Illustration of the zone model concept

In zone models, the source of the flow into the upper zone is the fire plume. All zone models have a plume equation. A few models allow the user to select among several plume equations. Most current zone models are based on an axisymmetric plume. Because present zone models assume that there is no pre-existing temperature variation in the space, they cannot directly handle stratification. Zone models also assume that the ceiling smoke layer forms instantly and evenly from wall to wall. This fails to account for the initial lateral flow of smoke across the ceiling. The resulting error can be significant in spaces having large ceiling areas.

Zone models can, however, calculate many important factors in the course of events (e.g., smoke level, temperature, composition, and rate of descent) from any fire that the user can describe. Most will calculate the extent of heat loss to the space boundaries. Several will calculate the impact of vents or powered exhaust, and some will predict the response of heater smoke-actuated detection systems.

3.1.2.1 Limitations of zone modeling

Zone models have been used in fire safety design for a long time with considerable success. However, despite the level of sophistication achieved up to the present moment, this approach suffers from a number of major problems.

The most important of these are as follows [12]:

- Zone models supply limited information about the fire environment. Since variables of interest are averaged over zones with significant spatial scale, resolution is poor and important local effects can not be traced. On the other hand, field models are able to achieve high spatial resolution, and their ability to provide such resolution is constantly increasing.
- The major drawback of zone models is the necessity of a priori knowledge of the structure of the flow. This knowledge should be extracted either from experiments, or from preliminary theoretical considerations. This means that the validity of assumptions involved in zone modeling should be confirmed in each particular case. This virtually means that zone model development can never be decoupled from supporting experimental studies. In the field modeling approach, this problem is overcome by resorting to the fundamental physical principles of mechanics and thermodynamics, which are universally true for any system under consideration. Therefore, field models are applicable for any situation, with the change in flow structure and fire environment being accounted for automatically.
- There may exist problems which are not tractable using the zone approach with required accuracy. For example, in a rapidly growing fire there may not be sufficient time for flow restructuring so that different zones can develop and be distinguished from each other. The difference between various zones may become fuzzy, which puts into question the possibility of the zone

approach. The zone approach is also questionable in the case of very complicated geometry, if the space is obstructed by a variety of combustible objects.

- Flow structure may change as a result of small changes in parameters. This can make zone model assumptions invalid and lead to erroneous results.

3.1.3 Field Models (CFD)

Field models (also referred to as computational fluid dynamics models) usually require large-capacity computer work stations or mainframe computers and advanced expertise to operate and interpret. Field models, however, can potentially overcome the limitations of zone models and complement. As with zone models, field models solve the fundamental conservation equations. In field models, however, the space is divided into many cells (or zones) and uses the conservation equations to solve the movement of heat and mass between these zones. As a result, CFD modeling presents a more scientifically accurate approach.

Using field modeling, a domain in space is first defined. This domain is the actual world for the simulation to be carried through and its proportions are determined by the size of the object that is to be simulated. The domain is divided into a large number of small control volumes, which in addition can be defined as being walls or obstacles of some kind, or simply to consist of fluid space or air. In this way, the actual geometry that is to be simulated is built up inside the computational world, the domain, defined earlier and relevant boundary conditions can be predetermined including restrictions and limitations on the solution. CFD technique is then applied in order to solve a set of non-linear partial differential equations derived from basic laws of nature. Most flows encountered in real life are very complex. This indicates that one has to incorporate various models in order to make simulations possible. In the case of fire, a combustion model is used to simulate the course of combustion, a turbulence model has to be included for the prediction of the buoyancy driven

turbulent flow as well as a radiation model to simulate the thermal radiation. Of course, there are many additional sub-models that can be included such as fire-spread models, soot models etc.

In computational fluid dynamics, one often talks about the use of a pre-processor, a solver and a postprocessor. The pre-processor is used to define the actual problem and includes grid generation, boundary conditions, selection of calculation models to be used and what output is required etc. As the name implies, the solver uses the input data to find a solution to the problem. Now, as the conservation equations are non-linear partial differential equations they have no simple analytical solutions. Instead, field models use different kinds of numerical techniques to find the solutions. The solutions obtained are then examined and presented using some post processor software. Figure 3.2 presents the basics steps of CFD analysis.

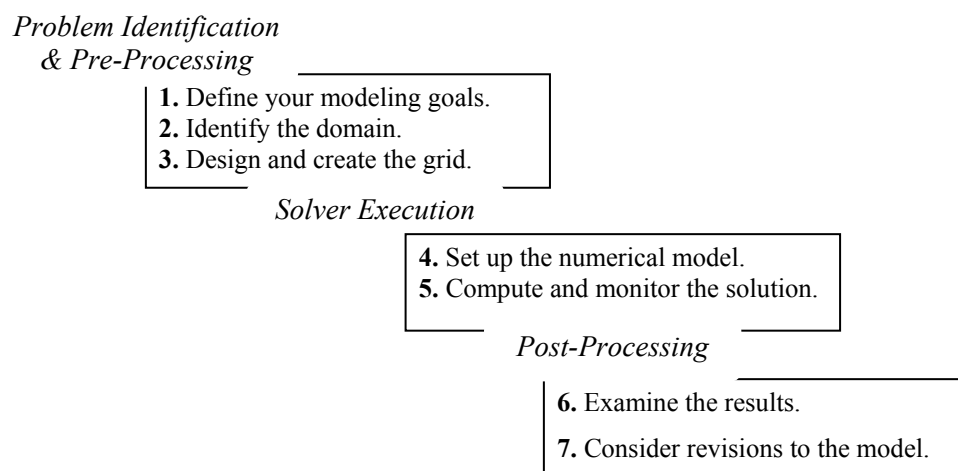


Figure 3.2 CFD analysis basic steps [24]

Given the rapid progress in computer power and the availability of this to a low cost, field models are not only a tool for the fire researchers but also applicable in

conventional fire safety engineering to optimize the fire safety in buildings et cetera. The accuracy of a simulation depends for example on factors such as the grid resolution and the specific models being used.

Through the use of small cells, field models can examine the situation in much greater detail and account for the impact of irregular shapes and unusual air movements that cannot be addressed by either zone models or algebraic equations. The level of refinement exceeds that which can usually be observed or derived from scale models.

3.1.3.1 CFD Modeling of Fire Application in Underground Transportation Systems

H. Xue, J.C. Ho and Y. M. Cheng (2001) [13] presented a comparison of different combustion models in enclosure fire simulation. In this study, three combustion models, the volumetric heat source model, the eddy break-up model and the presumed probability density function model, were examined in enclosure fire simulation. The computations were carried out using Fluent, a commercial CFD code. The governing equations were solved using the finite volume method in a staggered grid system. The algorithm employed was the SIMPLEC. Power-law scheme is used for the numerical simulation. The combustion models were compared and evaluated for their performance in predicting three typical enclosure fires, a room fire, a shopping mall fire and a tunnel fire. High Reynolds number turbulence $k-\varepsilon$ model with buoyancy modification and the discrete transfer radiation model were used in the simulation. Corresponding experimental data from the literature were adopted for validation. The volumetric heat model was the simplest model for combustion. The fire was modeled as a volumetric heat source, which was patched into the computational domain. In this model, the direct contribution of combustion species is neglected. The eddy break-up model was based on the solution of species transport equations for reactant and product concentrations. The reaction mechanism had to be explicitly defined and it could be simple or multi-stage reactions. The

reactions were assumed to be infinitely fast whenever fuel and oxidant simultaneously exist at a point. The presumed probability density function model was based on the solution of transport equations for one or two conserved scalars (the mixture fractions and/or its variance). The chemistry was modeled by equilibrium model, which assumes that the chemistry was rapid enough for chemical equilibrium to exist at the molecular level. It computed species from mixture fraction by an algorithm based on the minimization of Gibbs free energy. Individual component concentrations for the species of interest were derived from the predicted mixture fraction distribution. For a simple fuel/oxidizer system, the mixture fraction was defined as a ratio of rate of fuel consumption to sum of rate of fuel and oxygen combustion. To account for the radiative heat transfer in enclosure fires, the Discrete Transfer Radiation Model was incorporated into the turbulence $k-\varepsilon$ model together with three combustion sub-models. Heating or cooling of surfaces due to radiation and/or heat sources can be included in the model. The tunnel fire was simulated by burning liquefied petroleum gas (LPG) as a fuel. In the experimental study, two heat release rates, 3.15 and 4.75kW were studied under four different ventilation flow velocities at 0.13, 0.31, 0.52 and 0.61 m/s, respectively. The temperatures are measured at three cross-sections. Station 1 is located upstream at $x=0.9\text{m}$ and stations 2 and 3 are located downstream at $x=3.3\text{m}$ and $x=5.1\text{ m}$, respectively.

Predicted temperature distributions along verticals on the centerline of the tunnel were compared with the experimental measurements for the case at $U=0.13\text{ m/s}$ and $Q=3.15\text{ kW}$. It was observed that the temperature profile predicted by the eddy breakup model and the presumed probability density function model differed only slightly. The predicted temperature profiles are reasonable in most of the region at station 1 upstream and station 3 downstream. However, all three combustion models showed poor performance at station 2 downstream, a location near the fire source. The predicted temperature rise from the height of 0.15 m to 0.28 m is 550 °C, while experimental data showed that the temperature rise only reached 553 °C at the height of 0.26 m.

The heat release rate was changed from 3.15 to 4.75 kW. The corresponding temperature rise in the tunnel was increased. With the increase of the heat release rate, the difference in prediction of temperature between the presumed probability density function and the eddy breakup models appeared. The presumed probability density function model performed the best among the combustion models. The presumed probability density function model also showed its performance superior to other two models when the ventilation velocity is increased to 0.61 m/s.

Prediction of temperature and velocity fields in all the cases tested was not consistent. For the tunnel fire, the eddy breakup model and presumed probability density function model performed equally well. The performance of the presumed probability density function model was further improved at high heat release rate and high ventilation velocity. In general, the performance of presumed probability density function model was more consistent, although there was no distinct performance which could be commented as a good combustion model for enclosure fire simulation, especially at the flow region where fire source was nearby a large temperature gradient occurred. The current turbulent combustion models were inadequate to account for the interaction of combustion, turbulence, radiative heat transfer of participating media including smoke.

F. Chen, S. W. Chien, H. M. Jang and W. J. Chang (2003) [4] investigated the stack effects on smoke propagation in subway stations. The investigators computed the three dimensional smoke flow fields under various fires happened in a representative subway station of Taipei Rapid Transit System. The stack effect on smoke propagation in the Gong-Guan Subway Station, a typical mid-way station in the Taipei Rapid Transit System was examined. There were two floors in the station, one was the platform floor on the bottom and the other was the lobby floor on the top. The length of the station was 142.1 m and its width was 17.9 m. The height of the lobby floor and platform floor were 4.15 m and 5.15 m respectively. CFD was employed in order to investigate the smoke flow especially on the stack effect. A computer code, named CFX4 which utilized the finite volume method was employed

to solve the flow field. It was pointed out that a careful choice of a turbulence model was crucial in order to have a better simulation. The turbulence $k-\varepsilon$ model was able to simulate the flow in fire. The fire was simulated as a source of heat and smoke accounted for by CO_2 in which no combustion was considered. A fire having a heat release rate of 5 MW was produced 1.4×10^5 ppm/s. The boundary conditions for the flow in station are the no slip, no penetration and adiabatic for momentum, CO_2 and the temperature for the rigid walls enclosed the flow field. At the openings to the atmosphere, the atmospheric pressure instead of the detailed velocity distribution was given. Mass fraction of CO_2 and the temperature of surrounding atmosphere were specified in the portions of openings where the fresh air flowing in. During every time step in order to check the correctness of the computational results, they examined the conservation of mass in the enclosure by calculating the mass flow passing through the shafts. During calculation procedure no mechanical ventilation was turned on for the sake of studying stack effect. In the first case fire was located on the left of the lobby floor. The location factor dominated the smoke movement first, making the smoke move to the left-hand side of the station. Then the area factors took over to influence the smoke movement, implying that smoke preferred to go through the smaller area. Fire is located in the middle of the platform in the second case. In such a case, the smoke moved upwards rapidly, impinges on the ceiling and then spreads over to the two ends of station in the lobby floor. The smoke reached the two ends at almost the same time, while due to the smaller-area, the stack effect predominated the movement of smoke, inducing the smoke to move to the right. However, because the quantity of smoke is so large that smaller area was not sufficiently large to evacuate all the smoke moving to the right, the other exit started to help evacuate some of the smoke due to its large cross sectional area. Competition occurred in different stages, depending on the predominance of the location factor or the area factor. The area factor was the sole factor influencing the smoke movement, while still having two stages of influence: Firstly, a competition between the exits on the left and right. Secondly, a competition between the two exits on the right. The smoke eventually evacuated from the right exits. There are two factors influencing the stack effect in subway stations: the area factor and the location factor. Although

these two factors compete to predominate, a general rule-of-thumb is clear: the smoke will evacuate from the exit which the smoke reaches first, and then all or most of the smoke in the station will move towards this exit to evacuate. If there is no location factor, the area-factor will predominate the system; i.e. the smoke will evacuate from the exit of smaller area. However, if two factors become simultaneously effective, the location factor in general is more influential than the area factor.

S.K.L. Li and W.D. Kennedy (1999) [19] presented results of a study where CFD was the numerical tool used to analyze the ventilation performance in stations of the Buenos Aires Metro subway system. Both natural and mechanical ventilation options were studied. The study showed that although natural ventilation is sufficient to maintain the temperature criteria, it presented a potential egress problem by letting hot gases leave through the entranceways. The study took the following criteria into account. First one was identifying and evaluating feasible and cost-effective ventilation alternatives to meet the current industry standard NFPA 130 [6]. Performing subway environment simulation (SES) to determine the ventilation requirements for a tunnel emergency for a selected section of the system was the second criteria. Furthermore, performing CFD simulations to identify the most effective ventilation operating mode during a fire emergency in station was another criterion. The train heat release rate used for the analysis was a low-intensity fire of 1.8 MW which corresponded to a train fire involving only the under car combustible contents. They decided to locate a jet fans in the tunnel about 50 meters from each of the stations. The jet fan operating mode would be dependent on the location of the fire within the station. The SES program was utilized in order to provide the fundamental boundary conditions necessary for the CFD analysis. CFD simulations were performed to evaluate the station conditions resulting from a fire on board a train, stopped in a station, with and without mechanical ventilation. For natural ventilation, ambient pressure was assumed at all flow boundaries. For mechanical ventilation, simulations were performed to determine the airflow boundary conditions at the ends of the station. Ambient pressure conditions were used at

station entrances. Medrano and Pueyrredon Stations are selected for the simulations. Two fire scenarios were considered (1) a fire at either end of the station beyond the last exit or staircase (2) a fire between exits or staircases. The first scenario required the ventilation system to push smoke and hot gases toward the tunnel, or in direction opposite to that of the evacuating passengers. The second scenario required the ventilation system to force outside air through the station exits or stairways, thus maintaining the evacuation paths free of smoke and hot gases. Second fire scenario was considered the worse case of the two because of the proximity of the fire to the exits or staircases. A total of four steady state CFD simulations were performed, two of each station. The first simulation was used to evaluate the stations conditions when no mechanical ventilation is used. The second simulation evaluated the effectiveness of the jet fan ventilation system. The jet fan capacities used were those that satisfied the emergency requirements in the tunnel sections adjoining these stations. The analysis showed that natural ventilation would be insufficient to prevent the buildup of hot gases at the platform and mezzanine areas during a station fire and would not maintain acceptable conditions for evacuating passengers. The simulations showed that for a fire between exits or staircases, operating the jet fan system would draw in outside air through exits or stairways, thus maintaining an evacuation path free of hot gases. For a fire at either end of the station beyond the last exit or staircase, the jet fans should be operated in the same direction to generate longitudinal airflow in the direction opposite to the evacuation path. It was concluded that the jet fan system would be a viable and cost-effective alternative that would meet the established criteria for emergency ventilation in existing tunnels and stations.

D. McKinney, D. Brunner, M. Deng, and P.C. Miclea (1994 ICF Kaiser Engineers) [25] presented a study of critical velocity computation versus detailed modeling using the CFD code, FLUENT, for backlayering analysis in a typical tunnel fire scenario. The results of CFD analyses were given graphically and compared with the critical velocity calculations. The model used for their study simulated a rectangular cross-section tunnel 4 meter wide, 4.5 meters high, and 200 meters long. The model was aligned with the coordinate system axes, and grade was represented by dividing

the gravitational acceleration forces into horizontal and longitudinal components. For the model the horizontal component acted in the negative Z direction, making the slope uphill in the positive z direction. Turbulence was modeled using $k-\varepsilon$ model. Neither radiation nor heat conduction through the walls were considered in this analysis. The ambient temperature was taken at 0° Celsius. Smoke was represented as a separate, homogeneous fluid similar to air. Both smoke and air are considered incompressible. The ideal gas law was used to define the fluid properties. A molecular weight of 28 was assigned to air and 29 to smoke. The value for smoke was arbitrary. The density was computed as a function of temperature, pressure and smoke concentration. The fire was represented by injecting hot smoke, equivalent to a 14 MW fire, through an inlet in the top of the top center of the train. The train was 2.7 m, high by 2.4 m wide, for cross-sectional area of 11.52 m^2 . A blockage ratio of 0.36 was calculated for 18 m^2 tunnel. To represent a 14 MW fire with a heat of combustion of 14.5 kJ/g and a 14 to 1 air to fuel ratio, $50 \text{ m}^3/\text{sec}$ of 1210 K smoke was injected through a 50 m^2 inlet in the top the train. The results indicated that the general validity of the critical velocity concept and equation. A rather simplistic fire model injecting hot smoke through an inlet did not take into account the drafting effect of drawing cold air into the fire zone.

D. McKinney, M. Deng, and P.C. Miclea (1994 ICF Kaiser Engineers) [26] presented a continuation of the previous study comparing critical velocity and CFD results for a single-track tunnel with a higher blockage ratio than the original tunnel and for a double-track tunnel, each at two different grades. The two models used for this study each represented typical train tunnel configurations found in modern transit systems. FLUENT was used for back layering analysis in a typical transit tunnel fire scenario. The results of CFD analyses were given graphically and compared the results with the critical velocity calculations. Each of the models represented a 200 m long x 4 m high tunnel. The single-track tunnel is 4.5 m wide and the double-track tunnel is 8.5 m wide. The train in each case was represented a simple block $3 \text{ m} \times 3 \text{ m} \times 50 \text{ m}$ located midway along the length of the tunnel. The tunnels were each modeled at two different grades. The fire in each case was

modeled as a 10 MW heat source wrapped around both sides and the top of the train for a length of 15 m in the middle of the train. A user subroutine was used to add the heat as an enthalpy source, added a small amount of mass for the fuel, and converted the air to smoke at a rate consistent with amount of heat being added. A much more realistic approach was obtained than the injection of hot smoke used. For the single-track tunnel model the amount of backlayering obtained applying the annular area critical velocity was considered insignificant and no calculations were performed using the full area critical velocity. For double-track tunnel, the backlayering extended to the end of the train when using the annular area velocity and was limited to the fire zone when using the full area value.

D. Willemann and J. G. Sanchez (2002) [9] discussed some of the computational modeling techniques and analysis carried out to design a tunnel ventilation fan plant for the New York City Subway in order to improve the safety level in the system. Three levels of fires were considered: a 44 W (low intensity), which represents a low heat smoky tunnel condition, a 1.8 kW (intermediate intensity), which would be representative of an under-car train fire, and a 14.7 kW (high intensity), which would represent a fully engulfed car-train. It was emphasized that the fire model was critical in the CFD simulations. A simplified combustion process needed to be formulated identifying heat generation rates and fire products production rates. They used the SES results for providing system boundary conditions at some conditions. They used CFD analysis for the case where the velocity was lower the critical velocity. This study has shown how computer modeling techniques and analysis has helped the design of tunnel ventilation fan plants at New York City Transit.

F. Chen, S. W. Chien, H. Y. Chuay and S. C. Guo (2003) [5] investigated the effectiveness of the smoke control scheme of the Gong-Guan subway station of the Tapei Rapid Transit System. The three dimensional smoke flow fields under various fires happened in a representative subway station of Taipei Rapid Transit System were computed. CFD was employed in order to investigate the smoke flow. A computer code, named CFX4, which utilized the finite volume method, was

employed to solve the flow field. It was pointed out that a careful choice of a turbulence model was crucial in order to have a better simulation. The turbulence $k-\varepsilon$ model was able to simulate the flow in fire. The fire was simulated as a source of heat and smoke accounted for by CO_2 in which no combustion was considered. A fire having a heat release rate of 5 MW was produced 1.4×10^5 ppm/s. The boundary conditions for the flow in station are the no slip, no penetration and adiabatic for momentum, CO_2 and the temperature for the rigid walls enclosed the flow field. At the openings to the atmosphere, the atmospheric pressure instead of the detailed velocity distribution was given. Mass fraction of CO_2 and the temperature of surrounding atmosphere were specified in the portions of openings where the fresh air flowing in. The station was equipped with three mechanical systems to evacuate the smoke. They were tunnel ventilation fans located in the tunnel near the two ends of the platform floor, under platform exhaust located below the platform and smoke evacuate gate located on the ceiling of the lobby floor. It was concluded that a fire occurred at the center of the station was the most serious case for a smoke control strategy. The effects of smoke control schemes at a fire occurring at the center of the platform were compared. The tunnel ventilation fans and under platform exhaust system controlled the smoke generated by a fire occurring in the center of the station, and the smoke evacuate gate was an auxiliary equipment. It was also emphasized that for the case of a fire occurring at the two ends of the platform floor, the tunnel ventilation fans drove all the smoke into the tunnels near the fire, leaving both the platform and the lobby floors free of smoke. The effect of platform edge door on smoke control was examined. The platform edge door was a vertical wall made of a transparent material, partly or completely separating the spaces between the platform and the rails. On this transparent wall there were as many doors as on the train. The platform edge doors helped to control smoke efficiently.

N. Shahcheraghi, D. McKinney and P. Miclea (2002) [10] investigated the effect of fan start time on the performance of a subway station emergency ventilation system. The method included a time dependent fire growth within a transient computational fluid dynamics simulation of a train fire in the subway station. This study considered

four different emergency ventilation fan start times (0, 60, 180 and 420 seconds). In 960 seconds, 10 MW fire grew its full size. Summer condition was taken into consideration because the buoyancy forces temperature was warmer than the station interior temperature. Therefore, the buoyancy forces acted against the action of emergency ventilation system. Three boundary conditions were the tunnel openings, the fans and the mezzanine connections to the surface. The tunnel openings were defined as a mass flow boundary, where flow rates were determined from the SES simulation of fire. The initial tunnel boundary conditions were derived from the SES simulations. The fans were treated as constant volume flow rate boundaries and the mezzanine exit was specified as an opening to the outdoor ambient conditions. Walls were modeled as no slip boundaries with estimated roughness values of 0.25 cm. CFX-TASCFLOW version 2.11.02 was used during the simulation. The fire region was made of one train car volume, which was divided into six zones. The fire region growth was simulated by five consecutive step increased in the fire volume starting with the first zone and ending with the six zone (at which point the entire car was on fire). It was concluded that earlier start of ventilation system resulted in a better confinement of smoke and heat within the station during fire growth period.

K.C. Karki, S.V. Patankar, E. M. Rosenbluth and S.S. Levy (2000) [14] investigated the development and validation of a computational fluid dynamics model for longitudinal ventilation system using jet fans. The model included component models for turbulence, fire, radiation, smoke and jet fan. It was validated using the data from the Memorial Tunnel Fire Ventilation Test Program. The tunnel ventilation model was based on the general-purpose CFD code COMPACT-3D. It employed the buoyancy-augmented $k-\epsilon$ model to represent the turbulent transport and included component models for jet fans, ventilation ducts, fire, radiation heat transfer, and smoke. The fire was represented as a source of heat and mass. The model did not simulate the combustion process. Instead, the heat release rate due to combustion was defined as a volumetric heat source in a postulated fire region. As a result, information on the flame size and shape and the volumetric heat release rate and its distribution was necessary for the model. The heat release rate was computed from

the rate of fuel consumption, the heating value of the fuel and combustion efficiency. The model included two options for representing the radiation transport. In the radiative fraction approach, thermal radiation in the participating medium was ignored and a fixed fraction of the total heat released in the fire was assumed to be lost to the surroundings without affecting the temperature distribution within the tunnel; the remaining energy was transported away by the fluid. Experiments on diffusion flames indicate that the radiation fraction typically was in the range 0.2 to 0.4. In the detailed radiation treatment, the six-flux model was used for calculation of thermal radiation in the participating medium. The entire heat released in the fire region was introduced as source in the energy equation; the radiation model determined the amount of energy lost to the walls. Radiation fraction approach in order to decrease the computational effort and complexity was used. A separate conservation equation for smoke was solved. The rate of production of smoke was calculated from the specified rate of fuel consumption and the stoichiometric ratio of the fuel assuming complete combustion. A jet fan was represented as a constant volumetric flow rate device. A jet fan was simulated by a combination of sources and sinks. They presented specific details as follows: The diffusion coefficients for temperature and species concentration in the fan region were set to be zeros that there was no interaction between the fluid within the fan and the fluid on the outside. Mass and momentum sources were introduced in the fluid control volumes adjacent to the discharge end of the fan. The strengths of the mass and momentum sources were determined from the fluid density at the intake end of the fan, the fan capacity, and the discharge velocity. For energy equation, the total enthalpy entering the fan from the intake end was introduced as source at the discharge end. Thus, there was no energy addition within the jet fan. A similar practice was used for smoke. Mass sinks were introduced in the fluid control volumes next to the intake end of the fan. At a solid-fluid interface, the wall-function approach was use. For the momentum equations, the no-slip condition was imposed on the solid surfaces. For species concentration, the diffusion flux into the wall was zero. It was concluded that the model correctly predicted the air flow generated by a jet fan ventilation system. The simplified approach of representing the fire as a volumetric heat source and

neglecting the radiation component of the fire heat release rate was adequate for predicting the effects of fire in the far-field region of the tunnel.

M. Andersson, B. Hedskog and H. Nyman (2002) [11] investigated the single exit underground station of Zinkensdamm in Sweden in order to improve the escape situation in case of a fire on the platform. The improvements including installation of a detection system, installation of sprinkler system, establishment of fire rated constructions between platforms and escalators and pressurization of the escalator shaft were discussed. The station was an underground construction, which included three levels. They were platforms, escalator engine-room and ticket hall. The platform and ticket hall level was connected with three escalators and ticket hall was connected to the ground level through a staircase and elevator. The problem of the evacuation of the underground station Zinkensdamm was the fact that people on the station only had access to one exit. A probable smoke spread in case of a fire in a train on the platform was visualized with the help of CFD calculations. In the calculations, the program CFX 4.3 was used. In the calculations the fire was modeled using a given soot yield inserted into the cells of the volumetric heat source. The fire load was taken 4 MW. It was assumed that 9 percent of the fuel burnt was generated as effective soot particles and were spread in the calculation domain. The soot yield value of 0.09 represented the effective value of 300 m²/kg for the smoke potential of the fuel burnt. No initial flow was assumed in the station and the connecting tunnels when the fire started. The fire-induced flow was the only flow generated in the calculations. The tunnel openings ended in open spaces of calm air. The results from the calculations showed that the average temperature near the openings was calculated 70 °C, in a matter of sight (10 meter) occurred after approximately 3-4 minutes on the platform where the fire started. Simulation of the evacuation process was also performed with the help of the computer program STEPS (Simulator of Transient Evacuation and Pedestrian Movements). The large number of people and limited number of available escalators made that the results from the simulations indicated longer evacuation times than the normal situations. Nevertheless, a significant improvement could be pointed out since the evacuating people were

regarded as safe when they reached the area in front of the escalators. The results of the air flow measurement indicated the importance to stop all traffic in case of fire to avoid high air flows that affected the smoke spread to the escalator shaft. The CFD calculations and the simulations of the evacuation process indicated a significant improvement of the safety of the evacuating people.

3.1.3.2 CFD Fire Modeling Approach in This Thesis

The fire is represented as the source of heat, mass and a scalar quantity describing smoke concentration and visibility. Developing generic descriptions for the rate of heat release of fires, a “t-squared” approximation is used. The initial growth period is nearly always accelerating in real fires. A t-squared fire is one in which the burning rate varies proportionally to the square of time. The t-squared fire has been used extensively in the U.S. for the design of detection systems, and guidance on selecting values for the growth time associated with various materials available in NFPA 204M [22].

Fire is positioned at the bottom of the train. The fire is assumed to initiate under the train covering $\frac{1}{4}$ of the vehicle floor and start growing at zero second. The burning part of the train is modeled as a source of heater. The smoke is injected to the system from the floor of the burning part. The fire model used in CFD analyses is demonstrated in Figure 3.3

The smoke concentrations are reported in terms of a variable called “scalar”, so that a scalar value of 1 indicates a concentration of smoke and combustion products at the fire source. In other words, scalar value of 0.1 indicates a concentration of smoke and combustion products 10% of the value at the fire source.

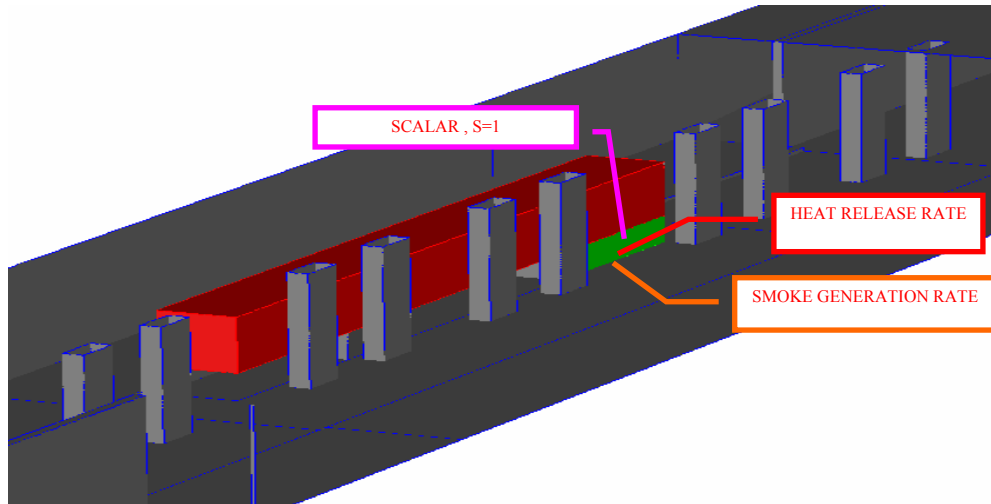


Figure 3.3 Fire modeling in the CFD analysis [1, 2]

The solution of the fundamental equations of the fluid motion using numerical techniques is obtained in CFD. The CFD analysis is performed in CFDesign7.0 in order to evaluate the fire safety during the station fire incidence. The region of interest is divided into numerous small volumes, or cells, and the equations are solved within each cell. As a result, variables (temperature, velocity and scalar) are solved within the calculation domain. Tetrahedral meshes are used in the analysis. Three dimensional transient models have been developed in which the basic equations for the conservation of mass, momentum and energy are solved at successive time steps. The duration of simulation is six minutes, selected based on the evacuation period of the passengers. These partial differential equations are solved numerically. The k - ϵ turbulence model is used in the analysis. The effect of buoyancy is included in the equations by solving the state equation. The variables of interest are as follows:

- Velocities in the three coordinates directions (U, V, W)
- Pressure (P)
- Temperature (T)
- Turbulence Kinetic Energy (k)

- Turbulence Dissipation Rate (ϵ)
- Scalar (S) (for smoke concentration and visibility)

The obtained results from CFDesign 7.0 are compared with the outputs of Fire Dynamics Simulator (FDS). The aim of this study is to understand how good CFDesign performs in a fire in a subway problem. FDS is a computational fluid dynamics model of fire-driven fluid flow. The software solves numerically a form of the Navier-Stokes equations appropriate for low-speed, thermally-driven flow with an emphasis on smoke and heat transport from fires. Smokeview is a visualization program that is used to display the results of the FDS simulation. FDS has been aimed at solving practical fire problems in fire protection engineering, while at the same time providing a tool to study fundamental fire dynamics and combustion. Additional information can be found in Appendix-B and FDS 4 Technical Manual [30]. FDS uses a mixture fraction combustion model. The mixture fraction is a conserved scalar quantity that is defined as the fraction of gas at a given point in the flow field that originated as fuel. The model assumes that combustion is mixing-controlled, and that the reaction of fuel and oxygen is infinitely fast. The mass fractions of all of the major reactants and products can be derived from the mixture fraction.

CHAPTER 4

CFDESIGN 7.0

4.1 Introduction

Here CFdesign 7.0 is utilized in the simulation of a fire incidence in the stations of an underground transportation system. This software can be used in order to test pumps, fans, blowers, compressors, turbomachinery, valves, pistons, hydraulic rams, and many other applications across all industries. CFdesign solves the mathematical equations which represent heat and momentum transfer in a moving fluid. The finite element method is used to discretize the flow domain, thereby transforming the governing partial differential equations into a set of algebraic equations whose solution represent an approximation to the exact (and most often unattainable) analytical solution. The numerical formulation is derived from the Simpler solution scheme [29]. Solution procedure of the software is shown in Figure 4.1.

Results are displayed at every step of the calculation using cutting planes, iso-surfaces, x-y plots, and particle traces. CFdesign has an ability of showing results from multiple analyses, to be viewed, compared, and contrasted. The interaction between a solid body in motion and the surrounding fluid is a key aspect to the design of many mechanical devices. It is capable of solving the problem where the interaction between a solid in motion and the surrounding fluid is important. The flow analysis is often just the beginning in many analysis-design projects. Results

from CFdesign can be applied as structural boundary conditions for subsequent analysis with many popular finite element analysis packages. Aerodynamic and hydrodynamic induced pressures as well as temperatures can be interpolated directly onto the finite element analysis mesh.

4.2. Physical Boundaries

Different kinds of physical boundaries are assigned in the CFdesign interface:

Inlets: Inlets are most often defined with either non-zero velocity components or a gage static pressure, etc. An inlet can be a fan. The inlet flow rate will vary with the pressure drop through the device. Volumetric flow rate can be assigned as an inlet condition. Total Pressure can be used at the inlet of supersonic flow models if that is the only quantity known. For heat transfer analyses, the temperature at all inlets has to be specified.

Outlets: The recommended outlet condition is a gage static pressure with a value of zero. If this condition is used at an outlet, then no other conditions should be applied to that outlet. If the outlet velocity or volumetric flow rate is known, then either of these conditions can be applied to the outlet. If this is done, then a pressure must be specified at the inlet.

Slip/Symmetry Walls: This condition allows fluid to flow along a wall. The fluid is prevented from flowing through the wall. However, this boundary condition can be used with a very low viscosity to simulate Euler or inviscid flow. Slip walls are also useful for defining a symmetry plane. The symmetry region does not have to be parallel to a coordinate axis. For axisymmetric analyses, the symmetry condition along the axis is automatically set, and does not need to be applied manually.

Unknown Inlet/Outlet: This is a “natural” condition meaning that boundary is open, but no other constraints are applied. This is most used for supersonic outlets where the outlet pressure or velocity is not known, and applying either condition would result in shock waves or expansion waves at the outlet.

Walls : AutoWall sets wall conditions automatically on all surfaces that are not defined as inlets, outlets, symmetry, slip, or unknown. It is not necessary to set a zero velocity (no-flow) condition at any fluid/solid interface. Wall turbulence conditions are set automatically. Walls with no specified thermal boundary conditions will be considered perfectly insulated for heat transfer calculations,

Periodic Boundaries: Periodic boundary conditions (cyclic symmetry) enable users to model a single passage of an axial or centrifugal turbomachine or of a non-rotating device with repeating features (passages). Periodic boundaries are always applied in pairs; the two members of a periodic pair have identical flow distributions.

Joule Heating Conditions: Joule heating is the generation of heat by passing an electric current through a metal.

Heat Transfer Boundary Types: A temperature condition constrains the applied region to that temperature throughout the entire analysis. It can also constrain the temperature of incoming flow. Heat flux is a surface condition that imposes a given amount of heat directly to the applied surface. Film coefficient (convection) is another surface condition that uses an applied convection coefficient and a surrounding temperature. This is most often used to simulate a cooling effect. Surface radiation is a surface condition that applies heat to a surface by use of a specified emissivity and a surrounding temperature. This is sort of a “radiation film coefficient” in that it exposes a surface to a given heat load using a source temperature and a surface condition. Heat generation is a volume condition that applies an amount of heat to a geometric volume

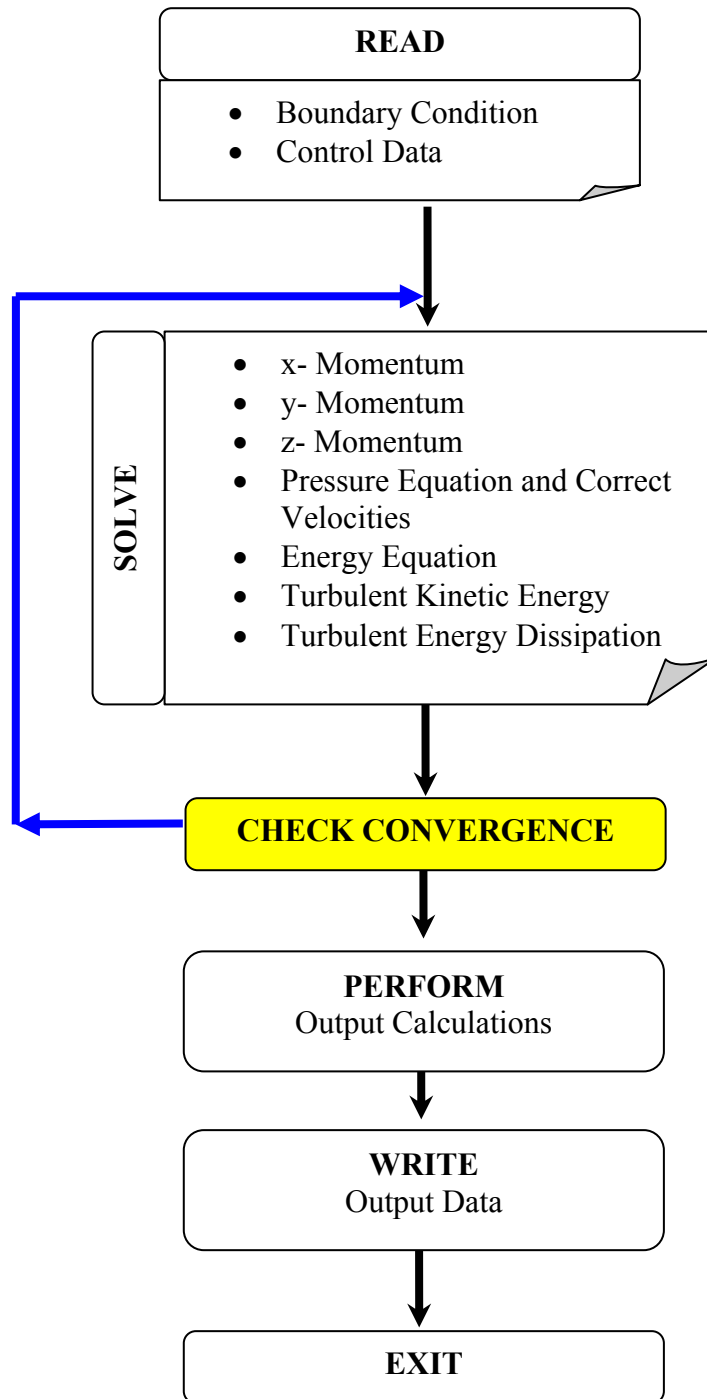


Figure 4.1 CFDesign solution procedure [29]

4.2.1 Surface Boundary Condition Details

Velocity : Velocity components are applied to an inlet (or outlet) surface.

Rotational Velocity : This condition applies a rotating velocity to a wall. It is applied by specifying a point on the axis of rotation, the direction of the axis of rotation, and the rotational velocity. This condition is used for simulating a rotating object in a surrounding flow.

Volume Flow Rate : A volume flow rate is applied to an inlet (or an outlet, if the applied direction is out of the model). This condition can only be applied planar entities.

Pressure : It can be defined as Gage (relative pressure) and Absolute (the sum of the gage and the reference pressure). Also it can be select either Static or Total. The recommended pressure condition for most analyses is Gage, Static.

Temperature : It can be defined in two different ways; either Static or Total. Static is the recommended temperature for most analyses. Total temperature should only be used as an inlet for compressible analyses with heat transfer.

Slip/Symmetry : There is no value associated with the slip condition.

Scalar : This is a unitless quantity ranging between 0 and 1 that represents the concentration of the tracking (scalar) quantity.

Humidity : This is a unitless quantity ranging between 0 and 1 that represents relative humidity (1 corresponds to a humidity level of 100%).

Steam Quality : This is a unitless quantity ranging between 0 and 1 that represents the steam quality (1 corresponds to a quality of 100% pure steam).

Heat Flux : This boundary condition can be applied to outer walls, to solid-solid interfaces, and to fluid-solid interfaces.

Total Heat Flux : This is a heat flux condition that is applied directly without having to divide by the surface area. This is very important because it allows to make parametric changes that might change the area, and not have to worry about recalculating the heat flux boundary condition.

Film Coefficient : Select the desired units, and enter a film coefficient (convection coefficient). Also, enter the reference temperature in the desired units.

Radiation : This condition simulates a radiative heat transfer between the selected surface(s) and some source outside of the model. The surface emissivity and the background temperature are the necessary inputs.

External Fan : The points of the known fan curve are entered. In order to model a fan that pulls flow, enter all flow rate and pressure values as negative.

Current : Used only to define a Joule heating analysis, apply the current to one end of the solid through which Joule heating is occurring. The current condition to apply is a total current, not a current density.

Voltage : Another condition used only for a Joule heating analysis. Apply a voltage to the other end of the heated solid. Alternatively, a voltage difference can be applied to the solid: a higher voltage on one side and a lower voltage on the other. In this case, omit the applied current condition.

Periodic : Periodic boundary conditions (cyclic symmetry) enable users to model a single passage of an axial or centrifugal turbomachine or of a non-rotating device with repeating features (passages). Periodic boundaries are always applied in pairs; the two members of a periodic pair have identical flow distributions. The two members of a periodic pair must be geometrically similar.

4.2.2 Volume Boundary Condition Details

Volumetric Heat Generation: This is a volume-based boundary condition. The applied condition is the amount of heat divided by the volume of the part.

Total Heat Generation: This is a volume-based boundary condition. The applied condition is the amount of heat on the part, and is not divided by the volume.

Temperature Dependent Heat Generation: This allows the heat generation to vary with temperature. Physically, such a condition allows for the simulation of a heating device that shuts off (or greatly de-powers) once a target temperature is reached. Temperature-dependent heat generation is available for both volumetric and total heat generation boundary conditions. It also allows for the simulation of industrial processes that operate within a narrow temperature band, and will adjust the heat input to maintain the target temperature.

4.2.3 Transient Conditions

To make a boundary condition that varies with time.

4.3 Installed Database Materials

Several variations of air and water are included with the software. These materials cannot be edited.

Table 4.1 List of materials in CFdesign 7.0 database [29]

Material	Descriptions
Air or Water Constant	The properties do not change.
Air -Water Buoyancy	Density changes with temperature. A buoyancy property should be selected when solving for natural convection.
Air-Water Not Standard	It should be used when temperature and/or pressure are far from standard conditions.
Air Moist	Useful for humidity (moist air) calculations. These properties are only for the gas.
H ₂ O Steam / Liquid	Useful for analyses of steam/water mixtures. Change the reference pressure if your operating conditions are at a different pressure.
Steam Buoyancy	Sets the properties of steam, but only allows density to vary with equation of state, not the steam tables. No other properties vary.
Steam Constant	Sets the properties of steam, but does not allow for any property variation. This is useful if the temperature and pressure variations are small.

4.3.1 Fluid Properties

The Material Editor is used to create materials different from those supplied with the software. There are six basic properties that are needed to define a fluid. Most of these properties can be made to vary with temperature, pressure or scalar, in several different ways. The following Table 4.2 lists the six properties and the available variational methods.

Table 4.2 List of properties and variational method [29]

Property	Variational Methods
Density	Constant, Equation of State, Polynomial, Inverse Polynomial, Arrhenius, Steam Table, Piecewise Linear, and Moist Gas
Viscosity	Constant, Sutherland, Power Law, Polynomial, Inverse Polynomial, Non-Newtonian Power Law, Hershel-Buckley, Carreau, Arrhenius, Piecewise Linear, and Steam Table, First Order Polynomial, Second Order Polynomial
Conductivity	Constant, Sutherland, Power Law, Polynomial, Inverse Polynomial, Arrhenius, Steam Table, Piecewise Linear
Specific Heat	Constant, Polynomial, Inverse Polynomial, Arrhenius, Steam Table, Piecewise Linear
C_p/C_v (gamma)	Constant
Emissivity	Constant, Piece-wise Linear variation with temperature

Several solid materials are included with the software. As mentioned, these materials cannot be edited, but each can be selected from the data base when creating a similar new material. Aluminum, copper, glass, steel etc. are some of the materials in the database.

4.4. Turbulence

The turbulence dialog is used to toggle turbulence on and off, to select the turbulence model and to modify the default values for the turbulence model parameters. If Laminar is selected, then the flow will be solved as laminar. If turbulent is selected (the default) then the analysis will be solved as turbulent. Most engineering flows are turbulent. Three turbulence models are available:

- The *constant eddy viscosity model* is slightly less rigorous than the other two models except for electronic cooling analyses, but more numerically stable. This is a good choice for lower speed turbulent flows and some buoyancy flows. This is also useful if one of the other two models caused divergence.
- *K-Epsilon*, the default turbulence model, is typically more accurate than the constant eddy viscosity, but more computational intensive and slightly less robust. It is not as resource intensive as the RNG model, but still gives good results.
- The *RNG turbulence model* is more computational intensive, but sometimes slightly more accurate than the k-epsilon model, particularly for separated flows. This model works best for predicting the reattachment point for separated flows, particularly for flow over a backward-facing step. When using the RNG model, it is often recommended to start with the k-epsilon model and after this model is fairly well converged, enable the RNG model.

4.5. Scalars

The scalars dialog controls the calculation of the scalar quantity. The transport of a general scalar variable will be modeled when general scalar option is selected. This scalar might be the salinity in a seawater fluid flow analysis, a mixture fraction in a multispecies analyses, smoke concentration in fire or some marker.

CHAPTER 5

CASE STUDIES

5.1 Introduction

Krakow Fast Tram consists of two stations and connecting tunnels. KCK station, one of the stations in Krakow Fast Tram, has a platform length of 55.5 m, a width of 14.8 m and a height of 4.75 m. The other station in Krakow Fast Tram is Polytechnika Station with a platform length of 55 m, a width of 21.25 m and height of 6.5 m. Three dimensional station geometries are drawn by using AutoDesk Mechanical Desktop 6.0 A fire load of 7.5 MW is assumed for the train fire in the analysis. The fire growth is represented as αt^2 . This fire representation is the most commonly used model in fire safety engineering. The fire growth factor (α) is taken as 47 W/s^2 which corresponds to the fast fire in NFPA 204M [22]. The fire is assumed to initiate under the tram covering $\frac{1}{4}$ of the vehicle floor and start growing at zeroth second. The heat release rate and smoke generation rate versus time is shown in the Figure 5.1 and Figure 5.2, respectively. In the analyses, it is assumed that all energy is transported by convection in order to reduce the computation time.

The station fire incidences are investigated for both of the stations. The CFD analysis is performed in CFDDesign7.0 in order to evaluate the fire safety during the station fire incidence. The CFD fire modeling approach is described in detail in Chapter 4. One of the case studies is compared with a code well known in the discipline, the Fire Dynamics Simulator, specifically developed for fire simulation.

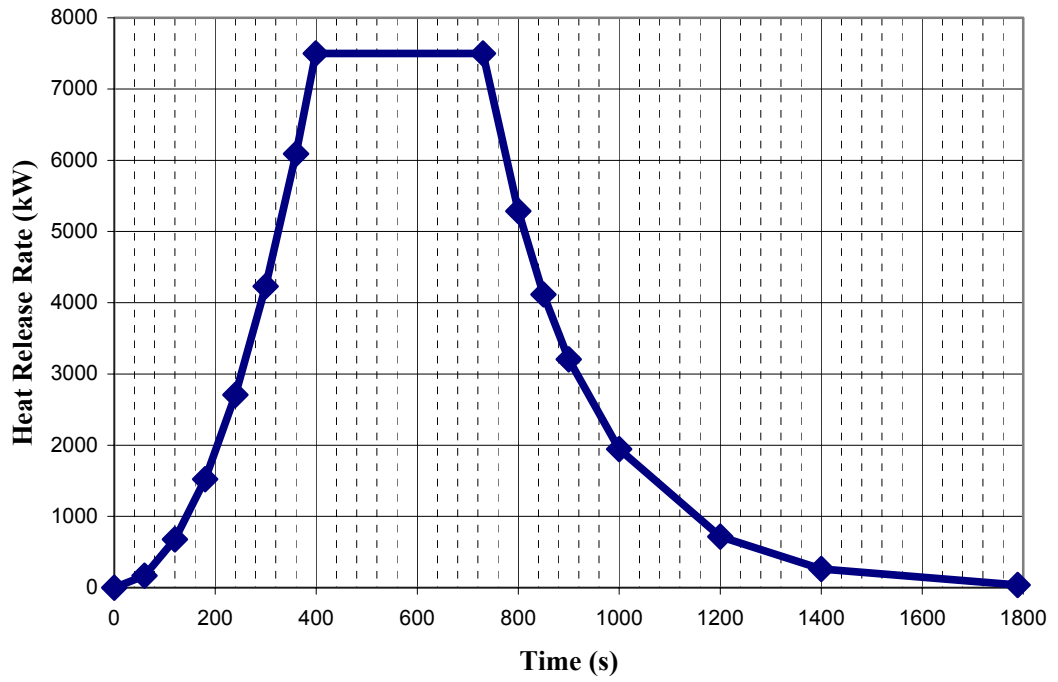


Figure 5.1 Heat release rate versus time [2, 3]

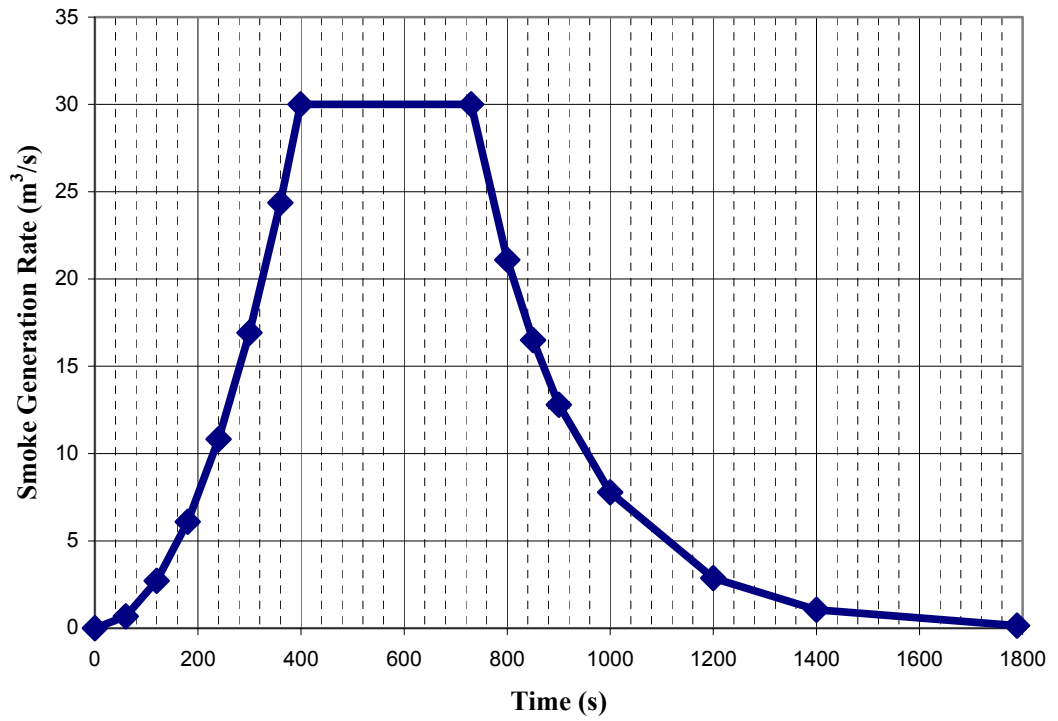


Figure 5.2 Smoke generation rate versus time [2, 3]

5.2 Case Study-1 KCK Station Fire

KCK station, one of the stations in Krakow Fast Tram, has a platform length of 55.5m, a width of 14.8 m and a height of 4.75 m. Four emergency ventilation fans having the same capacity ($80 \text{ m}^3/\text{s}$) are located on two sides of KCK station. Required fan capacities are calculated according to tunnel fire simulations in Subway Environmental Simulation (SES) program [28]. The fans have the ability to work in two modes of operation (supply or exhaust). The three dimensional representation of the station is shown in Figure5.3. The platforms and public areas of the concourse level of KCK station are represented up to the normal street exits. There are ten stairs to evacuate the passengers.

The emergency ventilation air is extracted via fans through the shafts over the running tunnels. Initially a steady state analyses are performed. Three different emergency ventilation scenarios are investigated. Firstly, all of the fans in the station operate in exhaust mode. Secondly, two fans near the fire location operate in exhaust as the other two fans do not work. Lastly, two fans near the fire source are in exhaust mode, whereas the other two operate in the supply mode. As a result of these studies, the most feasible scenario is found to be the second one, where the operation of two fans (those closer to the fire) is in exhaust mode. This results in the flow of fresh air on all four escape routes. In this mode smoky region gets smaller and it is impelled towards the operating fans. This is taken as the safe mode of fan operation. The results of this study are given in Appendix A.

Two unsteady fire scenarios are investigated in the analysis. In the first scenario, fire is located at the south end of the vehicle. The fans at the south side of the station work in exhaust mode. Figure 5.4 shows the ventilation scenario in the first case. They start operating 30 s after the initiation of the fire and reach the steady-state after 150 s. The simulation continues for 360 s (6 min) up to the fully developed state of fire sufficient for the evacuation of passengers from the platform level.

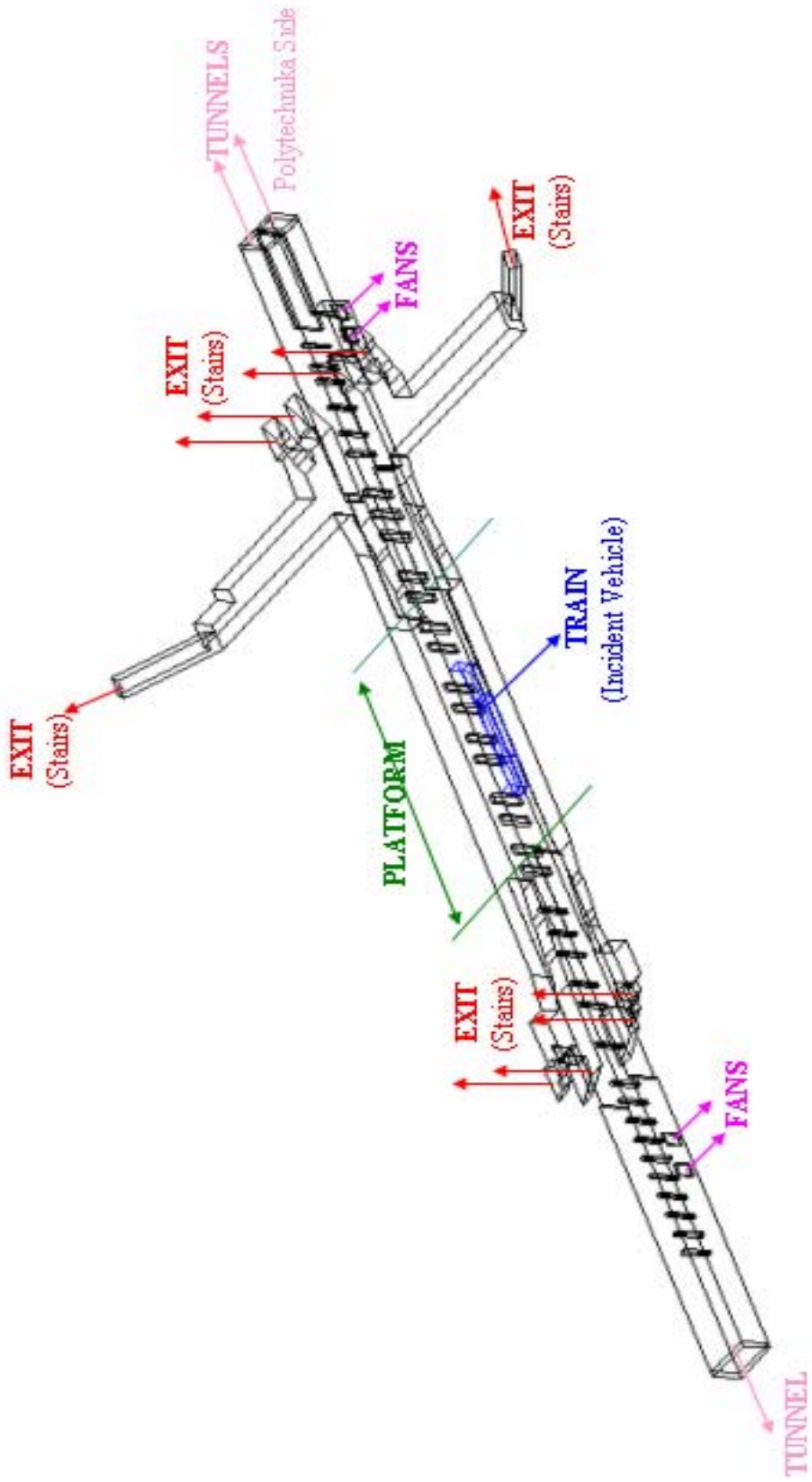


Figure 5.3 3-D representation of KCK Station in Krakow Fast Tram

In the second scenario, the fire is located at the north end of the vehicle. Here, the fans at the north side of the station work in exhaust mode. Figure 5.4 shows the ventilation scenario of the second case where the fan operation is similar to that in the first scenario (Figure 5.5). The number of computational elements in the simulation is 900 000 in KCK Station Fire. Each one is performed in four days.

Tunnel: Tunnels are represented using zero gage pressure boundaries, these boundaries have been enhanced with loss terms based on tunnel section length and tunnel friction factors. The temperature of the tunnels assumed to be the ambient temperature (20 °C).

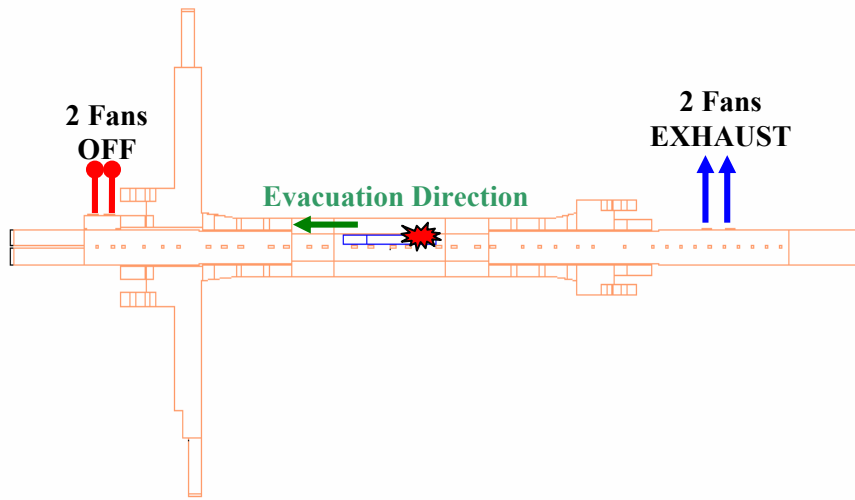
Train: The non-burning sections of the train are represented as solid regions within the model. The train is assumed to be mainly made of aluminum.

Fire: Fire is represented as a source of heat and smoke represented by the “scalar quantity”. Developing generic descriptions for the rate of heat release of fires, a “t-squared” approximation is used. The initial growth period is nearly always accelerating in real fires. A t-squared fire is one in which the burning rate varies proportionally to the square of time. Fire is positioned at the bottom of the train. The fire is assumed to initiate under the train covering $\frac{1}{4}$ of the vehicle floor.

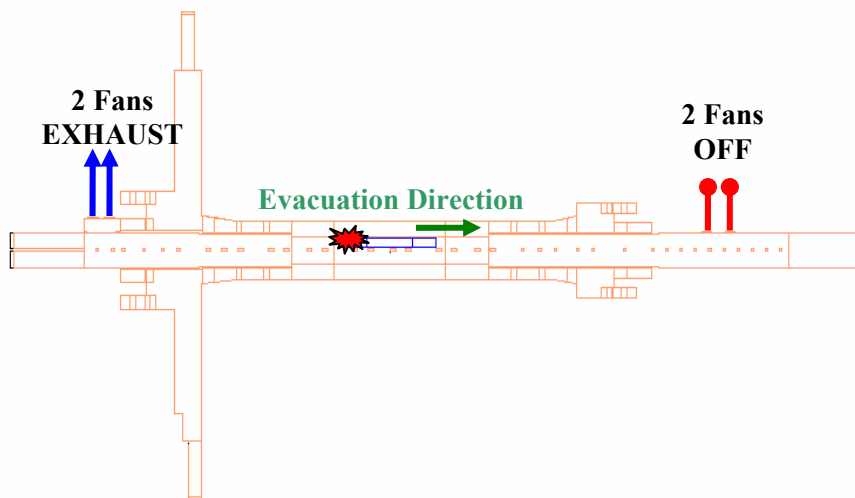
Wall: The no-slip boundary condition is applied to the walls.

Fans: Volumetric flow rate boundary condition is applied to the fan tunnel entrances. After 30 s, the fans start to operate and reach steady-state in a duration of two minutes.

Stairs: The exits (stairs) from the concourse level are represented using constant pressure boundaries (zero gage). The temperature of the exits is assumed to be at the ambient temperature of 20 °C.



SCENARIO-1



SCENARIO-2

Figure 5.4 Schematic drawing of fire and ventilation scenarios in KCK Station

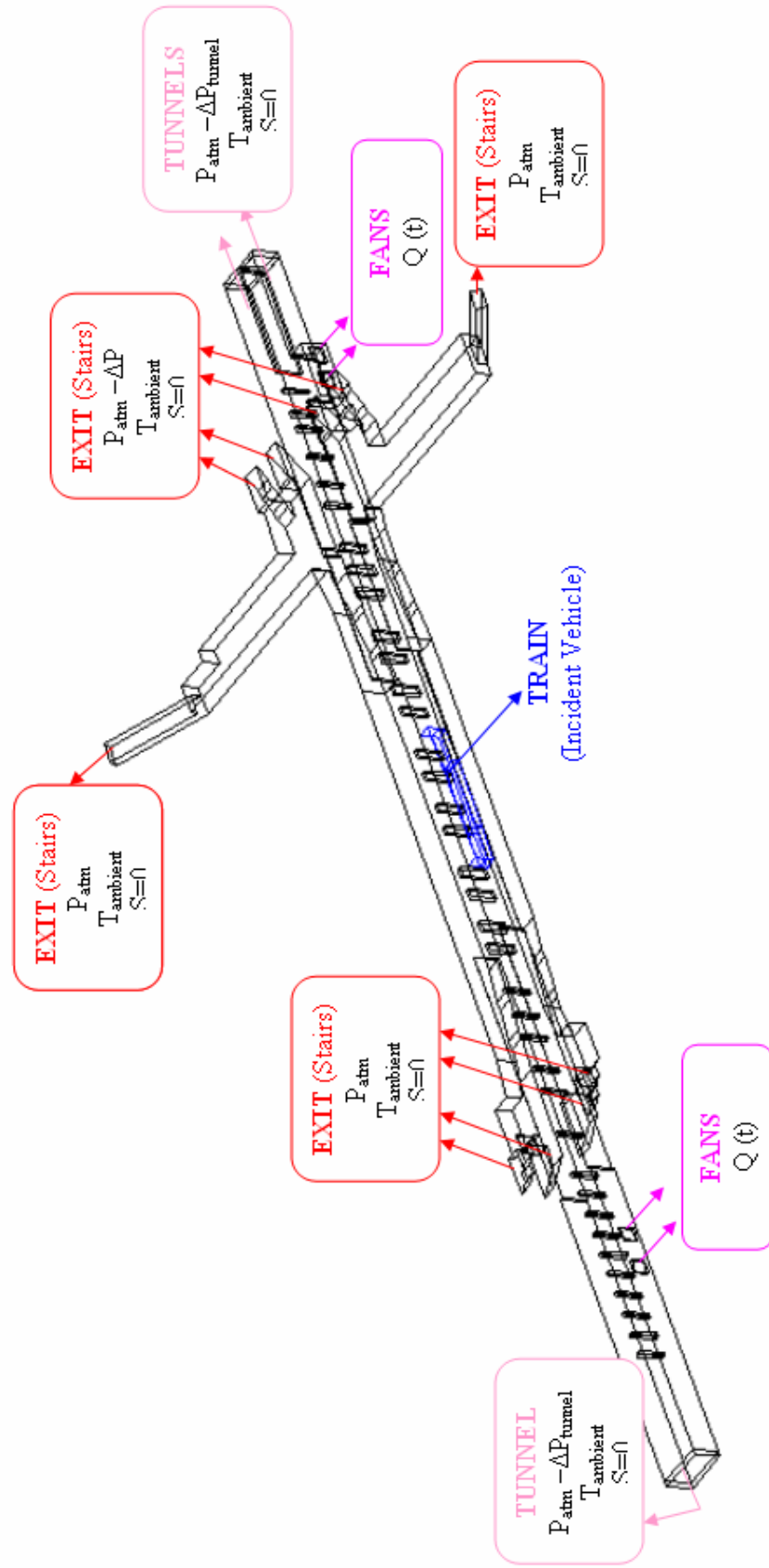


Figure 5.5 Boundary conditions applied in the CFD analysis for KCK Station

For both scenarios CFD simulation results are given in contour plots of temperature, velocity and scalar variable. Contour plots are given for sections 1, 2 and 3 which are shown in Figure 5.6 and Figure 5.7. Section 1 corresponds to a horizontal plane 2.5 m above floor level. Section 2 in Scenario 1, corresponds to the vertical plane which passes through the fire axis and Section 3 in Scenario 2, corresponds to the vertical plane which passes through the fire axis.

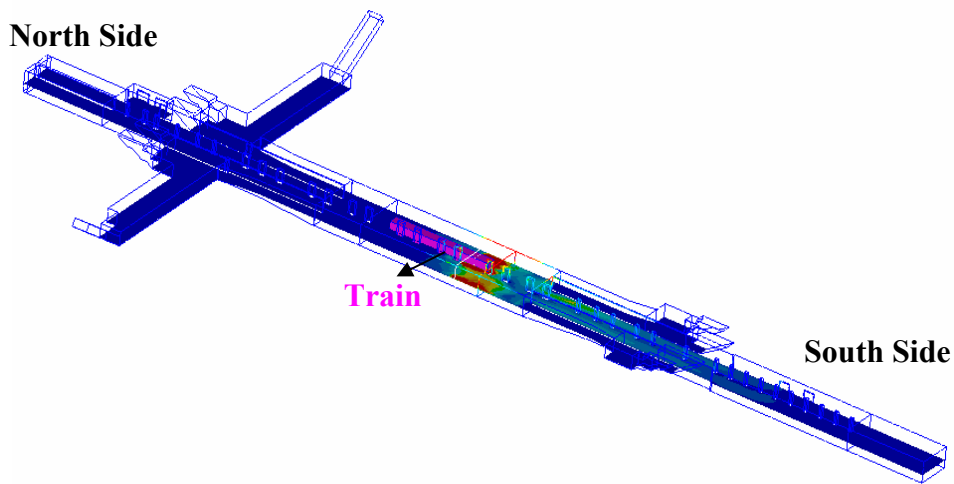


Figure 5.6 Section 1 (Horizontal plane 2.5 m above floor level)

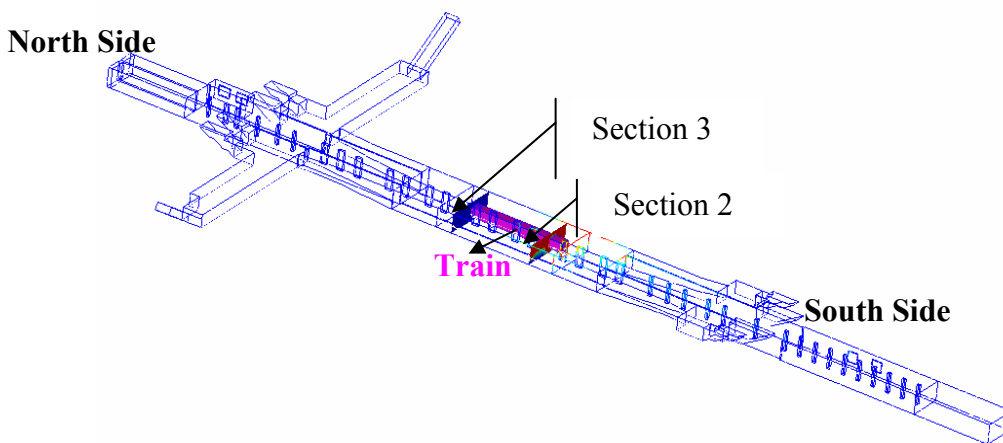


Figure 5.7 Section 2 and Section 3 (Vertical planes passing through fire axis)

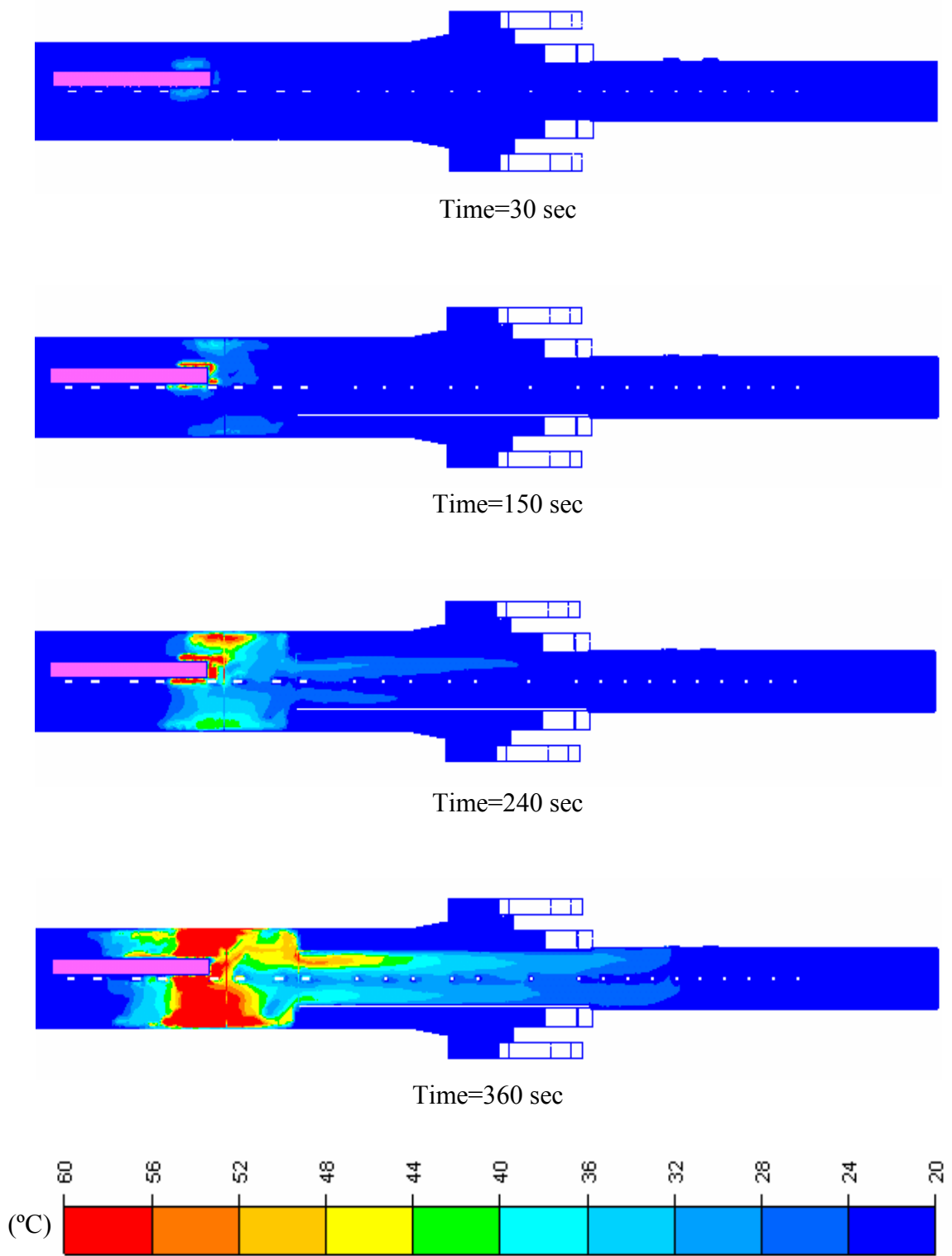
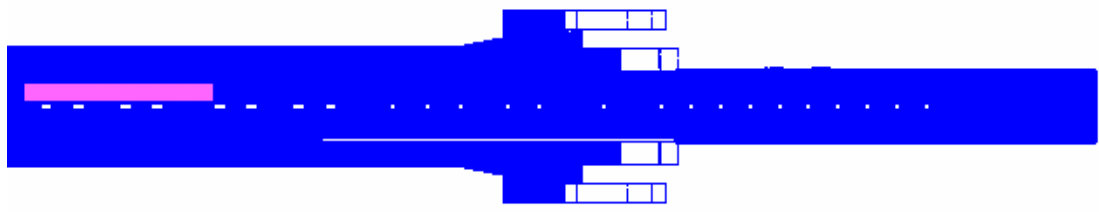
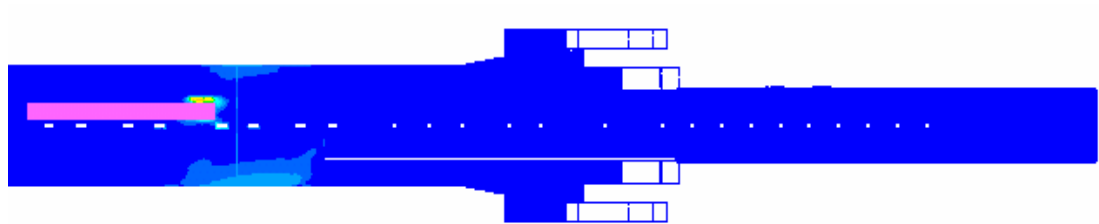


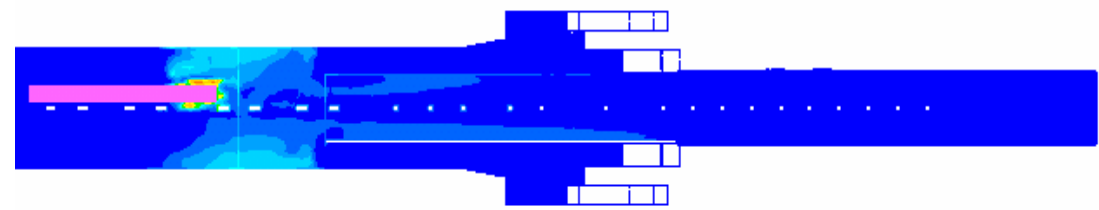
Figure 5.8 Temperature distribution at Section-1 (KCK Scenario-1)



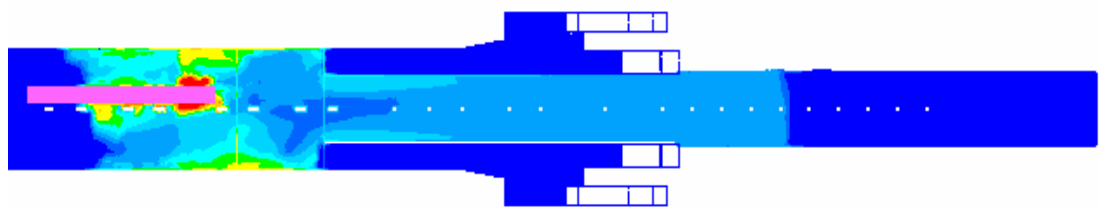
Time=30 sec



Time=150 sec



Time=240 sec



Time=360 sec



Figure 5.9 Scalar distribution at Section-1 (KCK Scenario-1)

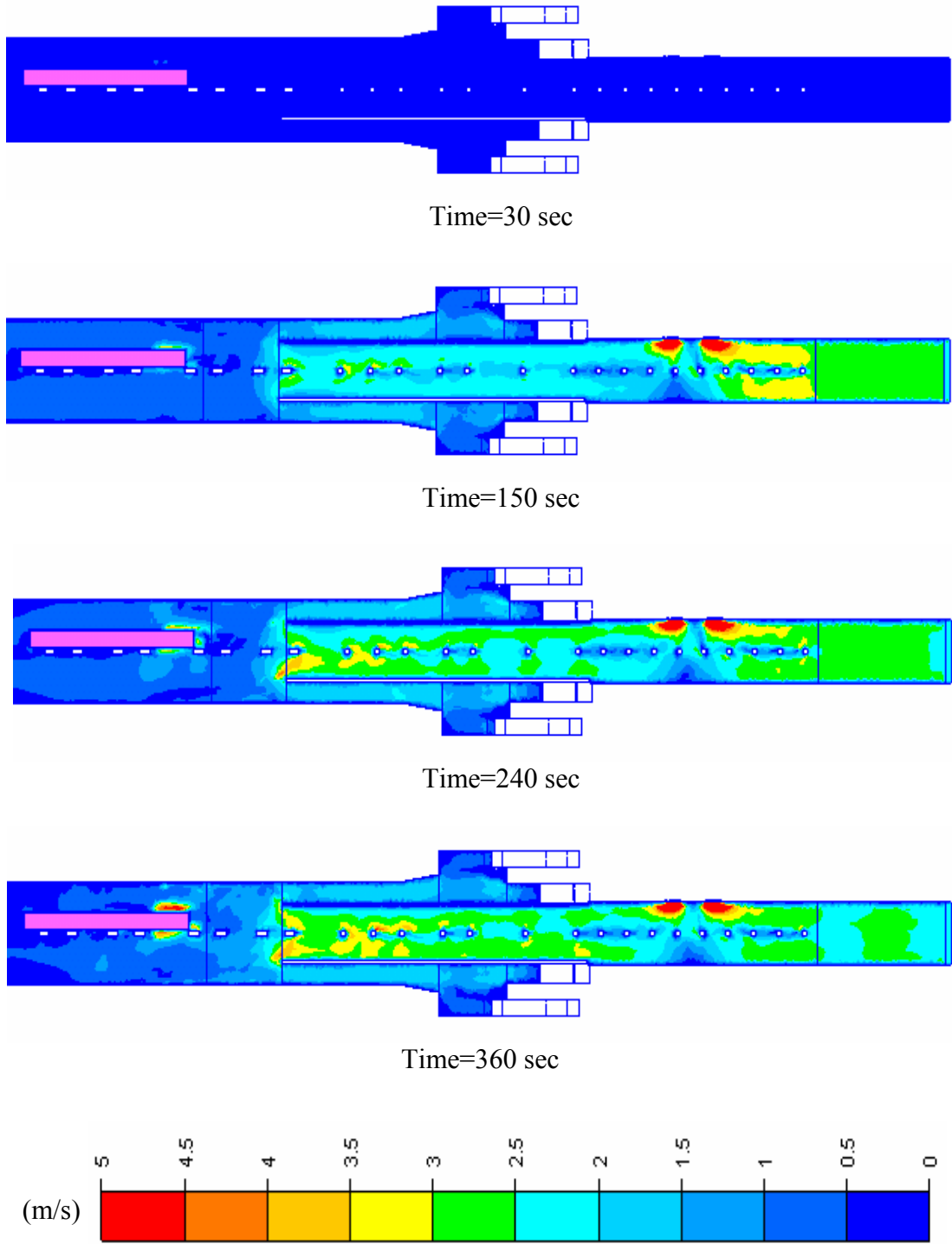


Figure 5.10 Velocity distribution at Section-1 (KCK Scenario-1)

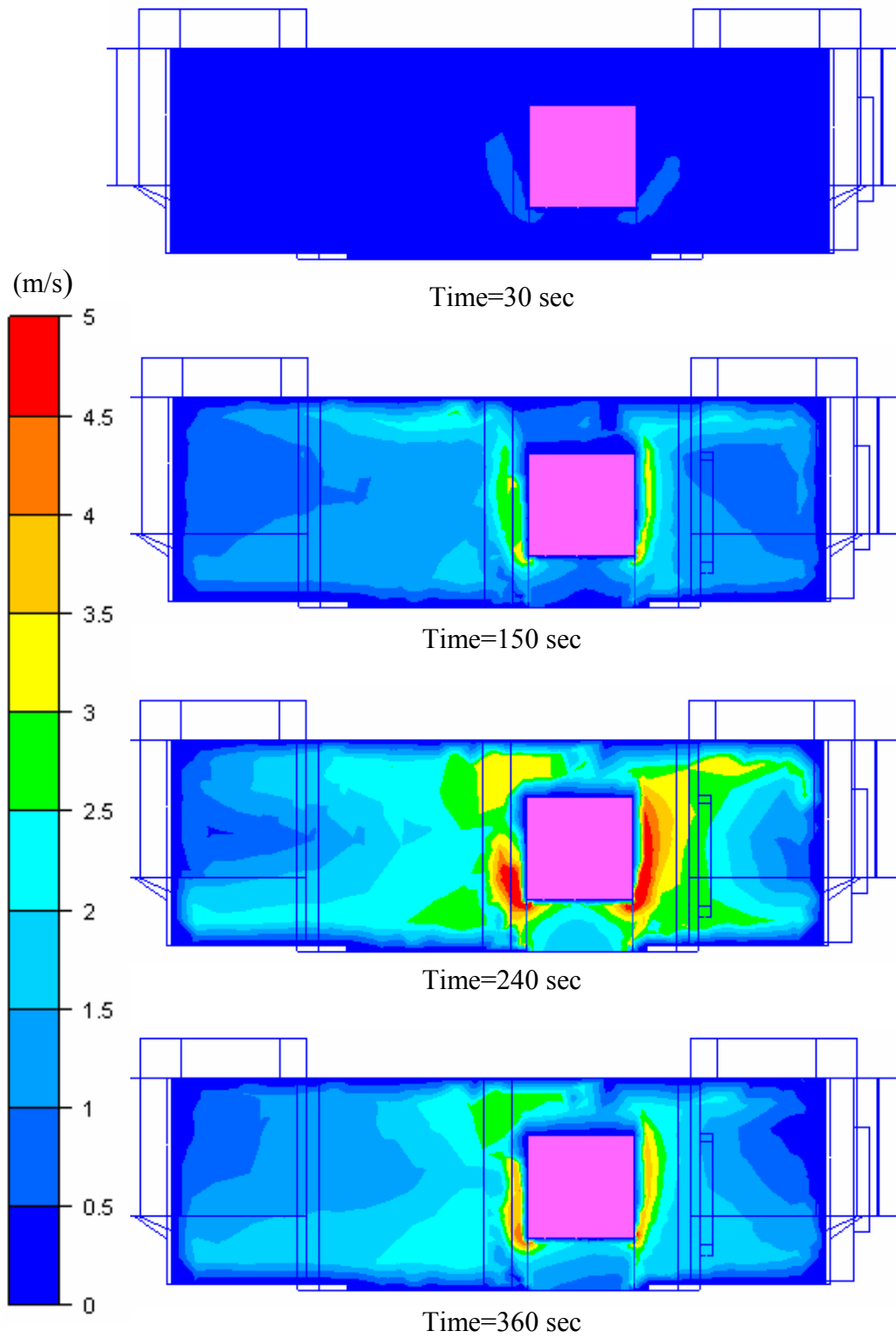


Figure 5.11 Velocity distribution at fire axis (KCK Scenario-1)

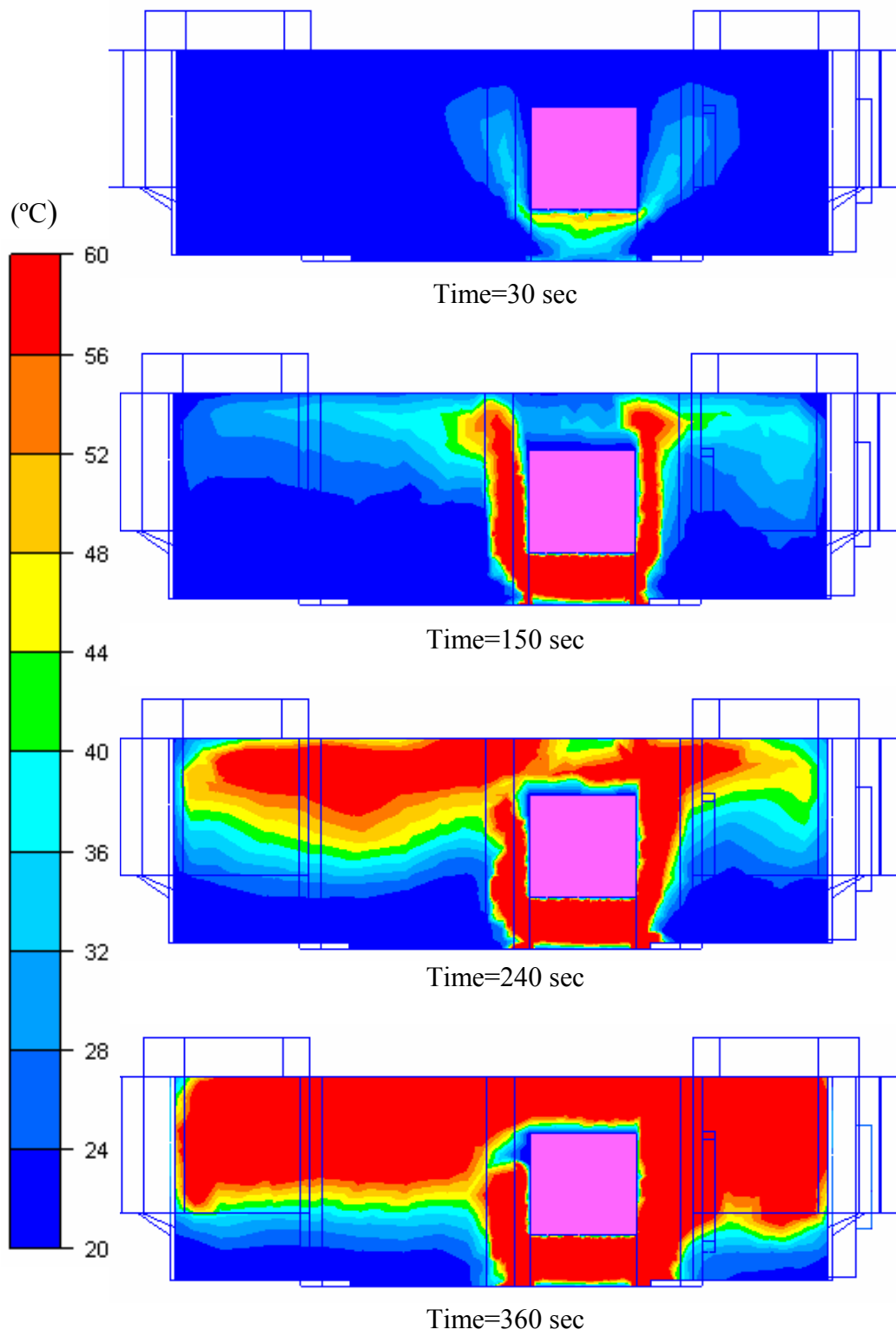


Figure 5.12 Temperature distribution at fire axis (KCK Scenario-1)

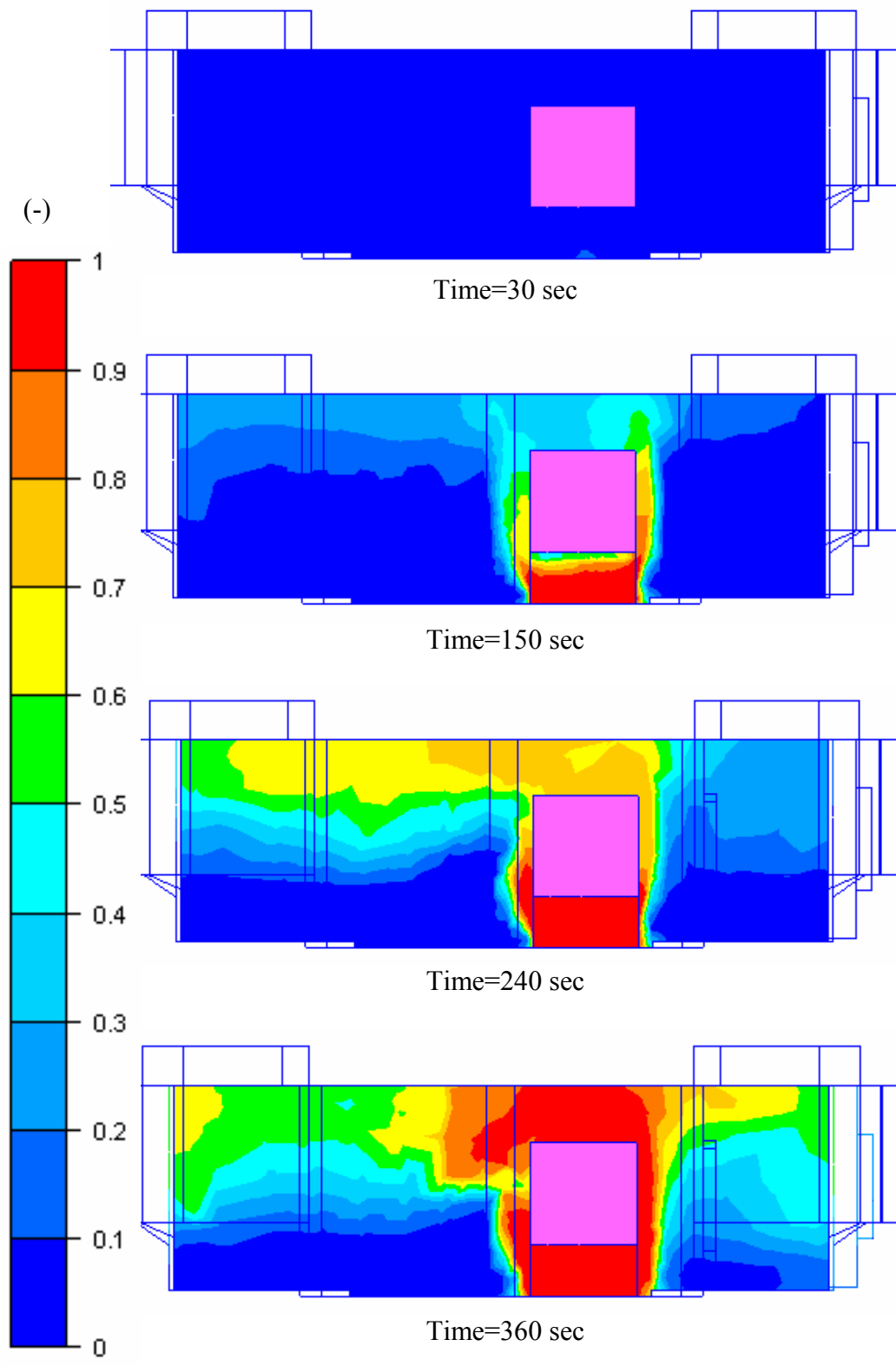


Figure 5.13 Scalar (S) distribution at fire axis (KCK Scenario-1)

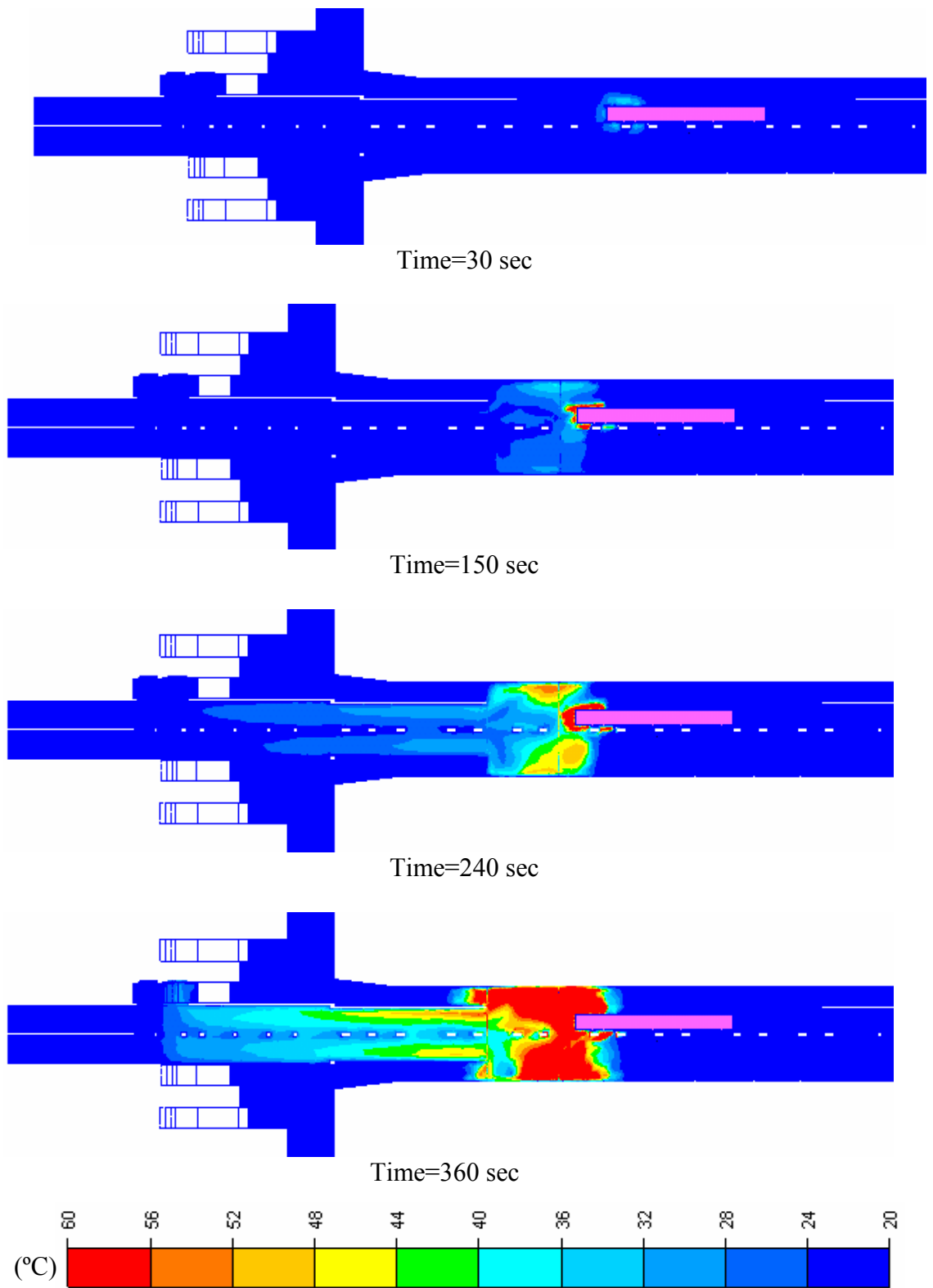


Figure 5.14 Temperature distribution at Section-1 (KCK Scenario-2)

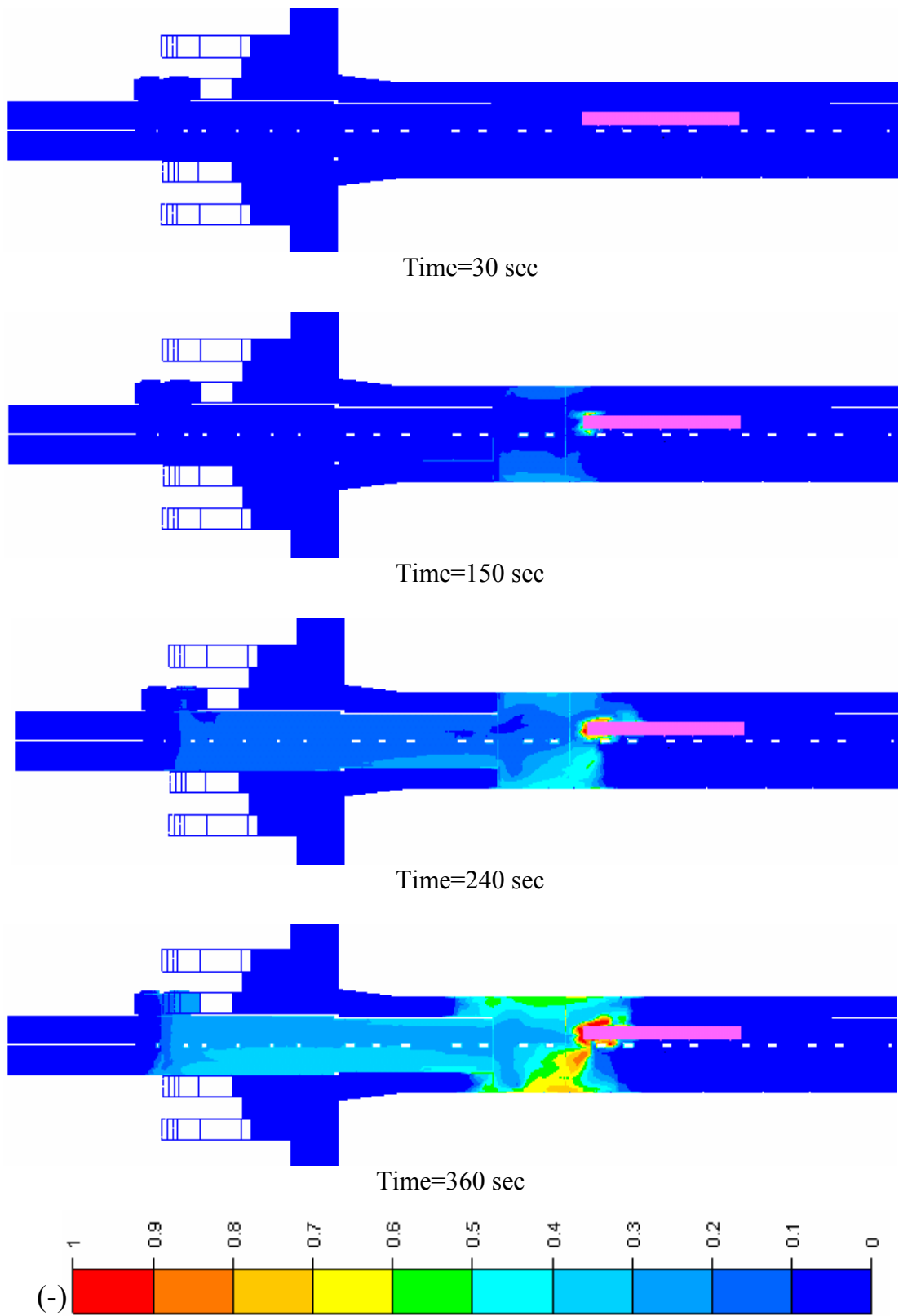


Figure 5.15 Scalar distribution at Section-1 (KCK Scenario-2)

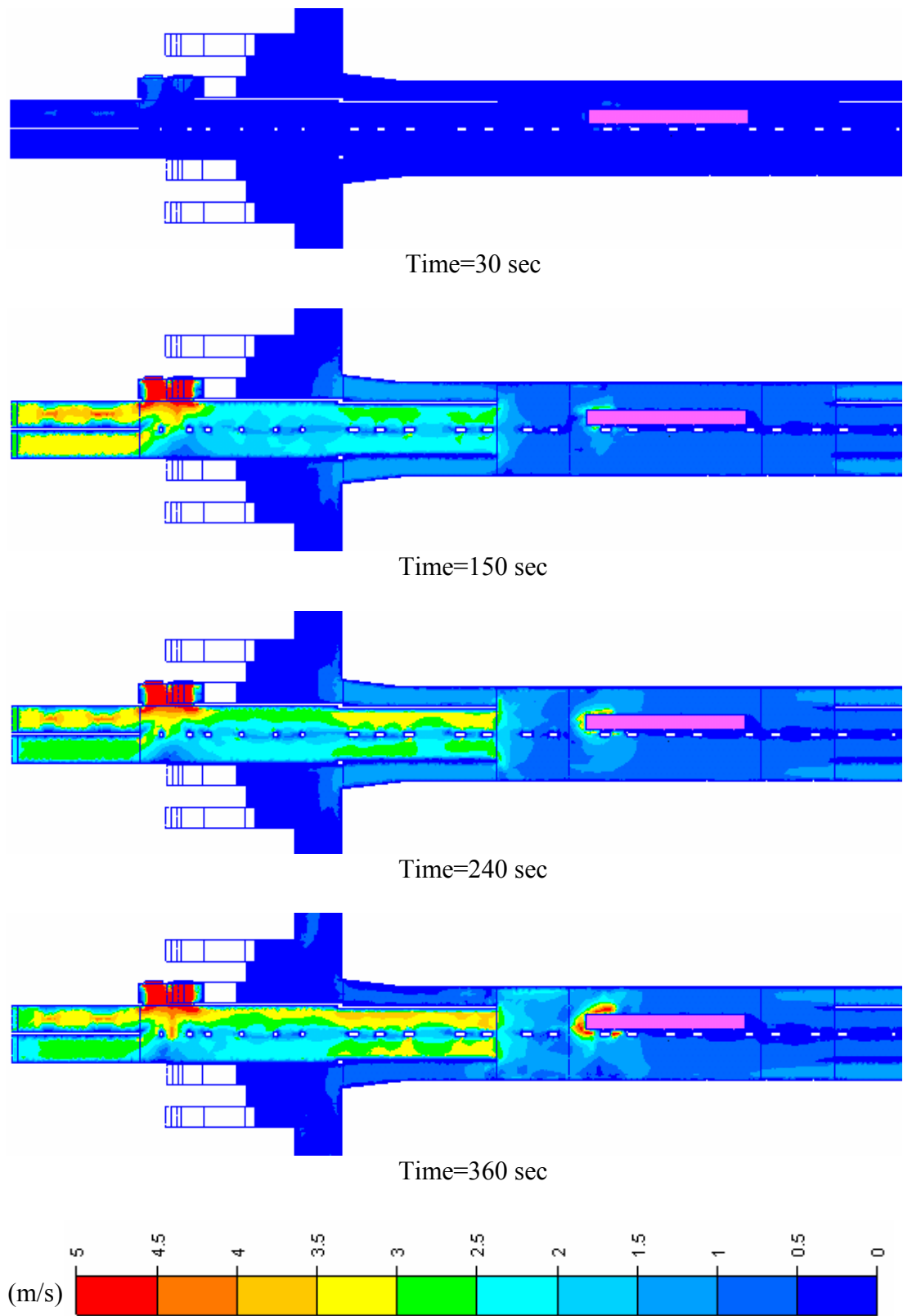


Figure 5.16 Velocity distribution at Section-1 (KCK Scenario-2)

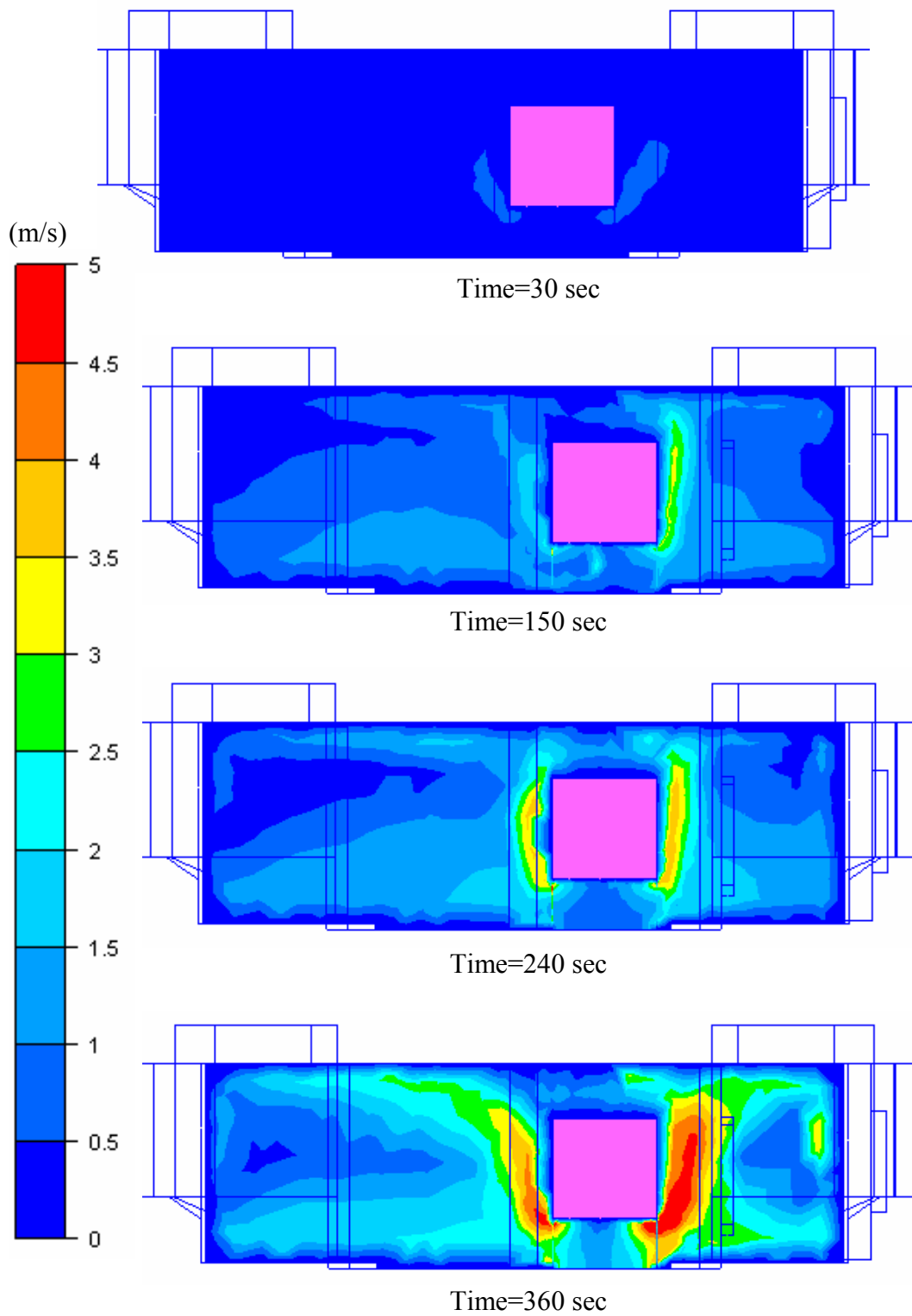


Figure 5.17 Velocity distribution at fire axis (KCK Scenario-2)

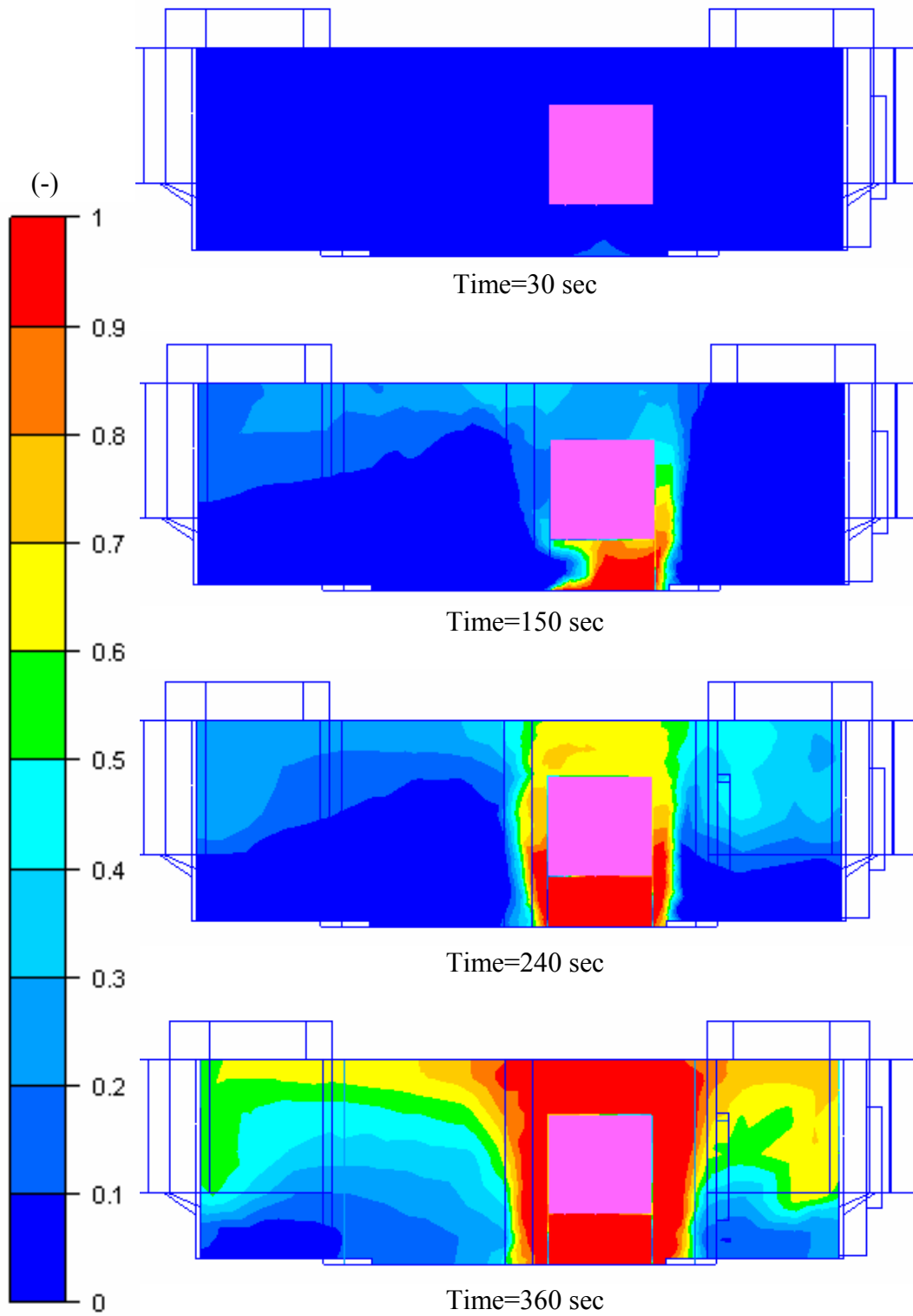


Figure 5.18 Scalar distribution at fire axis (KCK Scenario-2)

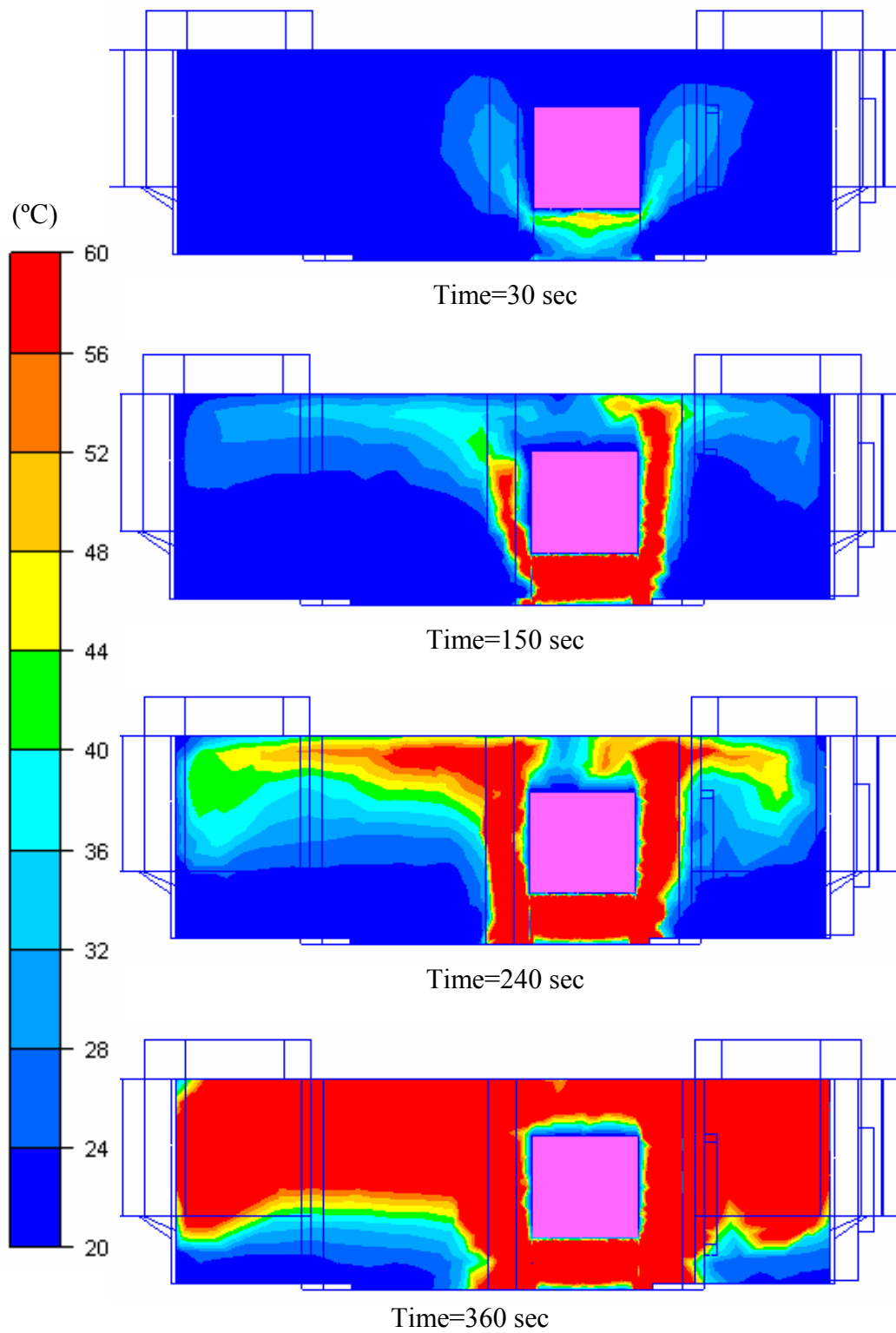


Figure 5.19 Temperature distribution at fire axis (KCK Scenario-2)

5.2.1 Results of KCK Station Train Fire

5.2.1.1 Scenario 1

Scenario 1 considers the fire at the south end of the train. In this case emergency ventilation fans at the south side of the station are switched on 30 seconds after the fire initiation. The main results of this scenario are presented graphically in Figures 5.8 to 5.13. The development of the fire and subsequent smoke movement is summarized in the following commentary.

Table 5.1 Commentary on Scenario 1 in KCK Station

Elapsed Time Fire Load:	Commentary
Time 30 sec (0.5 min) 42 kW	Smoke from the comparatively small fire has very low and localized effects near the fire source. The emergency ventilation fans are just started.
Time 150 sec(2.5 min) 1058 kW	The emergency ventilation fans have reached steady state. Some smoke rising from the sides has reached the top of the station and expand towards the other track. Smoke is slightly sucked towards the fans.
Time 240 sec (4 min) 2707 kW	The fans have been working at full load for 1.5 minutes and extraction of smoke towards the fans is visible. Smoke concentration increases in the tunnel section between the platform and the fans. It is clearly seen that no smoke exist on the evacuation routes and visibility is not hindered on these routes.
Time 360 sec (6 min) 6091 kW	The fans have been working at full load for 3.5 minutes and extraction of smoke towards the fans is visible. Smoke concentration further increases in the tunnel section between the platform and the fans. Smoke concentration also increases near the fire source due to increased fire load. It is clearly seen that no smoke exist on the evacuation routes and visibility is not hindered on these routes.

5.2.1.2 Scenario 2

Scenario 2 considers the fire at the north end of the train. In this case emergency ventilation fans at Polytechnika side of the station are switched on 30 seconds after the fire initiation. The main results of this scenario are presented graphically in Figures 5.14 to 5.19. The development of the fire and subsequent smoke movement is summarized in the following commentary.

Table 5.2 Commentary on Scenario 2 in KCK Station

Elapsed Time Fire Load:	Commentary
Time 30 sec (0.5 min) 42 kW	Fire Load 42 kW. Comparison of the results for Scenario 1 and Scenario 2 shows no significant effect in terms of temperature and smoke concentration. Similar to Scenario 1, smoke from the comparatively small fire has very low and localized effects near the fire source. The emergency ventilation fans are just started.
Time 150 sec(2.5 min) 1058 kW	Fire Load 1058 kW. The emergency ventilation fans have reached steady state. Some smoke rising from the sides has just reached the top of the station. Smoke is slightly sucked towards the fans.
Time 240 sec (4 min) 2707 kW	Fire Load 2707 kW. The fans have been working at full load for 1.5 minutes and extraction of smoke towards the fans is visible. Smoke concentration increases in the tunnel section between the platform and the fans and it is higher compared to Scenario 1, which is due to shorter Fan-Fire distance. It is also clearly seen that no smoke exist on the evacuation routes and visibility is not hindered on these routes.
Time 360 sec (6 min) 6091 kW	Fire Load 6091 kW. The fans have been working at full load for 3.5 minutes and extraction of smoke towards the fans is visible. Smoke concentration gets denser in the tunnel section between the platform and the fans. Smoke concentration also increases near the fire source due to increased fire load. Again, it is seen that no smoke exist on the evacuation routes and visibility is not hindered on these routes.

5.2.1.3 Evaluation

In the simulations the smoke distribution is given in terms of CO concentration and visibility by means of scalar quantities. The velocity and temperature contours are represented on the KCK station model in case of two possible fire incidences.

From these results it is shown that, station evacuation in case of a possible fire will not cause any problem to the passengers as far as CO, visibility and other smoke contents are considered. For the evacuation two of the four emergency fans at the fire side of the station are sufficient and are recommended to start 30 s after the initiation. The duration of evacuation process from the station is given to be 6 minutes.

If two fans closer to the fire side are operated, temperature and smoke distributions on the escape routes allow a safe evacuation. The maximum temperature in the evacuation direction does not exceed 60 °C. The concourse level remains clear of smoke for both scenarios.

It is important to use the emergency ventilation systems installed in the stations to control the smoke and heat generated by a fire. The ventilation systems should be activated as soon as possible (< 30s) after the onset of a fire incidence. The emergency ventilation fans are sufficient to remove the smoke from the station and create smoke free evacuation paths.

5.2.2. Comparison of Scenario-1 of KCK Station Fire with Fire Dynamics Simulator (FDS)

FDS is a computational fluid dynamics model of fire-driven fluid flow. The software solves numerically a form of the Navier-Stokes equations appropriate for low-speed, thermally-driven flow with an emphasis on smoke and heat transport from fires. The Fire Dynamics Simulator was developed and is currently maintained by the Fire Research Division in the Building and Fire Research Laboratory at the National Institute of Standards and Technology. It is found further information from Appendix-B and FDS 4 Technical Manual [30]. The results obtained from the simulations are given as contours plots of temperature, velocity and visibility at the level 2.5 m above the platform in Appendix-B. The obtained results from FDS are compared from the outputs of CFDesign 7.0. The comparison of CFDesign results with FDS is reasonable because FDS is checked by experiments in case of fire.

As far as temperature distribution is concerned, both programs' outputs give almost same results (Figure 5.14 & Figure B.3) up to time=240s. At the time of 30s, in the vicinity of fire there is small change in the temperature in the CFDesign analysis's result. At the time of 150 s, the high temperature regions (Temperature \geq 60 °C) start to be visualized in both simulations, and the fan's effects of temperature distributions are easily observed. At the time of 360 s high temperature region is larger in CFDesign 7.0 simulation results than FDS. This difference may be occurred due to larger estimation of smoke generation rate. In the FDS simulation, a mixture fraction combustion model is used. The mixture fraction is a conserved scalar quantity that is defined as the fraction of gas at a given point in the flow field that originated as fuel. The model assumes that combustion is mixing-controlled, and that the reaction of fuel and oxygen is infinitely fast. The mass fractions of all of the major reactants and products can be derived from the mixture fraction. The amount of combustion products is calculated automatically in the FDS simulation. In both of the simulations, the maximum temperature in the evacuation direction does not exceed 60 °C. Both simulations give favorable results for evacuation.

As far as velocity distribution is concerned, both programs' outputs give almost similar results in the duration of simulation. Small differences may occur due to inadequacy of FDS representation in round geometries. Both programs' results are consistent with each other.

If the visibility or smoke concentration distribution is investigated, CFDesign analysis gives more conservative results at the fire zone rather than FDS. As in the simulation of CFDesign, the ramp connecting the platform to the exits at the side of the fire location is affected from the smoke in FDS simulation at the time of 360 s.

In conclusion, both of the results verify that the emergency ventilation is capable of satisfying the requirements of NFPA-130 [6]. The compatibility of two results is proven that CFDesign software can be used as a design tool in order to investigate the sufficiency of emergency ventilation system as far as the smoke production rate is carefully determined. It can be noted that the effect of radiation heat transfer in case of fire is neglect in both simulation.

5.3 Case Study-2 Polytechnika Station Fire

Another station in Krakow Fast Tram is Polytechnika Station, which has a platform length of 55 m, a width of 21.25 m and height of 6.5 m. Likewise KCK Station, two pairs of emergency ventilation fans with a capacity of 80 m³/s are located on both sides of the station. SES program [28] is used in order to evaluate the required fan capacities during the tunnel fire simulations. The fans have the ability to work in two modes of operation (supply or exhaust). The three dimensional representation of the station is shown in Figure 5.20. The platform and public areas of the concourse level of the station are represented up to the normal street exits. There exist four stairs for evacuating the passengers.

Three different fire scenarios are investigated in case of a fire at Polytechnika Station. Ventilation scenarios in Polytechnika Station are shown in Figure 5.20. In all scenarios, fire is incident at south side of the tram. Unsteady analyses are presented in two ventilation scenarios. Based on the results obtained from KCK fire simulation, fans on the side of the fire are operated in exhaust mode. At first, whether such an operation with high temperature smoke going through the fans harm the fans and stop operation or not is checked. Then, the fire simulation is carried out unsteadily. Here in addition to exhaust fans, the fans at the other side of the station are operated in supply mode. (Figure 5.21) For all unsteady analyses, the fans start to operate in exhaust mode 30 s after the initiation of the fire and reach the steady-state after 150 s. The simulation continues for 360 s (60 min) taking the evacuation period of the passengers into account. Lastly, the third one is a steady analysis for investigating the effect of jet fan installations with fans nearest to the fire location in exhaust mode. After seeing that smoke and high temperature air is induced into the stairs and evacuation paths, additional precaution is necessary for the safety of passengers. The evacuation paths must be pressurized to obtain a smoke free evacuation path. Two similar jet fans with capacity of 6.3 m³/s (flow rate) and 32.1 m/s (discharge velocity) are attached to the ceiling along the evacuation paths one for each path in order to pressurize the environment. They work in a mode of injecting

air towards the platform. Identical boundary conditions are applied. (Figure 5.22)
The number of computational elements in the simulation is 1300000 in Polytechnika Station Fire. Each one is performed in five days.

The contours plots of temperature, scalar and velocity distributions are given at different locations: at 2.5 m above the platform and along the evacuation direction. The main results of these scenarios are presented graphically in Figures 5.23 to 5.37.

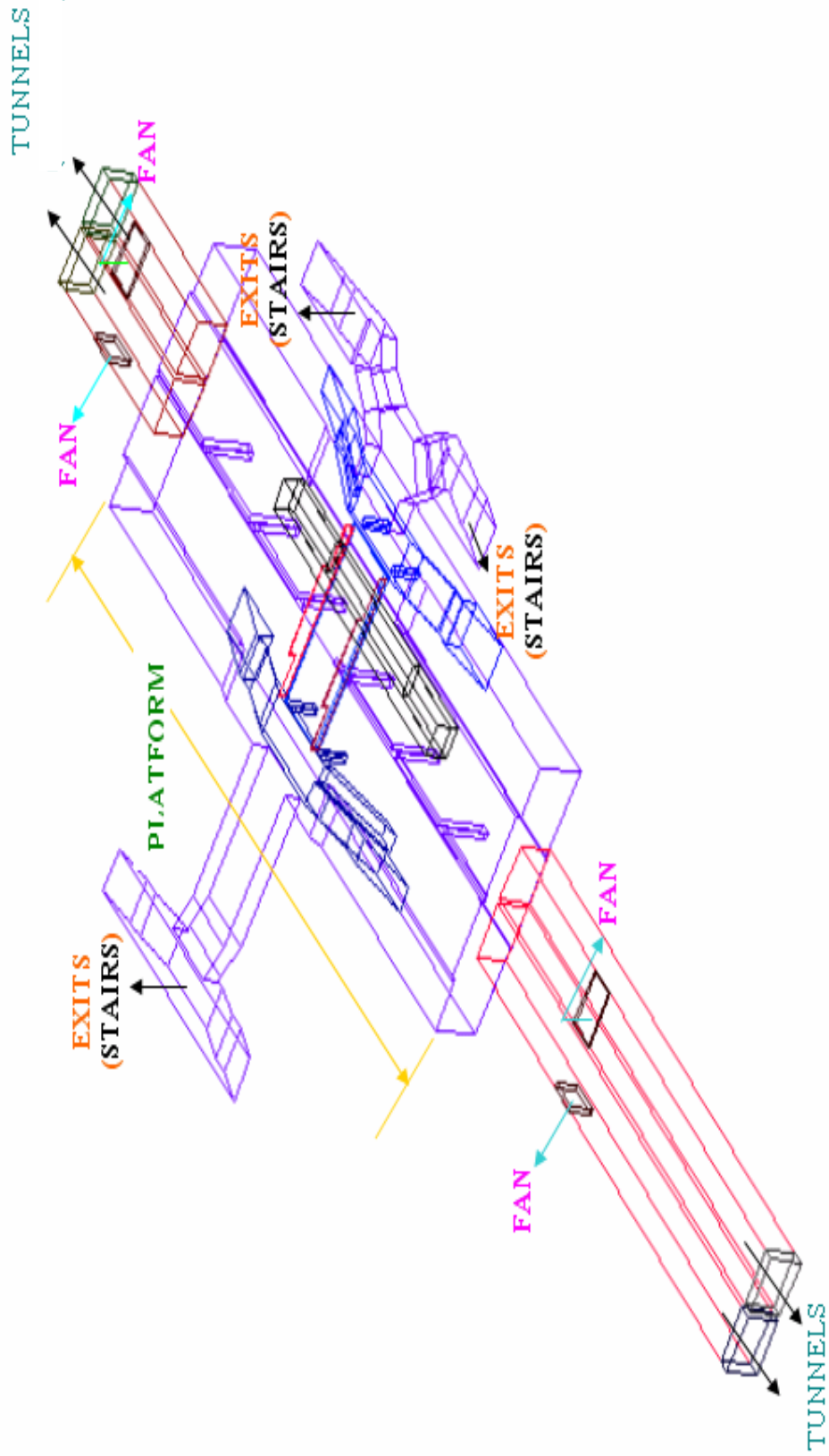


Figure 5.20 3D representation of Polytechnika Station In Krakow Fast Tram

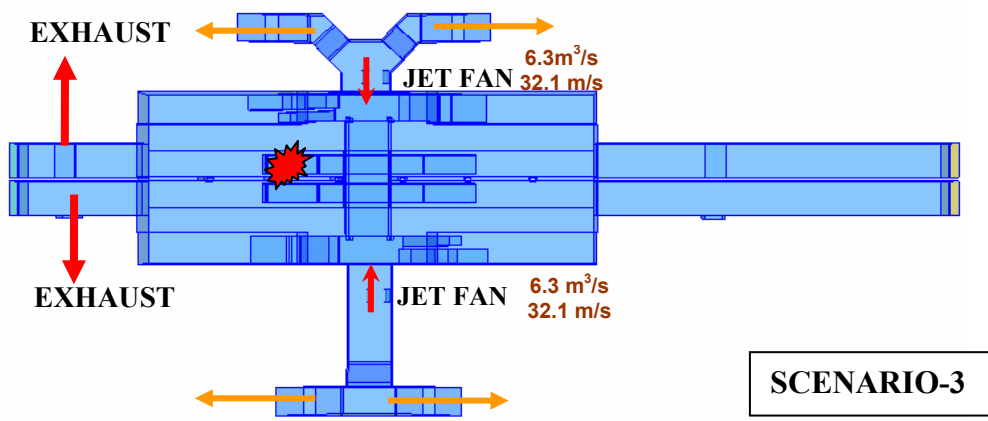
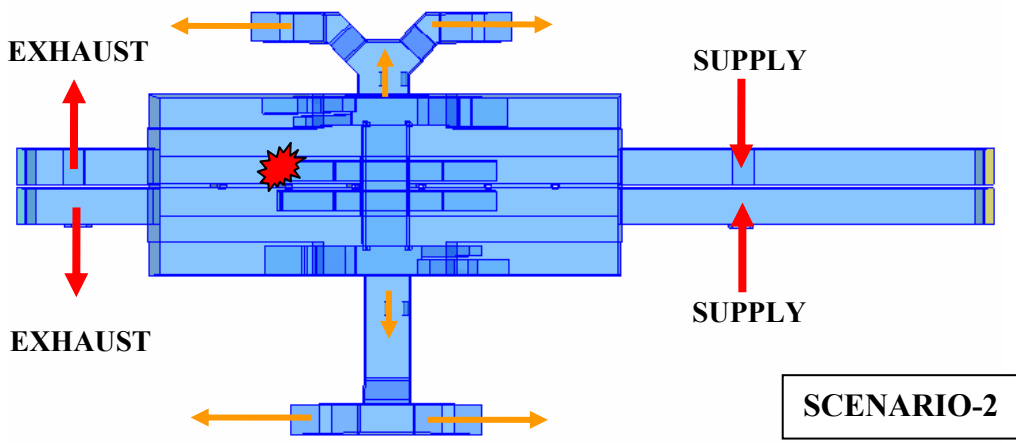
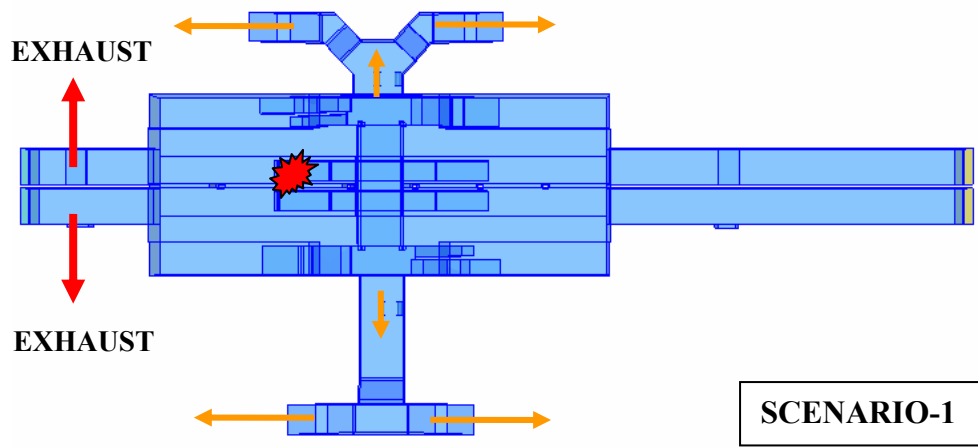


Figure 5.21 Schematic drawing of ventilation scenarios in Polytechnika

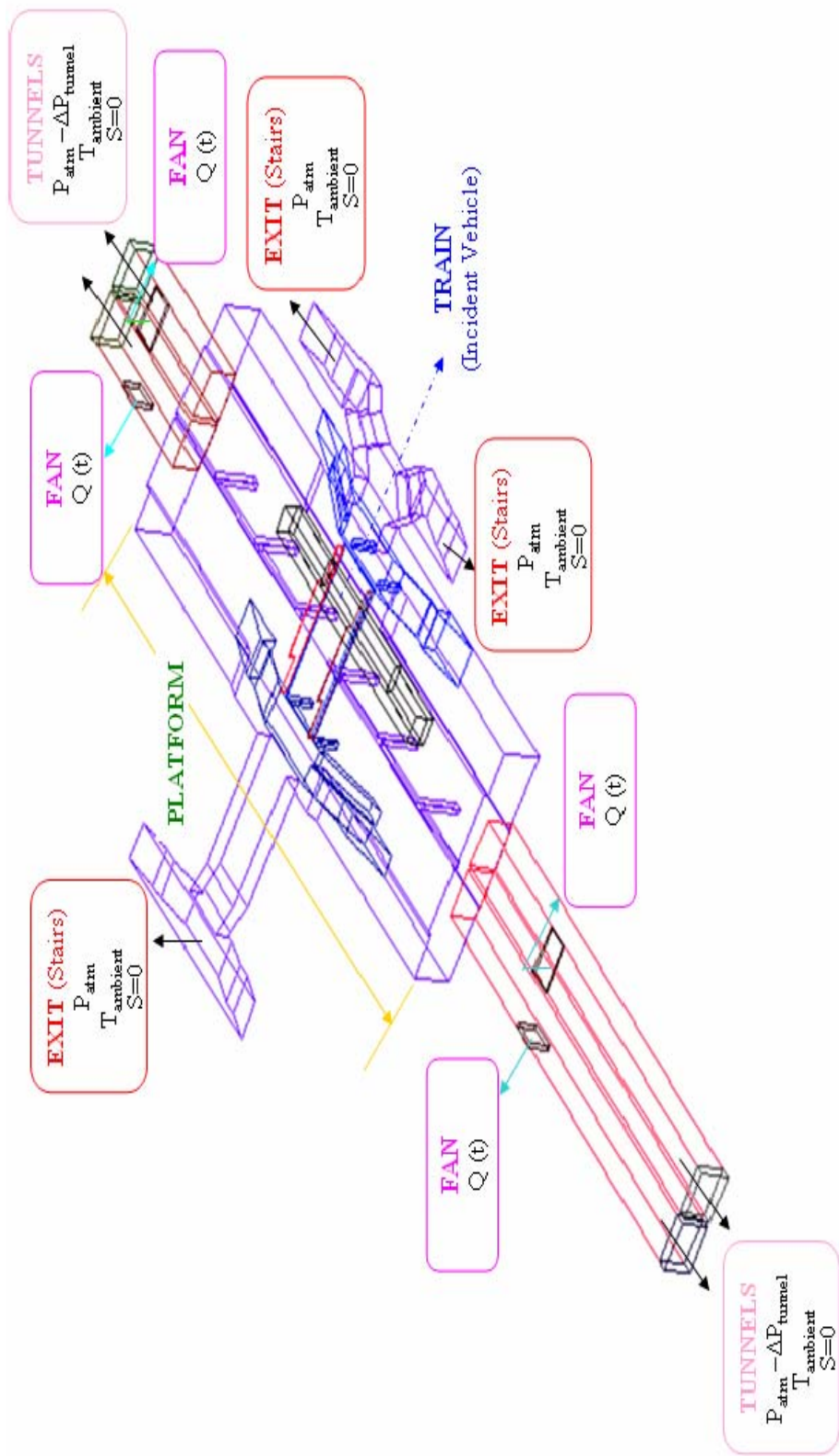


Figure 5.22 Boundary conditions applied in the unsteady CFD analyses for Polytechnika Station

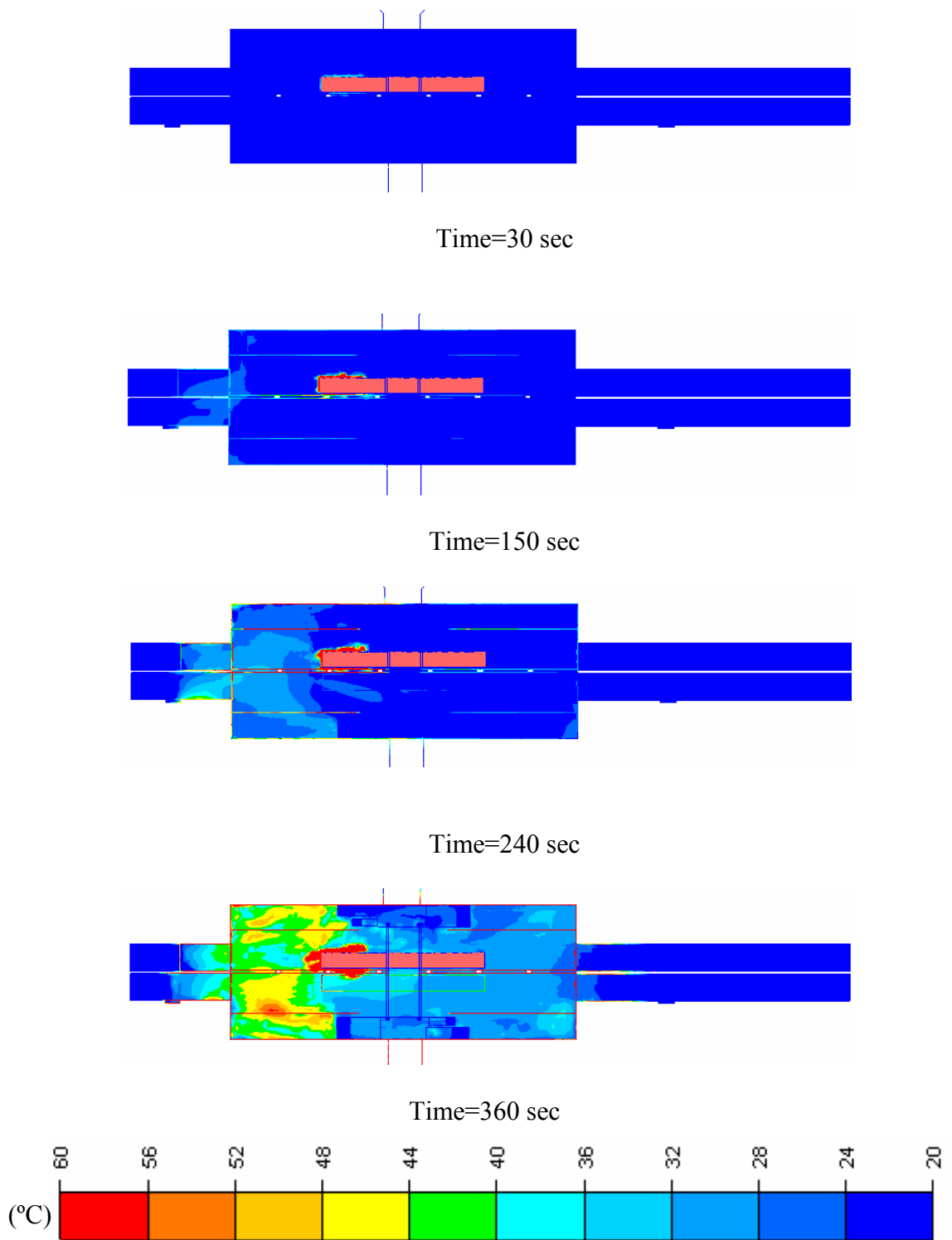


Figure 5.23 Temperature distribution at 2.5 m above the platform in Polytechnika Scenario-1

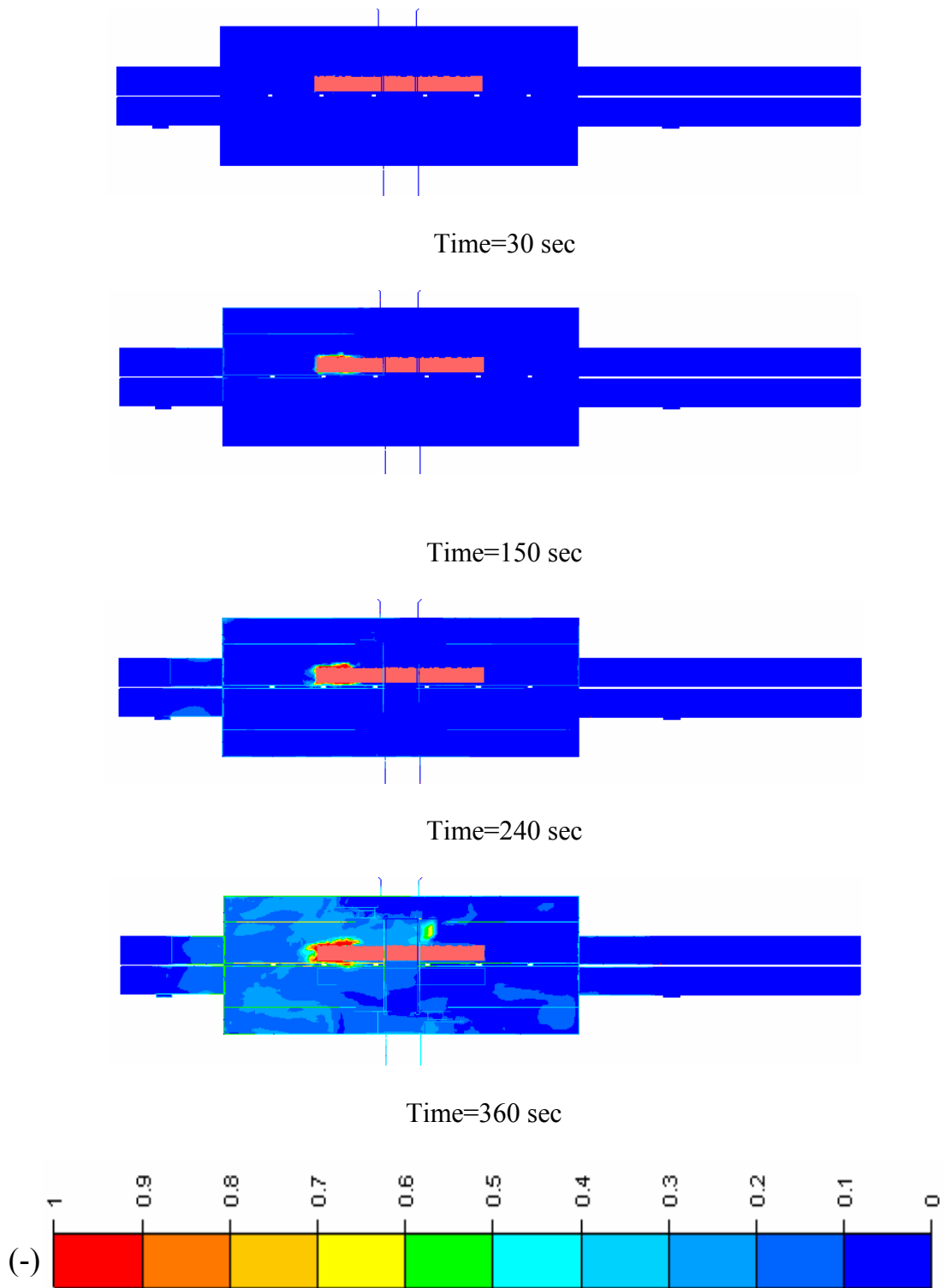


Figure 5.24 Scalar distribution at 2.5 m above the platform in Polytechnika Scenario-1

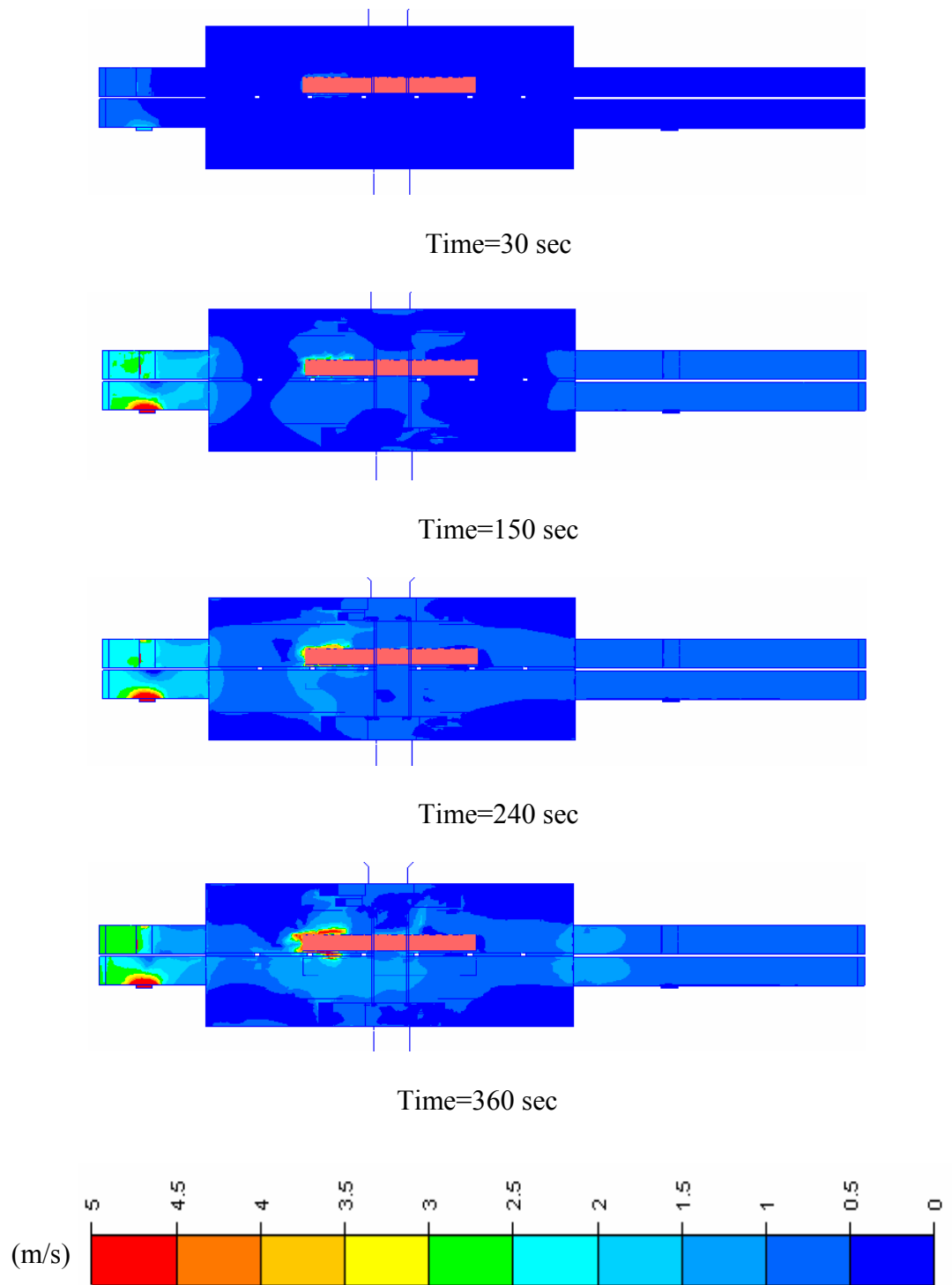


Figure 5.25 Velocity distribution at 2.5 m above platform level in Polytechnika Scenario-1

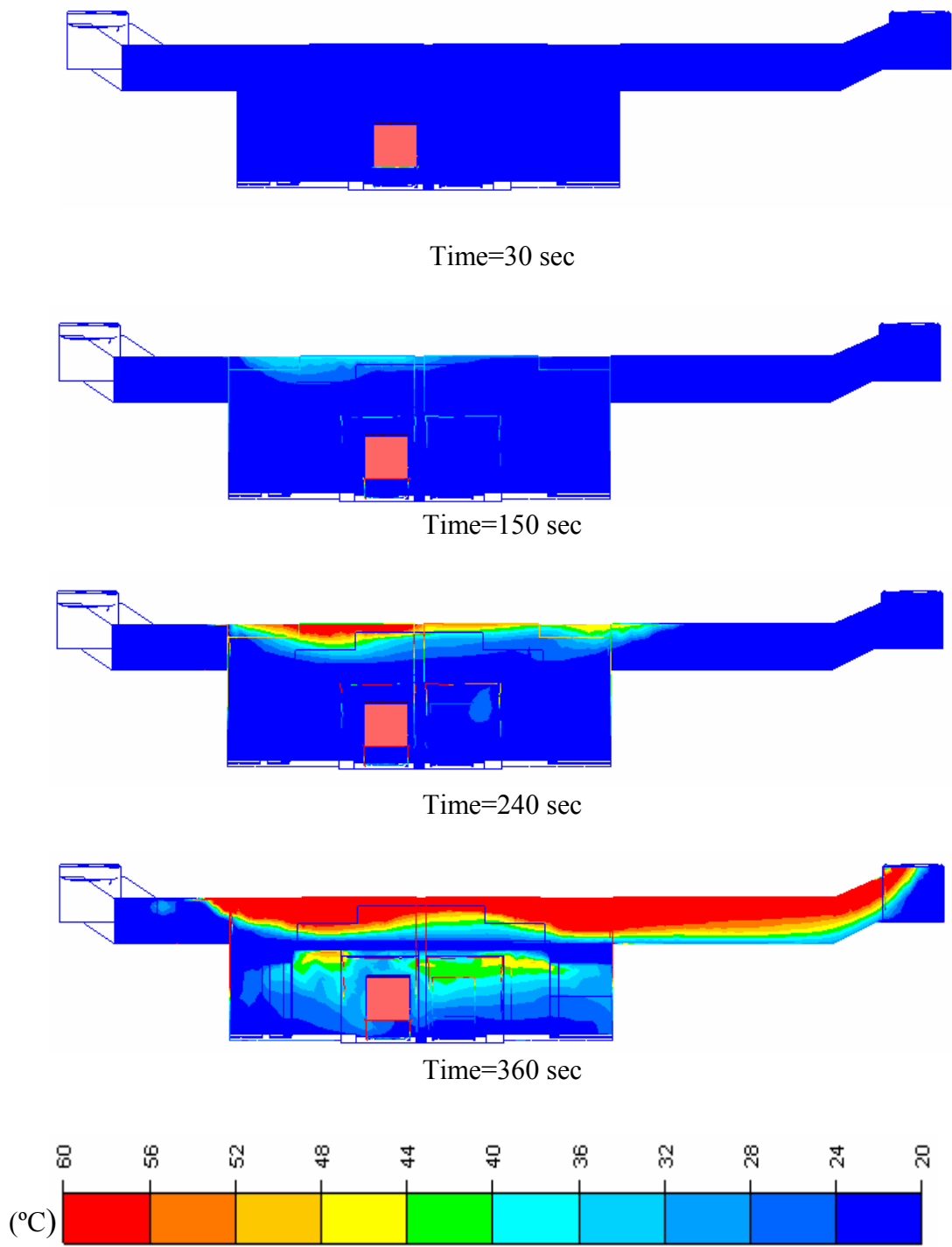


Figure 5.26 Temperature distribution along the evacuation direction in Polytechnika Scenario-1

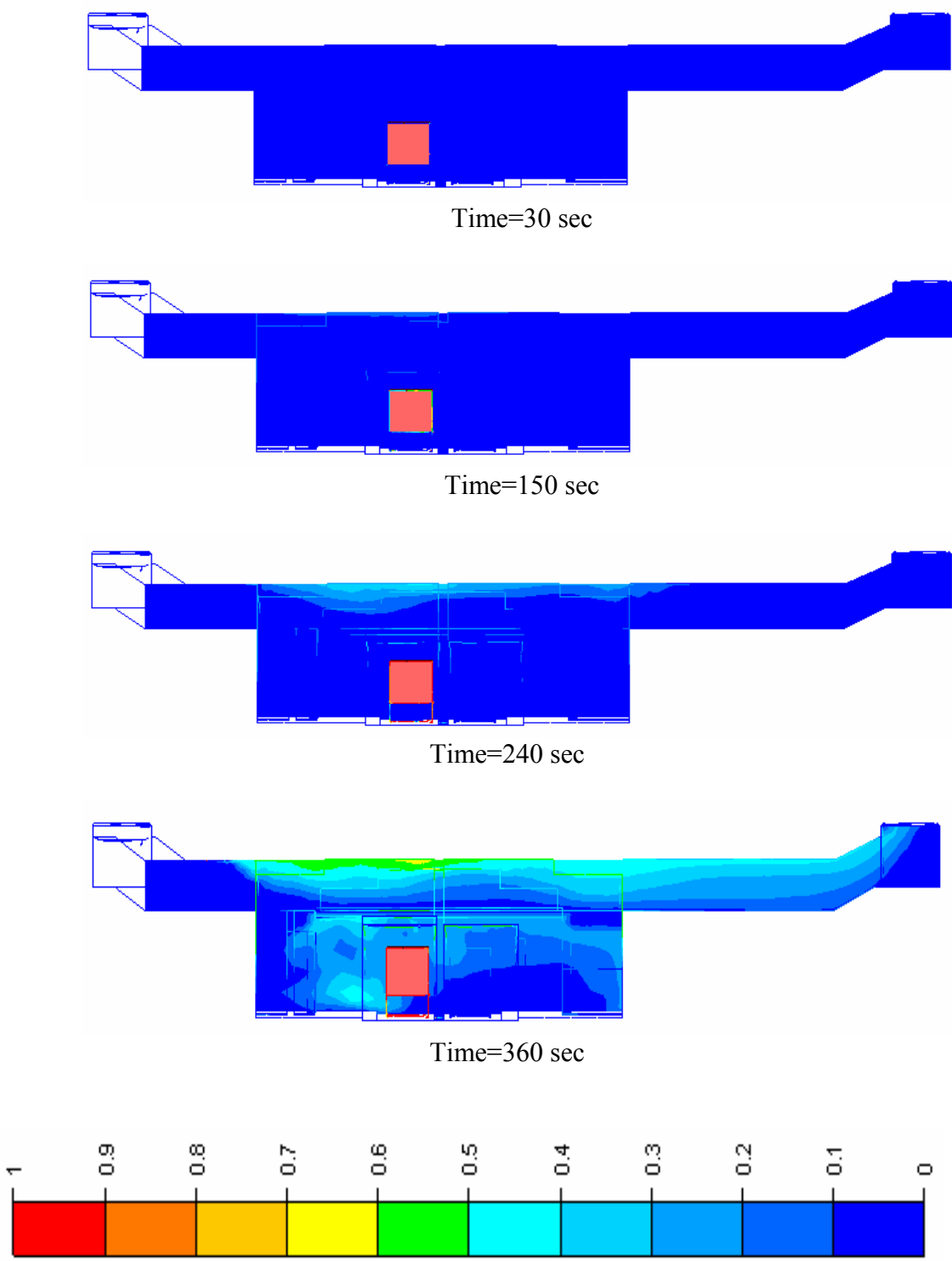


Figure 5.27 Scalar distribution along the evacuation direction in Polytechnika Scenario-1

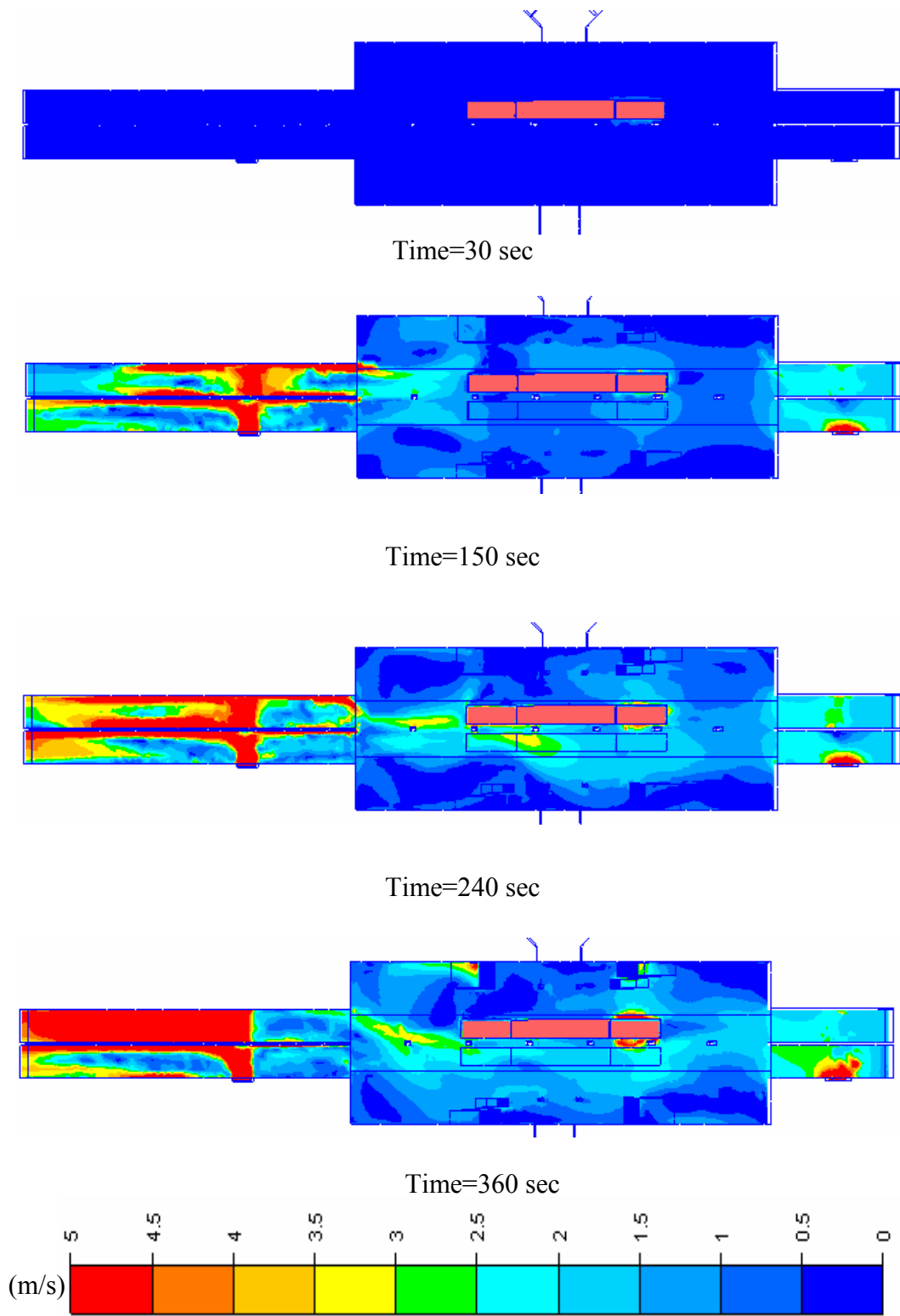


Figure 5.28 Velocity distribution at 2.5 m above platform level in Polytechnika Scenario-2

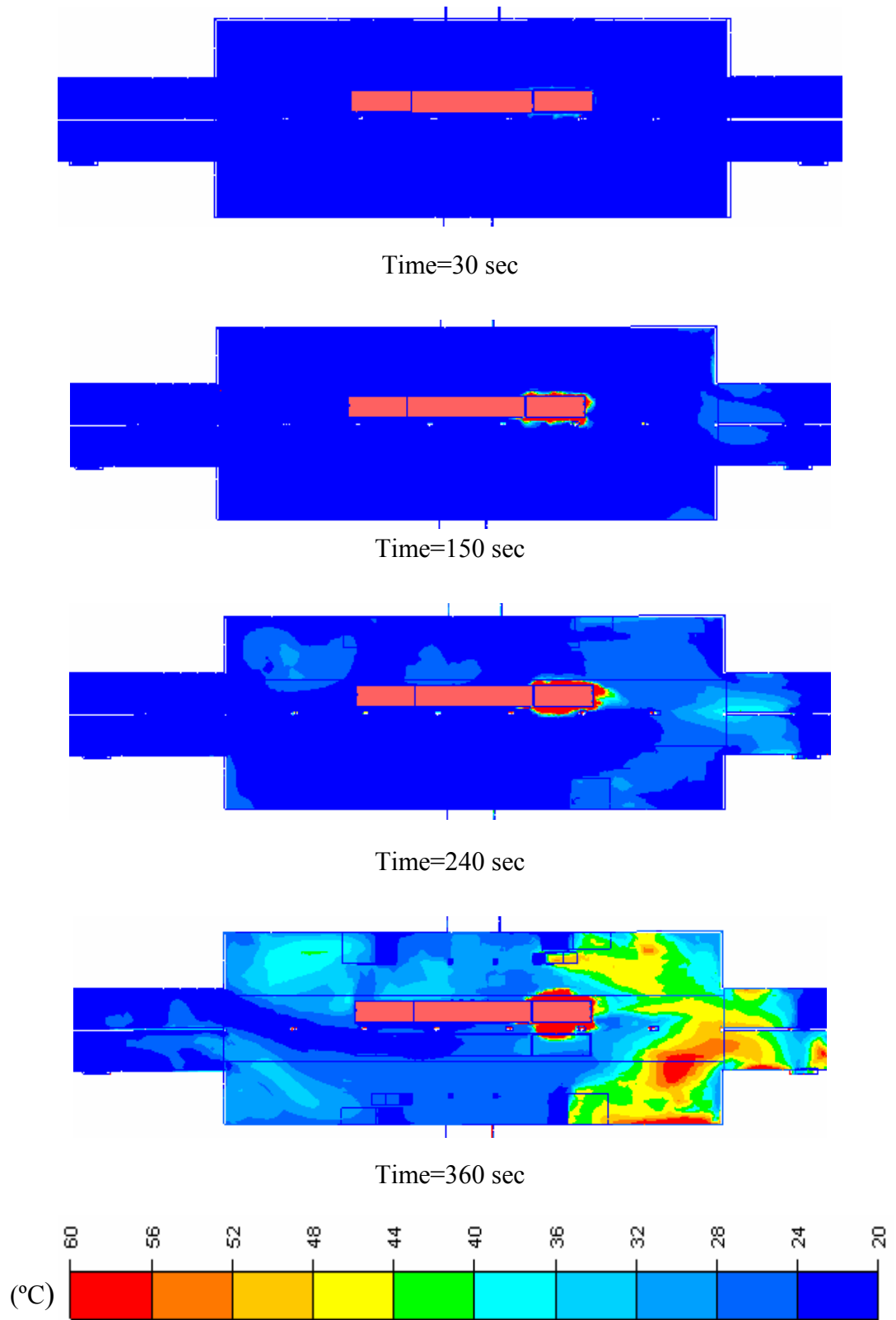


Figure 5.29 Temperature distribution at 2.5 m above platform level in Polytechnika Scenario-2

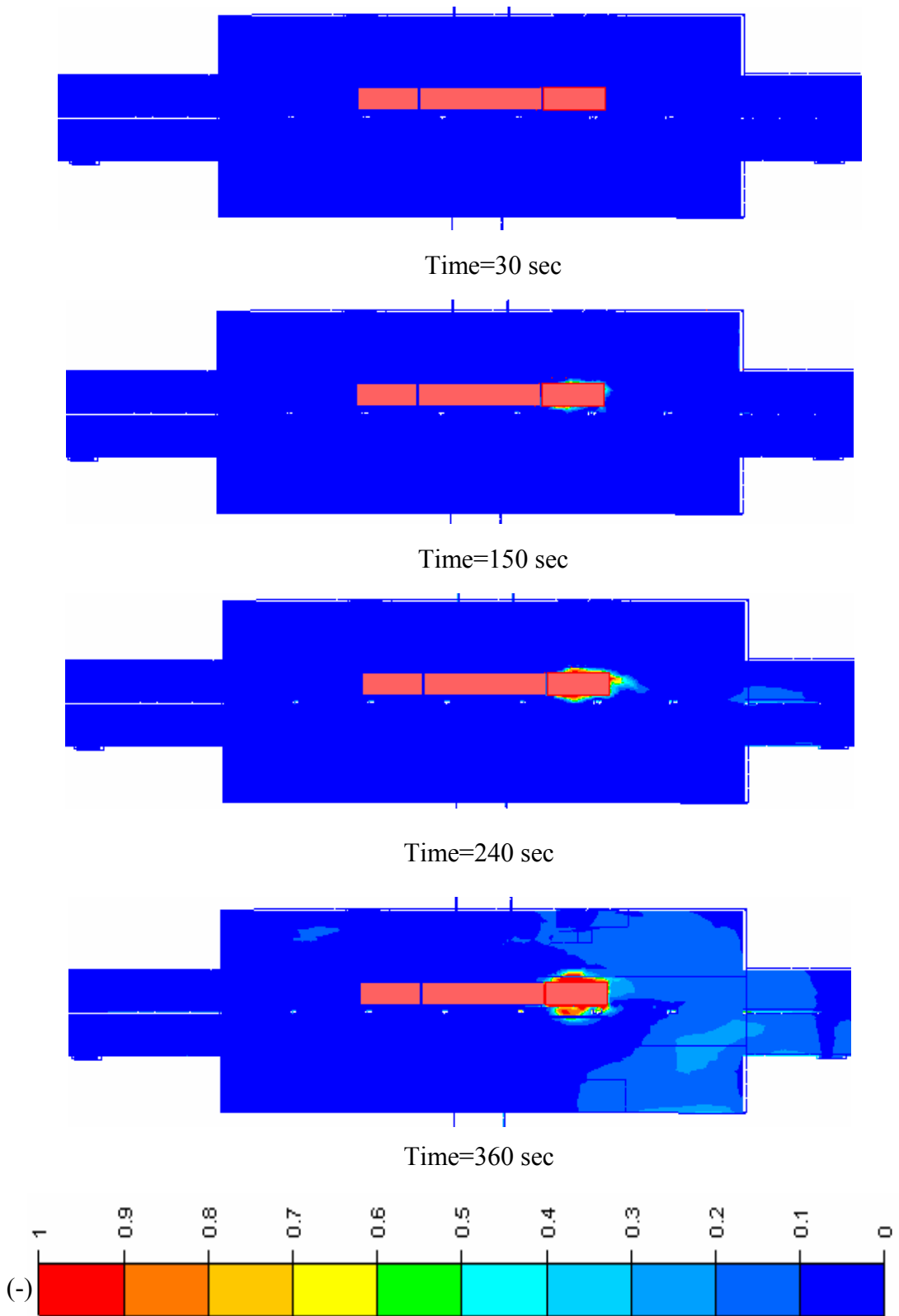


Figure 5.30 Scalar distribution at 2.5 m above platform level in Polytechnika Scenario-2

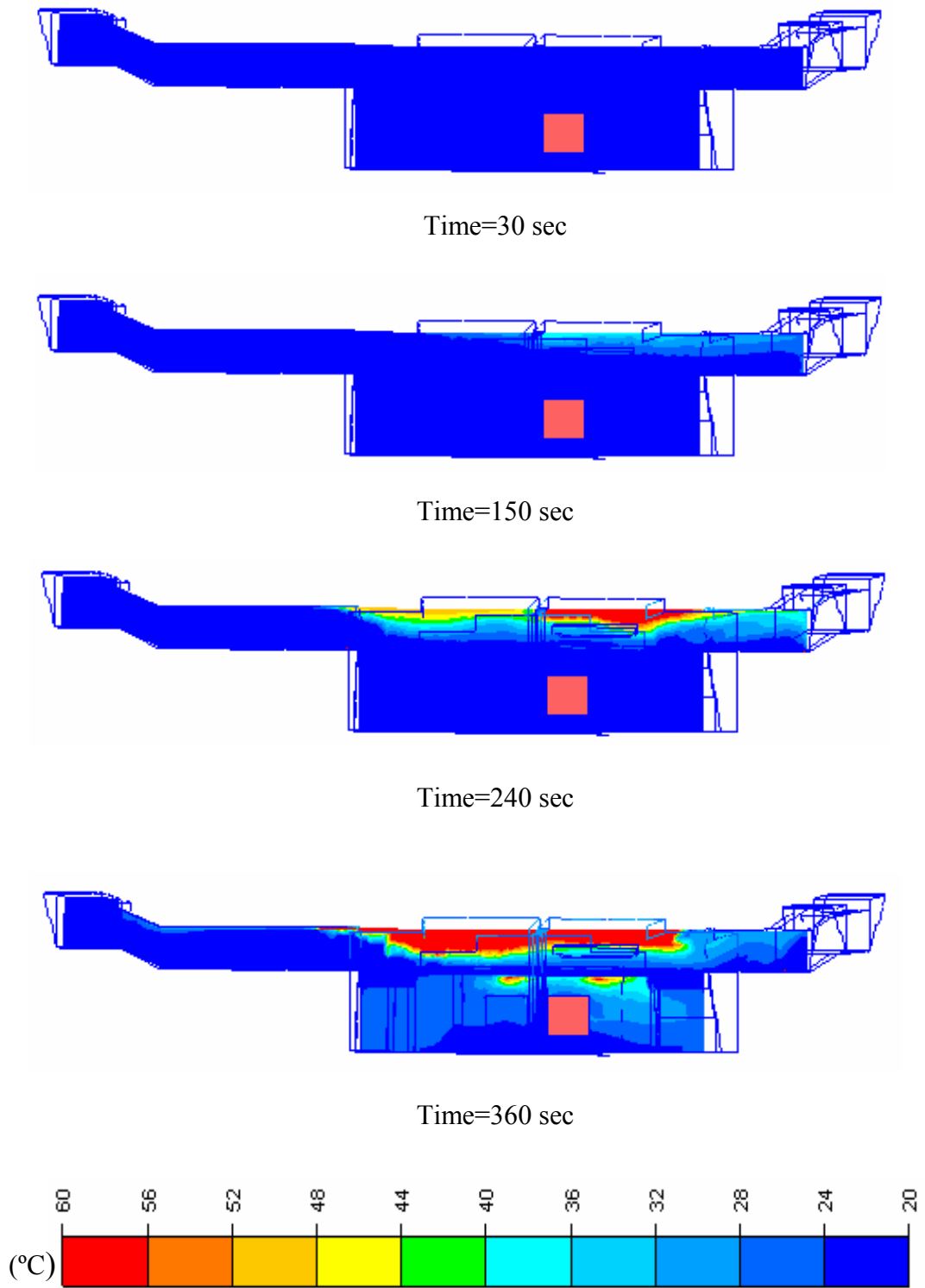


Figure 5.31 Temperature distribution along the evacuation direction in Polytechnika Scenario-2

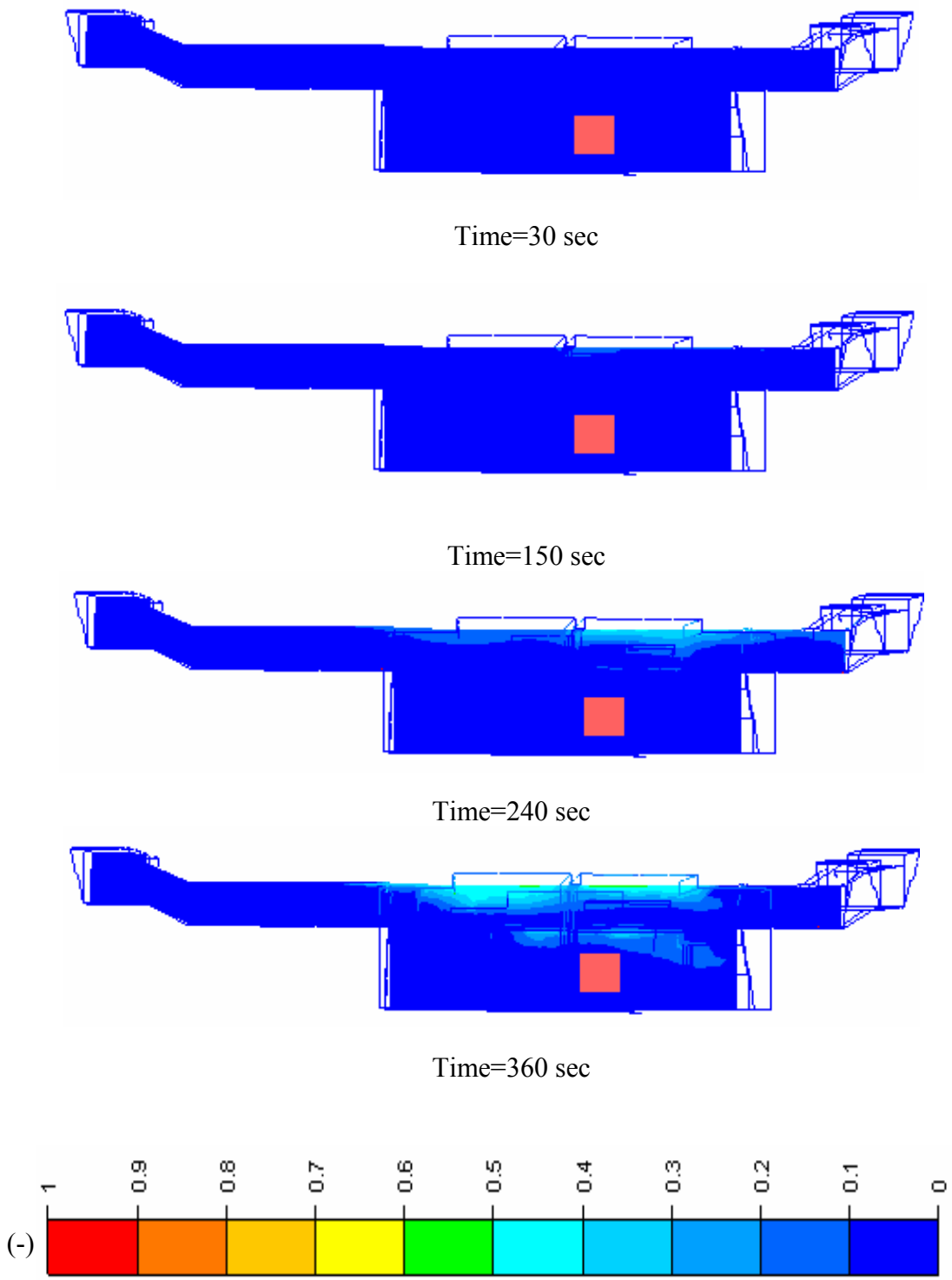


Figure 5.32 Scalar distribution along the evacuation direction in Polytechnika Scenario-2

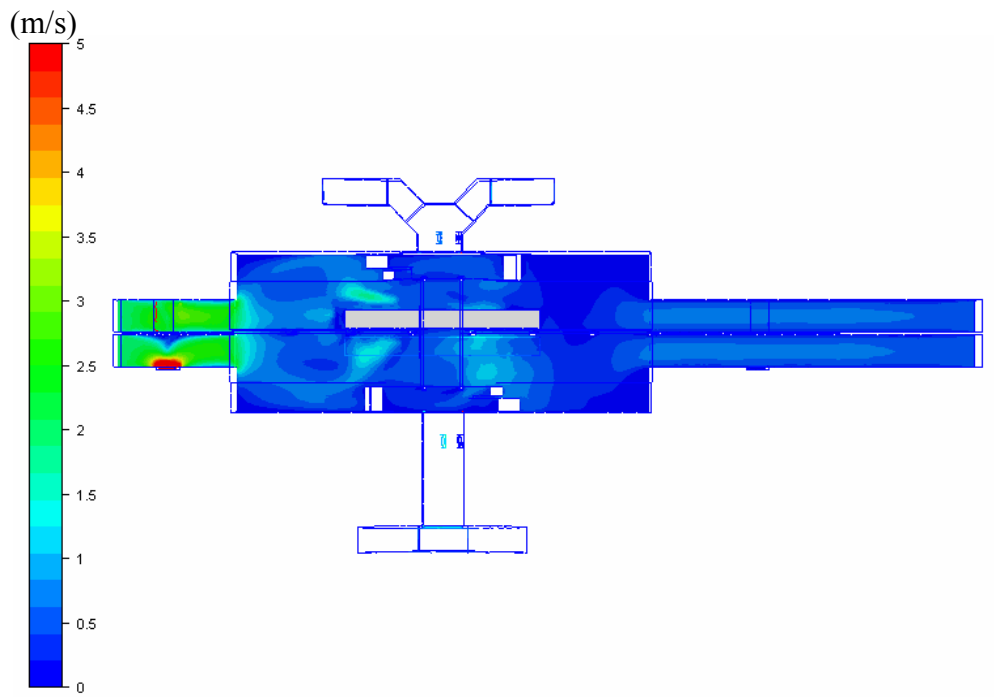


Figure 5.33 Velocity distribution at 2.5 m above platform level in Polytechnika Scenario-3

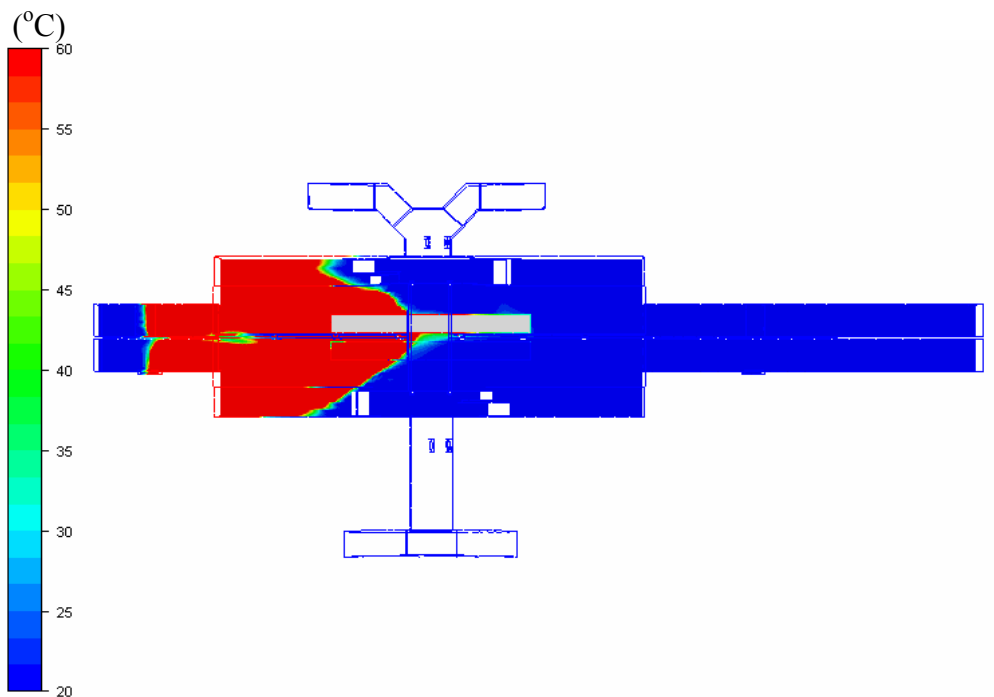


Figure 5.34 Temperature distribution at 2.5 m above platform level in Polytechnika Scenario-3

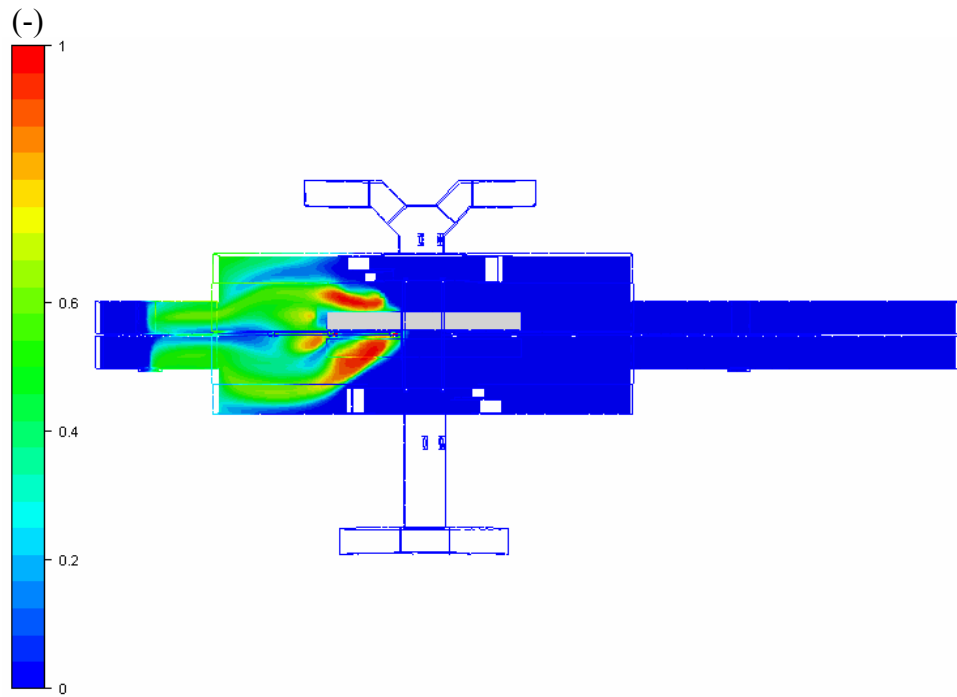


Figure 5.35 Scalar distribution at 2.5 m above platform level in Polytechnika Scenario-3

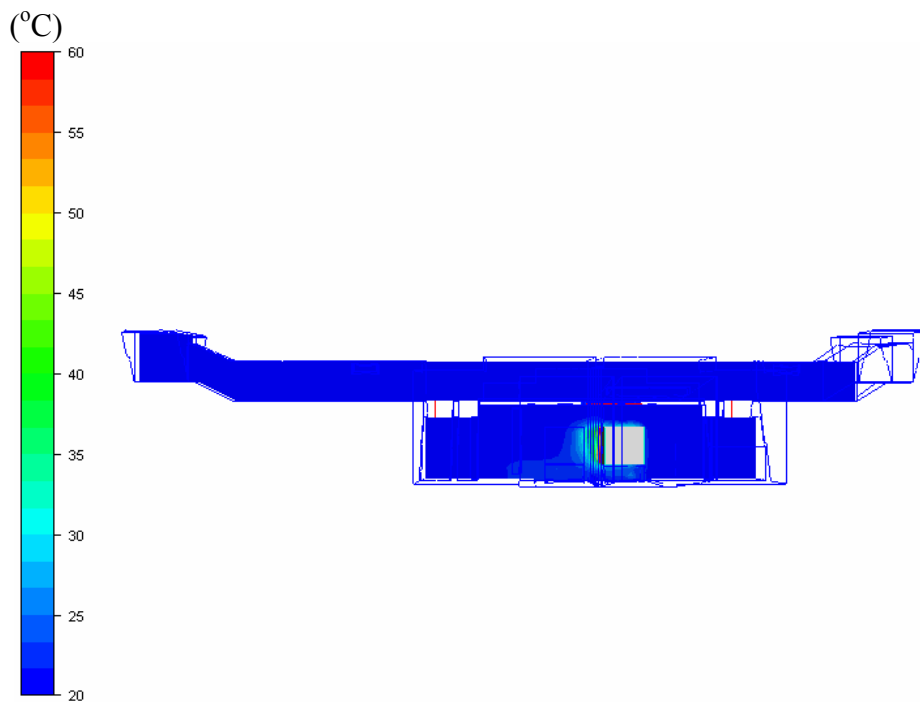


Figure 5.36 Temperature distribution along the evacuation direction in Polytechnika Scenario-3

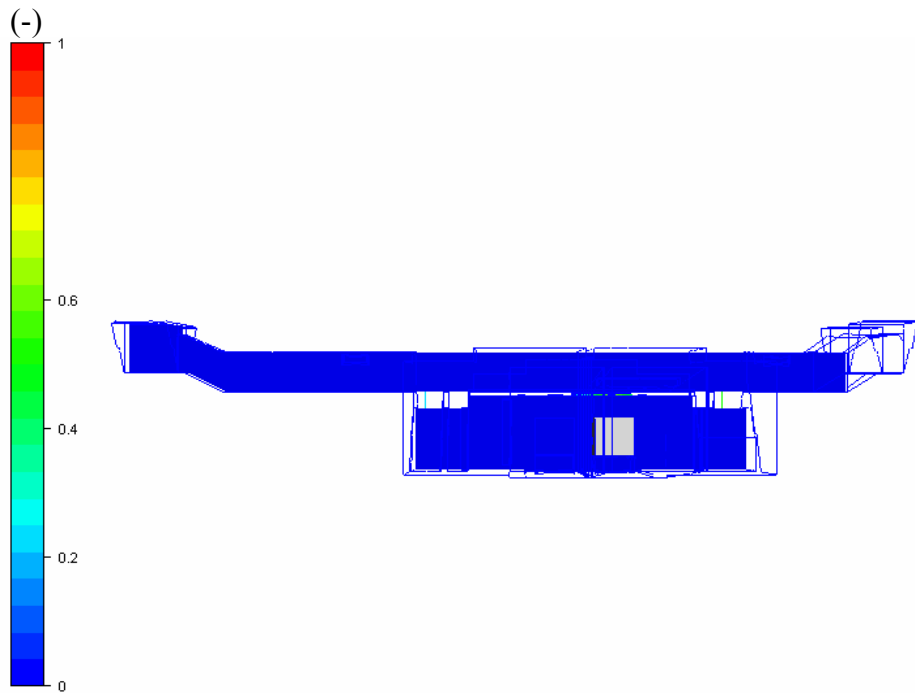


Figure 5.37 Scalar Distribution along the evacuation direction in Polytechnika Scenario-3

5.3.1 Results of Polytechnika Station Train Fire

5.3.1.1 Scenario-1

In this scenario, fire starts to burn at the south end of the train. Again, emergency ventilation fans at the south side of the station are switched on 30 seconds after the fire initiation. The main results of this scenario are presented graphically in figures 5.23 to 5.27. The development of the fire and subsequent smoke movement is summarized in the following commentary.

Table 5.3 Commentary on Scenario 1 in Polytechnika Station

Elapsed Time Fire Load:	Commentary
Time 30 sec (0.5 min) 42 kW	Change in the smoke concentration and temperature can be seen in a small region near the fire source. The emergency ventilation fans are just started. No danger to evacuees at this time.
Time 150 sec(2.5 min) 1058 kW	The emergency ventilation fans have reached steady state. Smoke region starts to expand in transverse direction. Flow developed by the fan activation is demonstrated.
Time 240 sec (4 min) 2707 kW	The fans have been working at full load for 1.5 minutes and extraction of smoke towards the fans is visible. Smoke accumulated over the ceiling expands towards the station. Visibility is satisfied the requirements. Evacuation path is free of smoke and high temperature. No danger to evacuees at this time.
Time 360 sec (6 min) 6091 kW	The fans have been working at full load for 3.5 minutes. It is demonstrated by the scalar and temperature distributions, the evacuation path is filled with smoke.

5.3.1.2 Scenario-2

In Scenario-2, fire starts to burn at the south end of the train. Emergency ventilation fans at the both side of the station are switched on 30 seconds after the fire initiation. The main results of this scenario are presented graphically in figures 5.28 to 5.32 The development of the fire and subsequent smoke movement is summarized in the following commentary.

Table 5.4 Commentary on Scenario 2 in Polytechnika Station

Elapsed Time Fire Load:	Commentary
Time 30 sec (0.5 min) 42 kW	The emergency ventilation fans are just started. Small region around the fire region affect the platform area as far as smoke concentration and temperature distribution are concerned.
Time 150 sec(2.5 min) 1058 kW	The emergency ventilation fans have reached steady state. Smoke rising from the sides has reached the top of the station and expands towards the other track. Smoke is slightly sucked towards the fans.
Time 240 sec (4 min) 2707 kW	The fans have been working at full load for 1.5 minutes and extraction of smoke towards the fans is visible. Smoke accumulated over the ceiling expands towards the station and reached to the evacuation path direction. Also, it is seen that smoke leaves the station through the nearest path. Therefore, high temperature and low visibility threaten the lives of the evacuees.
Time 360 sec (6 min) 6091 kW	The fans have been working at full load for 3.5 minutes and extraction of smoke towards the fans is visible. Smoke and temperature affected region is enlarged and it closes the entry of the evacuation path totally. Also, amount of smoke leaving the station through the exits increases. Lives of the evacuees are in danger.

5.3.1.3 Scenario-3

It is shown in the steady state analysis that pressurized the evacuation paths by using a jet fan results in a free of smoke evacuation paths. Addition of jet fans with the two operating emergency ventilation fans keeps the evacuation path below 60 °C. The concourse level remains clear of smoke. The jet effect pushes the smoke towards the fans. Therefore, NFPA 130 [6] requirements are satisfied.

5.3.1.4 Evaluation

In the first scenario, ventilation system is not capable of removing the smoke from the evacuation direction. Operation of fans near the fire is not sufficient. At the time of 360 s the corridor connecting the concourse level to the station exits is filled with smoke. Also, temperature distribution along the evacuation path is above 60 °C. In the second scenario, the fans at the other side of the station are operated in supply mode in addition to exhaust fans. The smoke and temperature level along the evacuation path is more favorable than the first scenario; whereas a propagated smoke layer hinders the visibility of passengers. In transient analyses, the emergency ventilation system located at Polytechnika station does not satisfy the requirements of NFPA 130 [6]. Because, the evacuation paths are filled with smoke and temperature along evacuation path is above 60 °C. It is recommended that in addition to fans placed at both side of the station, station fans or jet fans located at the evacuation paths are attached in order to pressurize the evacuation path for smoke free.

In Scenario-3, the addition of jet fans to the emergency ventilation system satisfies the requirements. From these results it is shown that, station evacuation in case of a possible fire will not cause any problem to the passengers as far as CO, visibility and other smoke contents are considered. The flow induced by the jet fans pushes the smoke towards the exhaust fans. For the evacuation, two of the four emergency fans at the fire side of the station and two jet fans located at the evacuation paths are sufficient. However, further analyses show that two jet fans are not sufficient for different fire locations. Additional precautions are necessary to have a fire safety in Polytechnika Station. A change in the position and number of jet fans and some modification in the station geometry are essential to satisfy the requirements of NFPA 130 [6].

CHAPTER 6

DISCUSSION AND CONCLUSION

6.1 Comments on the Results

It is apparent that one of the most critical and vital considerations in underground transportation system design is the need for a well-founded environmental control system. This system would include temperature and humidity control, circulation of fresh air to satisfy both normal and emergency requirements, and safety features in case of fire.

The Subway Environmental Simulation program has been designed with the ability to simulate the overall effects of a tunnel fire on the ventilation system. It can calculate the volumetric flow requirements of emergency ventilation system. However, the SES is a one-dimensional model. A realistic representation of flow physics within the complex station geometry is not achieved by SES program. CFD is used as a tool to evaluate the performance of emergency ventilation systems. SES can only be used in case of station fire to obtain boundary conditions.

In this study, CFD technique is utilized in order to examine the emergency ventilation requirements in case of fire in underground transportation system station. In case of a station fire in KCK and Polytechnika stations, CFD analyses are conducted to gain a better understanding of flow patterns and to determine smoke

propagation and temperatures on passenger escape routes and to evaluate if emergency fans will function and serve as intended.

The following conclusions are reached based on the results presented in the previous sections. Before the transient analysis, it is better to check the adequacy of emergency ventilation system fans in case of station fire by using the steady state analysis. The steady state analysis takes a short computation time in order to evaluate the adequacy of emergency ventilation system. Depending on the station geometry, the most appropriate ventilation scheme is determined. The most appropriate ventilation scheme is operation of fan closer to exhaust mode in a given situation.

The fan capacities in the system are calculated depending on the tunnel ventilation scenarios based on the design fire load. Whereas, it is not always the case that the fan capacities obtained in case of tunnel fire are not fulfilled the requirements of the station fire case. In this situation, additional fan e.g. station fan, jet fan or increasing the capacity of existing fans solve the problem.

The duration of fire to reach its full load varies depending on the fire growth factor. In this study, fire grows in a fast manner. Due to high temperature and smoke accumulation, the life of evacuees is threatened. From the transient analysis, it is important that emergency ventilation system is activated as soon as possible after the onset of an incident to provide protection and safety expected in a modern transit system. The smoke fills the compartment; therefore the evacuees have a difficulty to find a way to exit due to low visibility. It is vital to use emergency ventilation systems in the stations and tunnels to control the smoke and heat generated by a fire.

The construction of the underground transportation system is also important. In case of emergency, station will be designed according to NFPA 130 [6]. There shall be sufficient egress capacity to evacuate the platform occupant load from the station platform in 4 minutes or less. Also, the station shall be designed to permit evacuation from the most remote point on the platform to a point of safety in 6 minutes or less.

One of the case studies is compared with a code well known in the discipline, the Fire Dynamics Simulator, specifically developed for fire simulation. Both simulations give almost same results. Therefore, it can be said that the analyses performed in the thesis have a consistency in the field of interest.

In conclusion, many factors affect the safety of passengers in case of fire. These factors are examined carefully. For each station in underground transportation system, it is better to do CFD analysis in case of station fire.

6.2 Recommendations for Future Work

- If the emergency ventilation fans are started to operate in different instants, the effect of fan start time on the performance of an emergency ventilation system is to be investigated.
- Due to difficulties to calculate the emissivity of the components in the station, the simulations are performed neglecting the effect of radiation on heat transfer. The effect of radiation on temperature distribution should better be determined in future studies.
- Fire is assumed to grow in a fast manner in these simulations. Different fire growth rates are to be assumed and a transient CFD simulation of a train fire in the station is to be studied. In this manner, limiting capacity of the ventilation system will be determined.
- Different turbulence models are used in the simulations to evaluate the effects for predicting the flow in case of fire.

- CFD analysis results should be compared with the experimental results to verify them. If some fire experiments are designed in a future study and if the results can be used to verify some of these simulations, it will be very useful.

REFERENCES

- [1] Eralp, O.C.; Başıme, E.; Kayılı, S.; Musluoğlu, E. ; “A CFD Analysis of Station Fire Incidents and Determination of Passenger Evacuation Scenarios”, International Congress: Safety Innovation Criteria Inside Tunnels, June 29,30 and July 1 2005 (Accepted for congress)
- [2] Eralp, O. C.; Krakow Fast Tram CFD Fire & Smoke Movement Study in KCK Station, METU, September 2004
- [3] Eralp, O. C.; Krakow Fast Tram Emergency Ventilation in Tunnels, METU, September 2004
- [4] Chen, F. ; Chien, S. W. ; Jang, H. M.; Chang W. J.; ”Stacks Effects On Smoke Propagation In Subway Stations”, Continuum Mechanics Thermodynamics v 15, 2003, p. 425-440
- [5] Chen, F.; Chien, S. W. ; Chuay, H. Y. ; Guo, S. C.; “Smoke Control Of Fires In Subway Stations” , Theoretical and Computational Fluid Dynamics v16,2003, p 349-368
- [6] NFPA, NFPA 130-Standard for Fixed Guideway Transit System, National Fire Protection Association, 2003

- [7] Musluoğlu, E.; “Simulation of A Fire Incidence in Underground Transportation Systems”, M. Sc. Thesis, Middle East Technical University Mechanical Engineering Department, 2003
- [8] Düzce, A.,” Simulation Of Ventilation In The Stations Of Underground Transportation Systems”, M. Sc. Thesis, Middle East Technical University Mechanical Engineering Department, 2003
- [9] Willemann, D.; Sanchez, J. G.; “Computer Modeling Techniques and Analysis Used In Design Of Tunnel Ventilation Fan Plants For The New York City Subway”, Proceedings of the 2002 ASME/IEEE Joint Rail Conference, 2002
- [10] Shahcheraghi, N.; McKinney, D.; Miclea, P.; “The Effect Of Emergency Fan Start Time On Controlling The Heat and Smoke From A Growing Station Fire A Transient CFD Study”, Tunnel Fires 4th International Conference, 2-4 December 2002
- [11] Andersson, M.; Hedskog, B.; Nyman, H.; “Concept To Improve The Possibilities Of Escape From A Single Exit Underground Station”, Tunnel Fires 4th International Conference, 2-4 December 2002
- [12] Novozhilov, V.; “Computational Fluid Dynamics Modeling of Compartment Fires”, Progress in Energy and Science27, 2001, p 611-666
- [13] Xue, H.; Ho, J.C.; Cheng Y. M.; “Comparison Of Different Combustion Models In Enclosure Fire Simulation “ ,Fire Safety Journal v36, 2001, p.37-54
- [14] Karki, K. C.; Patankar, S. V.; Rosenbluth E. M. ; Levy, Sam S. ; “CFD Model For Jet Fan Ventilation Systems”, Proceedings of the 10th International

Symposium on Aerodynamics and Ventilation of Vehicle tunnels Principles, Analysis and Design,2000

- [15] Çoruh, M. M.; “Simulation of Ventilation in Underground Transportation Systems”, M. Sc. Thesis, Middle East Technical University Mechanical Engineering Department, 2000
- [16] Enclosure Fire Dynamics, Karlsson, B.; Quintiere, J.G., CRC Press, 2000
- [17] An Introduction to Fire Dynamics, 2nd ed., Drysdale, D., 1999
- [18] Carlsson, J.; “Fire Modeling Using CFD- An Introduction to Fire Safety Engineers”, Lund Institute of Technology Department of Fire Safety Engineering Report 5025, 1999
- [19] Li,Silas K.L.; Kennedy, W. D.; ”A CFD Analysis Of Station Fire Conditions In The Buones Aires Subway System “, ASHRAE Transactions v105, 1999, p410 -413
- [20] MacDonald, M; “CFD Fire and Smoke Movement Study”, Ankara Metro Report, December 1997
- [21] MacDonald, M; “Vehicle Fire Load Calculation and Fire Simulation”, Ankara Metro Report, November 1997
- [22] NFPA, NFPA 204M- Guide for Smoke and Heat Venting, National Fire Protection Association, 1995
- [23] NFPA, NFPA 92B- Guide for Smoke Management Systems in Malls, Atria and Large Areas, National Fire Protection Association, 1995

- [24] An Introduction to Computational Fluid Dynamics- The Finite Volume Method, Versteeg, H.K.; Malalasekera W., Prentice Hall, 1995
- [25] Mckinney, D.; Brunner, D.; Deng, M.; Miclea, P. C.; “Critical Velocity Of Air Versus Detailed Modeling Using Computational Fluid Dynamics In Tunnel Fires” ,1994 ,ICF Kaiser Engineers
- [26] Mckinney, D.; Brunner, D.; Deng, M.; Miclea, P. C.; “Critical Velocity Of Air Versus Detailed Modeling Using Computational Fluid Dynamics In Tunnel Fires (Part-2)” ,1994 ,ICF Kaiser Engineers
- [27] “Fire Protection Handbook”, NFPA, Seventh Edition , 1991
- [28] Subway Environmental Design Handbook, V.1, Principles and Applications, 2nd ed., U.S. Department of Transportation, 1976
- [29] CFDESIGN 7.0, User’s Guide, Blue Ridge Numerics Inc.
- [30] NIST FIRE DYNAMICS SIMULATOR (FDS) VERSION 4 Technical Reference Guide, NIST Special Publication 1018

APPENDIX -A

STEADY STATE EMERGENCY VENTILATION SCENARIOS IN KCK STATION

Three different steady state emergency ventilation scenarios are performed. Firstly, all of the fans in the station operate in exhaust mode. Secondly, two fans near the fire location operate in exhaust as the other two fans do not work. Lastly, two fans near the fire source are in exhaust mode when the other two are in supply mode. These modes are summarized in the Table A.1 below and also shown in Figure A.1. The results obtained are shown in Figure A.2-Figure A.5

Table A.1 Steady state emergency ventilation scenarios

Scenarios	Fan-1	Fan-2	Fan-3	Fan-4
Scenario-1	ON Exhaust	ON Exhaust	ON Exhaust	ON Exhaust
Scenario-2	OFF	OFF	ON Exhaust	ON Exhaust
Scenario-3	ON Supply	ON Supply	ON Exhaust	ON Exhaust

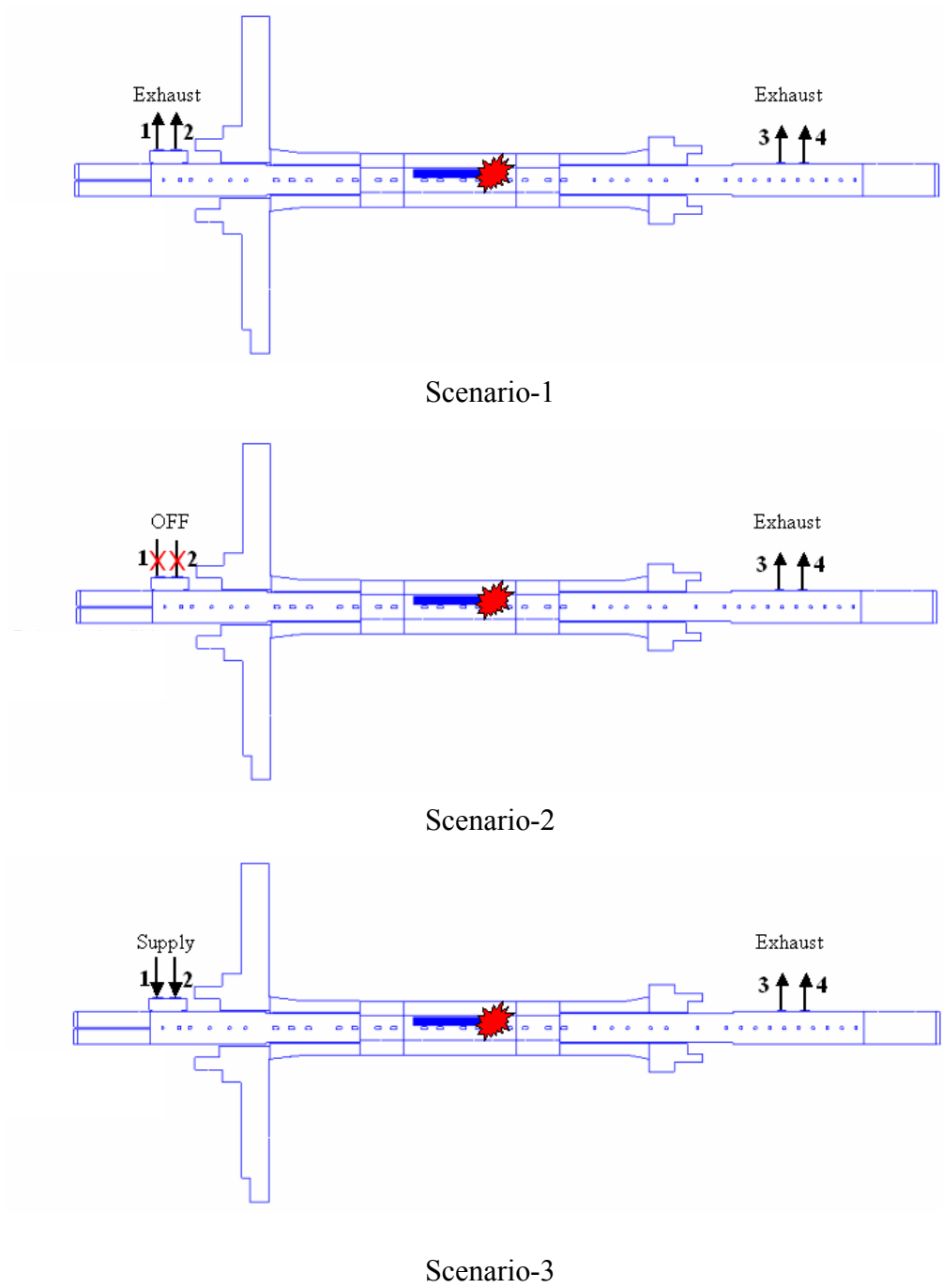
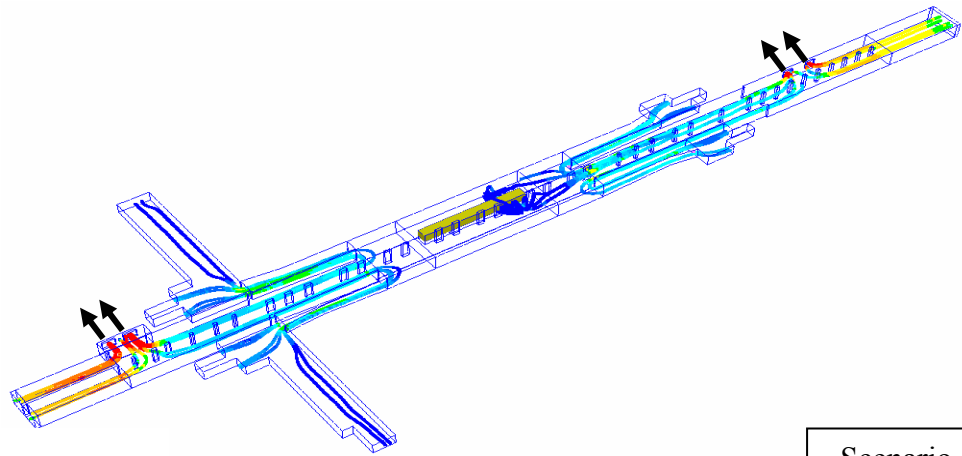
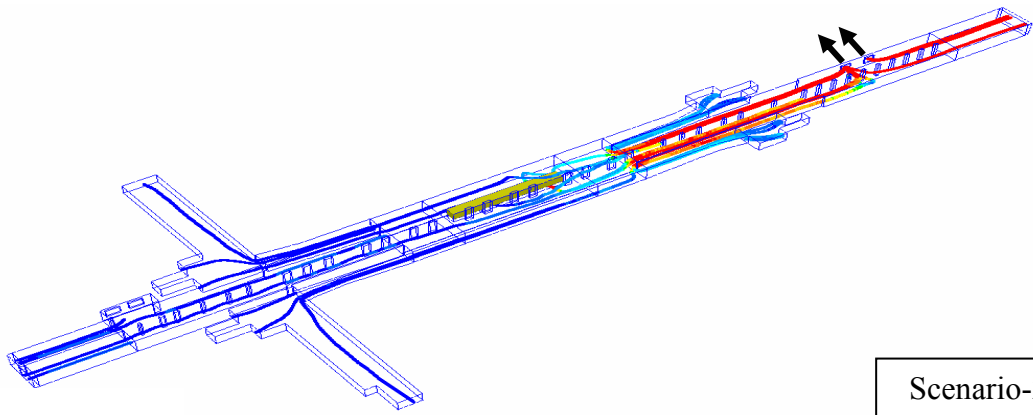


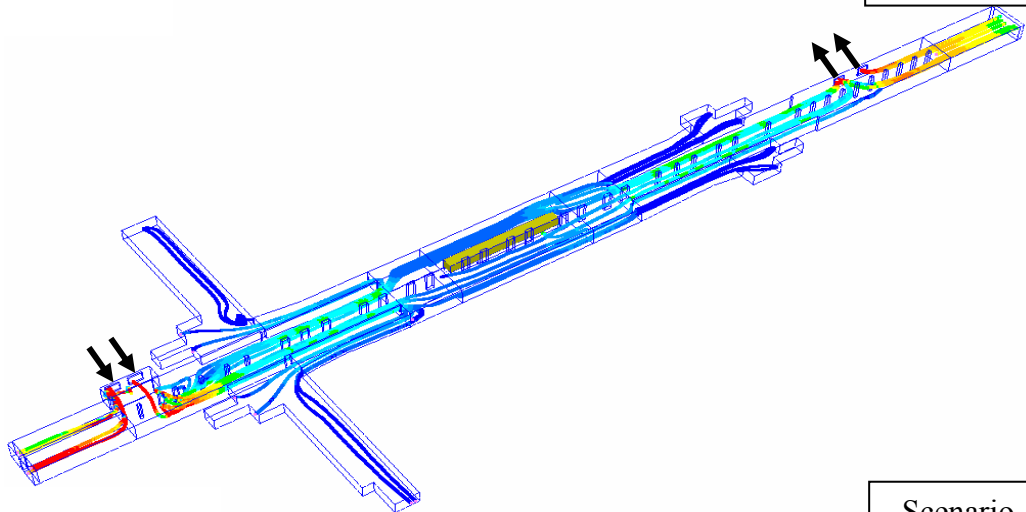
Figure A.1 Schematic drawing of steady state emergency ventilation scenarios in KCK Station



Scenario-1



Scenario-2



Scenario-3

Figure A.2 Stream tracers for ventilation scenarios in KCK Station

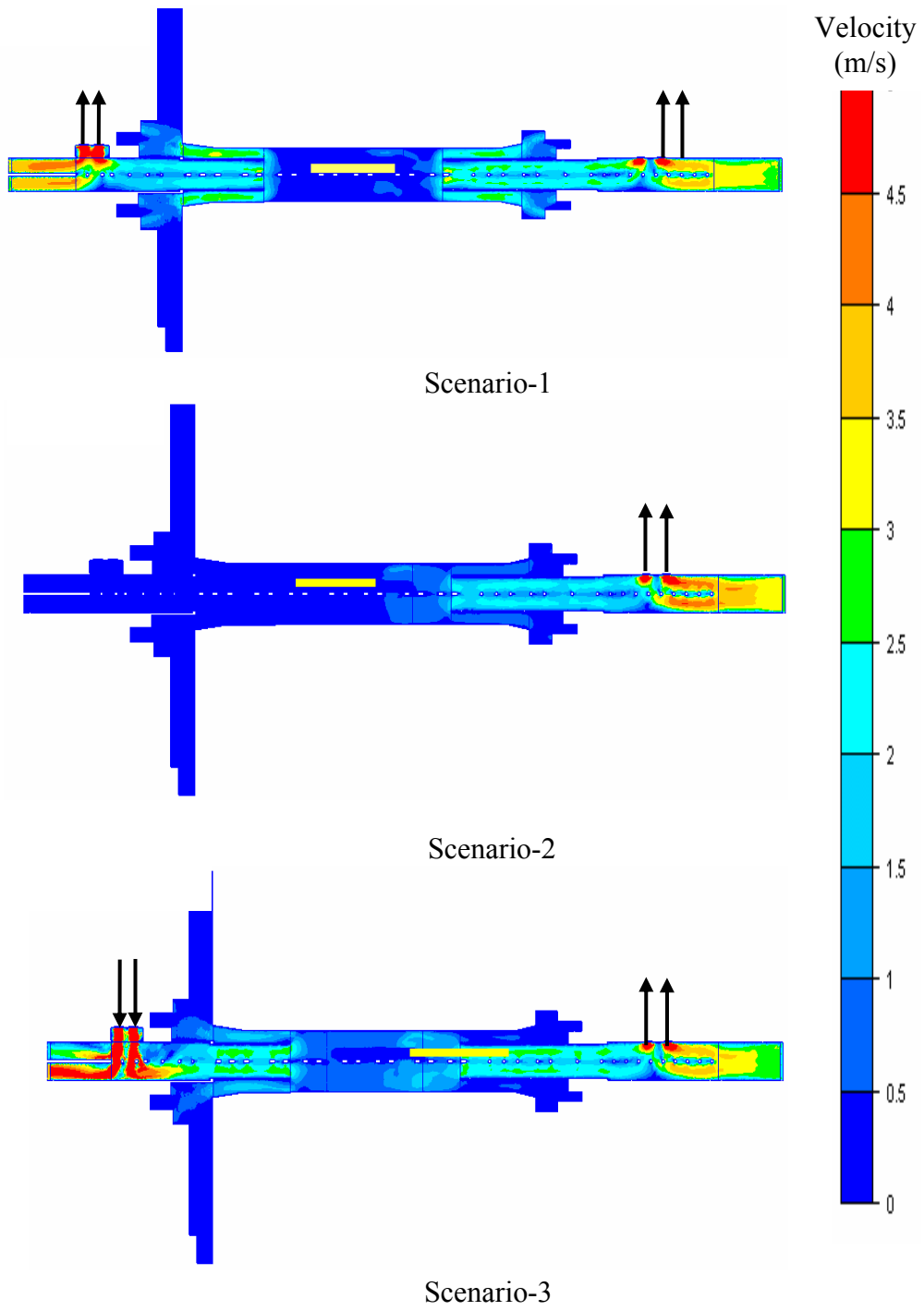


Figure A.3 Velocity distribution in ventilation scenarios

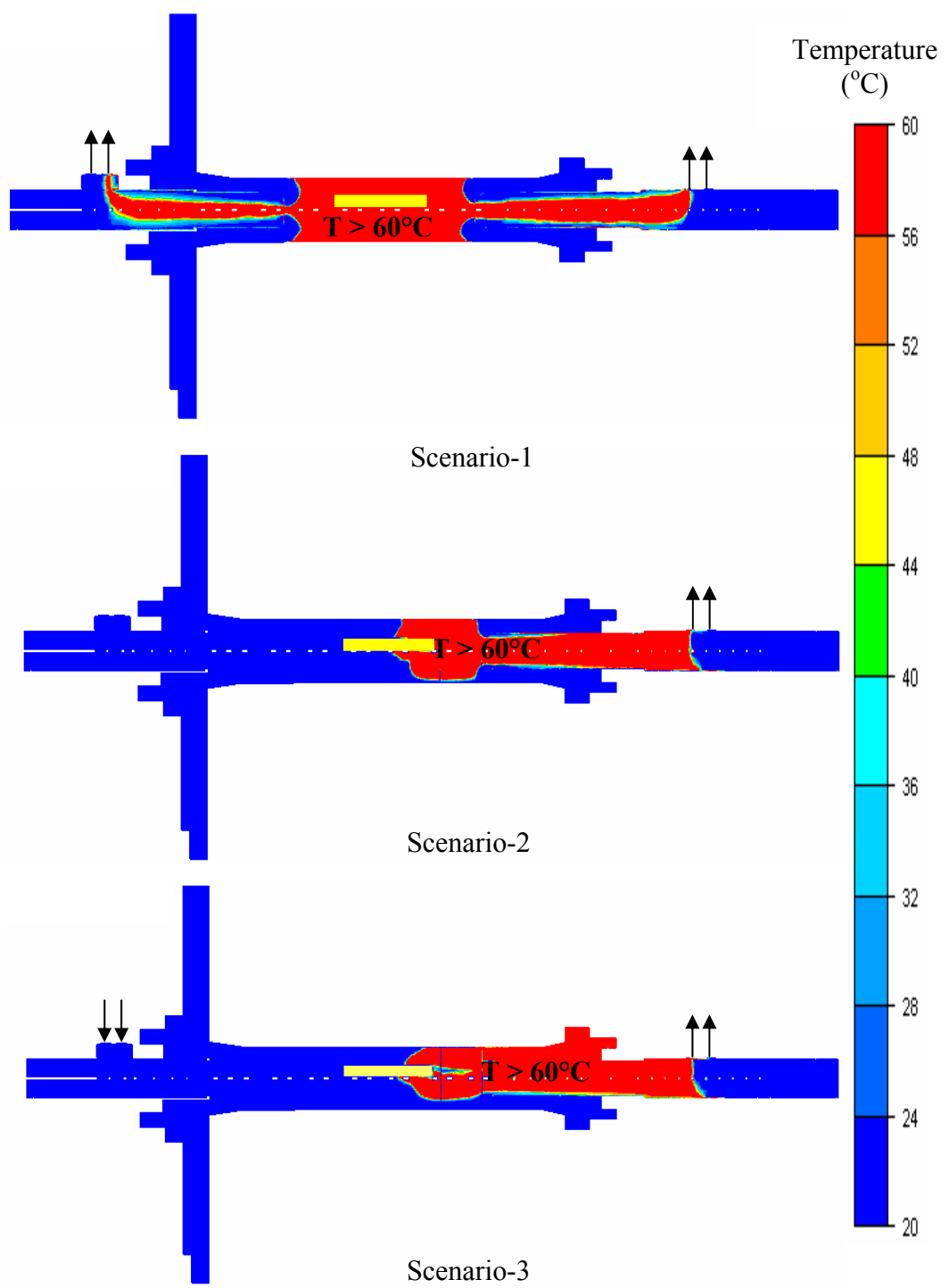


Figure A.4 Temperature distribution in ventilation scenarios

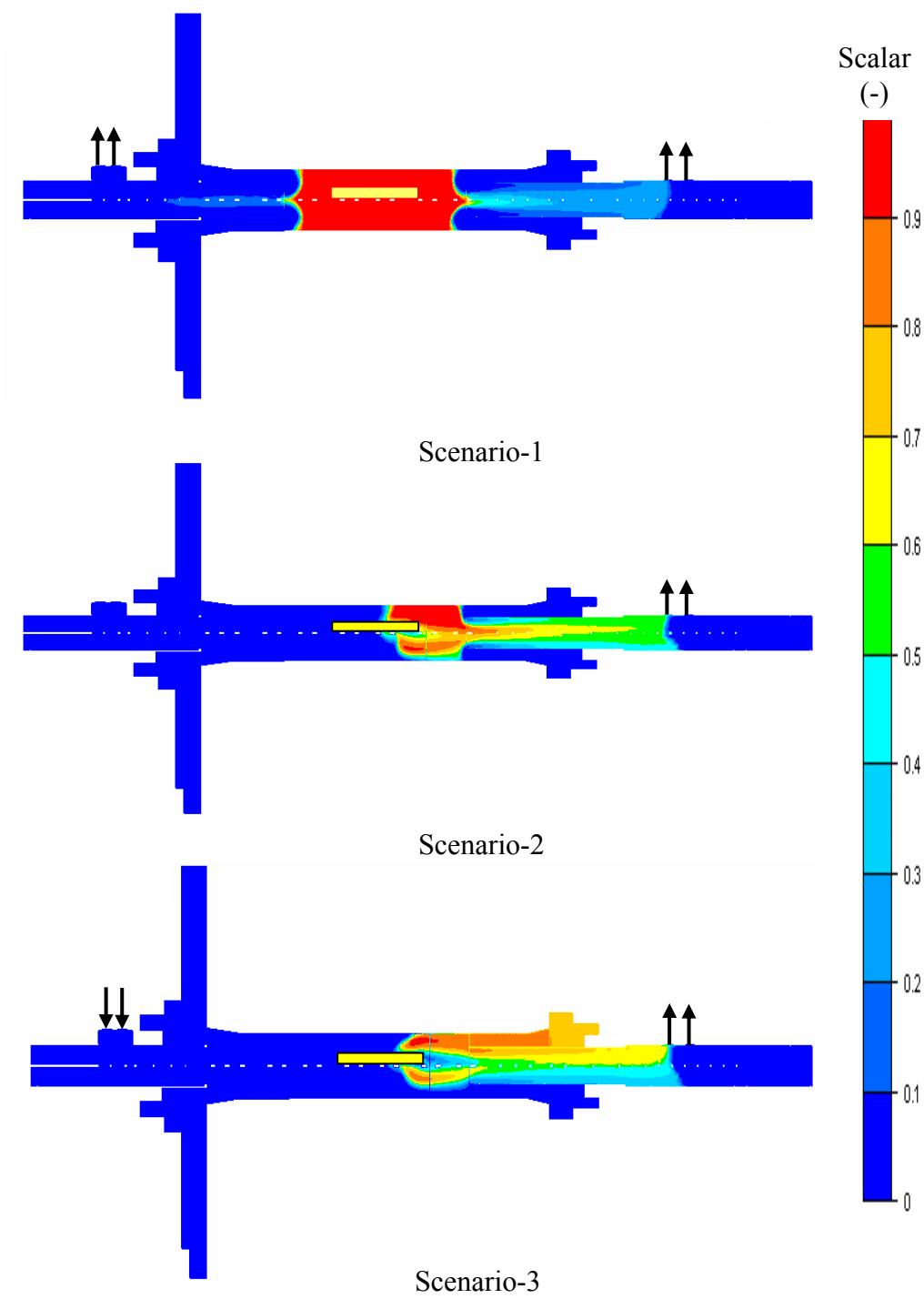


Figure A.5 Scalar distribution in ventilation scenarios

As a result of these trial scenarios, the following observations are made:

- Operation of four fans in exhaust mode (Scenario-1) results in flow of fresh air on all four escape routes. However, in this mode a stagnant smoke region is observed at the center of the station.
- Operation of two fans (those closer to the fire) in exhaust mode (Scenario-2) results in flow of fresh air on all four escape routes. In this mode smoke region gets smaller and it moves towards the operating fans. This is taken as the safe mode of fan operation.
- Operation of two fans in supply mode and two fans in exhaust mode (Scenario-3) results in flow of fresh air on all three escape routes. However, in this mode one of the escape routes is filled with smoke and hot gases.

APPENDIX -B

DESCRIPTION OF THE FIRE DYNAMICS SIMULATOR & KCK STATION FIRE SIMULATION RESULTS WITH FDS

B.1 FIRE DYNAMICS SIMULATOR

The name of the program is the NIST Fire Dynamics Simulator or FDS. The Fire Dynamics Simulator (FDS) was developed and is currently maintained by the Fire Research Division in the Building and Fire Research Laboratory at the National Institute of Standards and Technology (NIST). NIST founded in 1901 is a non-regulatory federal agency within the United States Commerce Department's Technology Administration. NIST's mission is to develop and promote measurement, standards, and technology to enhance productivity, facilitate trade, and improve the quality of life. FDS is a Fortran 90 computer program that solves the governing equations of fluid dynamics, and Smokeview is a companion program written in C/OpenGL programming language that produces images and animations of the results. FDS is released publicly since 2000. The present version of FDS is 4, released in July 2004 [30].

FDS is a computational fluid dynamics (CFD) model of fire-driven fluid flow. The software solves numerically a form of the Navier-Stokes equations appropriate for low-speed, thermally-driven flow with an emphasis on smoke and heat transport from fires. Smokeview is a visualization program that is used to display the results of

an FDS simulation. About half of the applications of the model have been for design of smoke handling systems and sprinkler/detector activation studies. The other half consists of residential and industrial fire reconstructions. Throughout its development, FDS has been aimed at solving practical fire problems in fire protection engineering, while at the same time providing a tool to study fundamental fire dynamics and combustion. Smokeview performs this visualization by presenting animated tracer particle flow, animated contour slices of computed gas variables and animated surface data. Smokeview also presents contours and vector plots of static data anywhere within a scene at a fixed time.

FDS computes the temperature, density, pressure, velocity and chemical composition within each numerical grid cell at each discrete time step. There are typically hundreds of thousands to several million grid cells and thousands to hundreds of thousands of time steps. In addition, FDS computes at solid surfaces the temperature, heat flux, mass loss rate, and various other quantities. It must be carefully selected what data to save, much like one would do in designing an actual experiment. Even though only a small fraction of the computed information can be saved, the output typically consists of fairly large data files. Typical output quantities for the gas phase include:

- Gas temperature
- Gas velocity
- Gas species concentration
- Smoke concentration and visibility estimates
- Pressure
- Heat release rate per unit volume
- Mixture fraction (or air/fuel ratio)
- Gas density
- Water droplet mass per unit volume

On solid surfaces, FDS predicts additional quantities associated with the energy balance between gas and solid phase, including

- Surface and interior temperature
- Heat flux, both radiative and convective
- Burning rate
- Water droplet mass per unit area

Global quantities recorded by the program include:

- Total Heat Release Rate (HRR)
- Sprinkler and detector activation times
- Mass and energy fluxes through openings or solids

B.1.1 Features of FDS

Hydrodynamic Model: FDS solves numerically a form of the Navier-Stokes equations for low-speed, thermally-driven flow with an emphasis on smoke and heat transport from fires. The core algorithm is an explicit predictor-corrector scheme, second order accurate in space and time. Turbulence is treated by means of the Smagorinsky form of Large Eddy Simulation.

Combustion Model: For most applications, FDS uses a mixture fraction combustion model. The mixture fraction is a conserved scalar quantity that is defined as the fraction of gas at a given point in the flow field that originated as fuel. The model assumes that combustion is mixing-controlled, and that the reaction of fuel and oxygen is infinitely fast. The mass fractions of all of the major reactants and products can be derived from the mixture fraction.

Radiation Transport: Radiative heat transfer is included in the model via the solution of the radiation transport equation for a non-scattering gray gas, and in some limited cases using a wide band model. The equation is solved using a technique similar to finite volume methods for convective transport, thus the name given to it is the Finite Volume Method. Using approximately 100 discrete angles, the finite volume solver requires about 15 % of the total CPU time of a calculation, a modest

cost given the complexity of radiation heat transfer. Water droplets can absorb thermal radiation. This is important in cases involving mist sprinklers, but also plays a role in all sprinkler cases. The absorption coefficients are based on Mie theory.

Geometry: FDS approximates the governing equations on a rectilinear grid. The user prescribes rectangular obstructions that are forced to conform with the underlying grid.

Multiple Meshes: This is a term used to describe the use of more than one rectangular mesh in a calculation. It is possible to prescribe more than one rectangular mesh to handle cases where the computational domain is not easily embedded within a single mesh.

Boundary Conditions: All solid surfaces are assigned thermal boundary conditions, plus information about the burning behavior of the material. Usually, material properties are stored in a database and invoked by name. Heat and mass transfer to and from solid surfaces is usually handled with empirical correlations.

B.1.2 Limitations of the Model

Although FDS can address most fire scenarios, there are limitations in all of its various algorithms. Some of the more important limitations of the model are:

Low Speed Flow Assumption: The use of FDS is limited to low-speed flow with an emphasis on smoke and heat transport from fires. This assumption rules out using the model for any scenario involving flow speeds approaching the speed of sound, such as explosions, choke flow at nozzles, and detonations.

Rectilinear Geometry: The efficiency of FDS is due to the simplicity of its rectilinear numerical grid and the use of fast, direct solvers for the pressure field. This can be a limitation in some situations where certain geometric features do not

conform to the rectangular grid, although most building components do. There are techniques in FDS to lessen the effect of “sawtooth” obstructions used to represent nonrectangular objects, but these cannot be expected to produce good results if, for example, the intent of the calculation is to study boundary layer effects. For most practical large-scale simulations, the increased grid resolution afforded by the fast pressure solver offsets the approximation of a curved boundary by small rectangular grid cells.

Fire Growth and Spread: Because the model was originally designed to analyze industrial-scale fires, it can be used reliably when the heat release rate of the fire is specified and the transport of heat and exhaust products is the principal aim of the simulation. In these cases, the model predicts flow velocities and temperatures to an accuracy within 5 % to 20 % of experimental measurements, depending on the resolution of the numerical grid. However, for fire scenarios where the heat release rate is predicted rather than prescribed, the uncertainty of the model is higher. There are several reasons for this: (1) properties of real materials and real fuels are often unknown or difficult to obtain, (2) the physical processes of combustion, radiation and solid phase heat transfer are more complicated than their mathematical representations in FDS, (3) the results of calculations are sensitive to both the numerical and physical parameters.

Combustion: For most applications, FDS uses a mixture fraction combustion model. The mixture fraction is a conserved scalar quantity that is defined as the fraction of gas at a given point in the flow field that originated as fuel. The model assumes that combustion is mixing-controlled, and that the reaction of fuel and oxygen is infinitely fast, regardless of the temperature. For large-scale, well-ventilated fires, this is a good assumption. However, if a fire is in an under-ventilated compartment, or if a suppression agent like water mist or carbon dioxide is introduced, fuel and oxygen may mix but may not burn. Also, a shear layer with high strain rate separating the fuel stream from an oxygen supply can prevent combustion from taking place. The physical mechanisms underlying these phenomena are complex,

and even simplified models still rely on an accurate prediction of the flame temperature and local strain rate.

Radiation: Radiative heat transfer is included in the model via the solution of the radiation transport equation for a non-scattering gray gas, and in some limited cases using a wide band model. The equation is solved using a technique similar to finite volume methods for convective transport. There are several limitations of the model. First, the absorption coefficient for the smoke gas is a complex function of its composition and temperature. Because of the simplified combustion model, the chemical composition of the smoky gases, especially the soot content, can affect both the absorption and emission of thermal radiation. Second, the radiation transport is discretized via approximately 100 solid angles. For targets far away from a localized source of radiation, like a growing fire, the discretization can lead to a non-uniform distribution of the radiant energy. This can be seen in the visualization of surface temperatures, where “hot spots” show the effect of the finite number of solid angles. The problem can be lessened by the inclusion of more solid angles, but at a price of longer computing times. In most cases, the radiative flux to far-field targets is not as important as those in the near-field, where coverage by the default number of angles is much better.

B.2 FDS Input Data File for KCK Station Fire

```
&HEAD CHID='KCK',TITLE='KCK STATION Fire' /
&GRID IBAR=512,JBAR=180,KBAR=18 /   Grid dimensions
&PDIM XBAR0=0.0,XBAR=438,YBAR0=-
43.75,YBAR=50.12,ZBAR0=0.0,ZBAR=4.75 /

&TIME TWFIN=400. / Total simulation time
&MISC TMPA=20.0,
REACTION='WOOD',NFRAMES=80,DTCORE=30,BACKGROUND_SPECIES='
AIR',
RADIATION=.FALSE.,RESTART=.TRUE./

&SURF ID='FIRE',PART_ID='tracers',HRRPUA=480.77 ,TAU_Q=-399./
7.5 MW FIRE 15.6 m^2 alfa t2 fire
&SURF ID='SHAFTLEFT', VOLUME_FLUX=80,
RAMP_V='SHAFTLEFT RAMP'/
&SURF ID='SHAFTRIGHT',VOLUME_FLUX=80,
RAMP_V='SHAFTRIGHT RAMP'/

&RAMP ID='SHAFTLEFT RAMP', T=0.0, F=0.0/
&RAMP ID='SHAFTLEFT RAMP', T=30.0, F=0.0/
&RAMP ID='SHAFTLEFT RAMP', T=150.0, F=1.0/
&RAMP ID='SHAFTLEFT RAMP', T=400.0, F=1.0/
&RAMP ID='SHAFTRIGHT RAMP', T=0.0, F=0.0/
&RAMP ID='SHAFTRIGHT RAMP', T=30.0, F=0.0/
&RAMP ID='SHAFTRIGHT RAMP', T=150.0,F=1.0/
&RAMP ID='SHAFTRIGHT RAMP', T=400.0,F=1.0/
&OBST XB=0.0,438,-43.75,50.12,0.0,4.75,          COLOR='WHITE' /
&VENT XB=193.07,199.57,5.21,7.61,0.0,0.0,          SURF_ID='FIRE'
,RGB = 0.86,0.58,0.44/          FIRE location
&OBST XB= 193.07, 219.07, 5.21, 7.61, 1.15, 3.45,
SURF_ID='STEEL',COLOR='MAGENTA',PERMIT_HOLE=.FALSE./
NON burning section of train

&OBST XB= 123.24, 123.84, 4.24 ,4.87, 0.0 ,4.75, COLOR='BLUE'
,PERMIT_HOLE=.FALSE./
&OBST XB= 127.68, 128.68, 4.24 ,4.87, 0.0 ,4.75, COLOR='BLUE'
,PERMIT_HOLE=.FALSE./
&OBST XB= 130.68, 131.68, 4.24 ,4.87, 0.0 ,4.75, COLOR='BLUE'
,PERMIT_HOLE=.FALSE./
&OBST XB= 136.34, 137.04, 4.24 ,4.87, 0.0 ,4.75, COLOR='BLUE'
,PERMIT_HOLE=.FALSE./
&OBST XB= 141.83, 142.53, 4.24 ,4.87, 0.0 ,4.75, COLOR='BLUE'
,PERMIT_HOLE=.FALSE./
```

&OBST XB= 146.21, 146.91, 4.24 ,4.87, 0.0 ,4.75, COLOR='BLUE'
,PERMIT_HOLE=.FALSE./
&OBST XB= 154.16, 155.76, 4.24 ,4.87, 0.0 ,4.75, COLOR='BLUE'
,PERMIT_HOLE=.FALSE./
&OBST XB= 158.53, 160.13, 4.24 ,4.87, 0.0 ,4.75, COLOR='BLUE'
,PERMIT_HOLE=.FALSE./
&OBST XB= 163.28, 164.88, 4.24 ,4.87, 0.0 ,4.75, COLOR='BLUE'
,PERMIT_HOLE=.FALSE./
&OBST XB= 171.78, 173.38, 4.24 ,4.87, 0.0 ,4.75, COLOR='BLUE'
,PERMIT_HOLE=.FALSE./
&OBST XB= 176.16, 177.76, 4.24 ,4.87, 0.0 ,4.75, COLOR='BLUE'
,PERMIT_HOLE=.FALSE./
&OBST XB= 182.56, 184.16, 4.24 ,4.87, 0.0 ,4.75, COLOR='BLUE'
,PERMIT_HOLE=.FALSE./
&OBST XB= 186.93, 188.53, 4.24 ,4.87, 0.0 ,4.75, COLOR='BLUE'
,PERMIT_HOLE=.FALSE./
&OBST XB= 195.41, 197.01, 4.24 ,4.87, 0.0 ,4.75, COLOR='BLUE'
,PERMIT_HOLE=.FALSE./
&OBST XB= 199.81, 201.41, 4.24 ,4.87, 0.0 ,4.75, COLOR='BLUE'
,PERMIT_HOLE=.FALSE./
&OBST XB= 206.21, 207.81, 4.24 ,4.87, 0.0 ,4.75, COLOR='BLUE'
,PERMIT_HOLE=.FALSE./
&OBST XB= 210.58, 212.18, 4.24 ,4.87, 0.0 ,4.75, COLOR='BLUE'
,PERMIT_HOLE=.FALSE./
&OBST XB= 219.08, 220.68, 4.24 ,4.87, 0.0 ,4.75, COLOR='BLUE'
,PERMIT_HOLE=.FALSE./
&OBST XB= 223.46, 225.06, 4.24 ,4.87, 0.0 ,4.75, COLOR='BLUE'
,PERMIT_HOLE=.FALSE./
&OBST XB= 229.86, 231.46, 4.24 ,4.87, 0.0 ,4.75, COLOR='BLUE'
,PERMIT_HOLE=.FALSE./
&OBST XB= 234.23, 235.83, 4.24 ,4.87, 0.0 ,4.75, COLOR='BLUE'
,PERMIT_HOLE=.FALSE./
&OBST XB= 243.18, 243.88, 4.24 ,4.87, 0.0 ,4.75, COLOR='BLUE'
,PERMIT_HOLE=.FALSE./
&OBST XB= 247.93, 248.63, 4.24 ,4.87, 0.0 ,4.75, COLOR='BLUE'
,PERMIT_HOLE=.FALSE./
&OBST XB= 252.31, 253.01, 4.24 ,4.87, 0.0 ,4.75, COLOR='BLUE'
,PERMIT_HOLE=.FALSE./
&OBST XB= 258.71, 259.41, 4.24 ,4.87, 0.0 ,4.75, COLOR='BLUE'
,PERMIT_HOLE=.FALSE./
&OBST XB= 263.08, 263.78, 4.24 ,4.87, 0.0 ,4.75, COLOR='BLUE'
,PERMIT_HOLE=.FALSE./
&OBST XB= 271.78, 272.48, 4.24 ,4.87, 0.0 ,4.75, COLOR='BLUE'
,PERMIT_HOLE=.FALSE./
&OBST XB= 279.78, 280.48, 4.24 ,4.87, 0.0 ,4.75, COLOR='BLUE'
,PERMIT_HOLE=.FALSE./

&OBST XB= 283.78, 284.48, 4.24 ,4.87, 0.0 ,4.75, COLOR='BLUE'
 ,PERMIT_HOLE=.FALSE./
 &OBST XB= 287.78, 288.48, 4.24 ,4.87, 0.0 ,4.75, COLOR='BLUE'
 ,PERMIT_HOLE=.FALSE./
 &OBST XB= 291.78, 292.48, 4.24 ,4.87, 0.0 ,4.75, COLOR='BLUE'
 ,PERMIT_HOLE=.FALSE./
 &OBST XB= 295.78, 296.48, 4.24 ,4.87, 0.0 ,4.75, COLOR='BLUE'
 ,PERMIT_HOLE=.FALSE./
 &OBST XB= 299.78, 300.48, 4.24 ,4.87, 0.0 ,4.75, COLOR='BLUE'
 ,PERMIT_HOLE=.FALSE./
 &OBST XB= 303.78, 304.48, 4.24 ,4.87, 0.0 ,4.75, COLOR='BLUE'
 ,PERMIT_HOLE=.FALSE./
 &OBST XB= 307.78, 308.48, 4.24 ,4.87, 0.0 ,4.75, COLOR='BLUE'
 ,PERMIT_HOLE=.FALSE./
 &OBST XB= 311.78, 312.48, 4.24 ,4.87, 0.0 ,4.75, COLOR='BLUE'
 ,PERMIT_HOLE=.FALSE./
 &OBST XB= 315.78, 316.48, 4.24 ,4.87, 0.0 ,4.75, COLOR='BLUE'
 ,PERMIT_HOLE=.FALSE./

&HOLE XB=145.41,153.11,19.5,50.12,0.0,4.75 /
 &HOLE XB=131.0,153.11, 9.6,19.5,0.0,4.75 /
 &HOLE XB=153.11,178.32, 9.6,11.95,0.0,4.75 /
 &HOLE XB=178.32,233.82,-2.85,11.95,0.0,4.75 /
 &HOLE XB=233.82,258.57,9.6,11.95,0.0,4.75 /
 &HOLE XB=258.57,275.4,9.6,16.65,0.0,4.75 /
 &HOLE XB=233.82,258.57,-0.5,-2.85,0.0,4.75 /
 &HOLE XB=258.57,275.4,-0.5,-7.55,0.0,4.75 /
 &HOLE XB=147.86,153.11,-36.97,-43.75,0.0,4.75 /
 &HOLE XB=145.41,153.11,-10.4,-36.97,0.0,4.75 /
 &HOLE XB=131.0,153.11, -0.5,-10.4,0.0,4.75 /
 &HOLE XB=153.11,178.32, -0.5,-2.85,0.0,4.75 /
 &HOLE XB=0.0,120.0,4.85,9.1,0.0,4.75 /
 &HOLE XB=0.0,120.0,0.0,4.25,0.0,4.75 /
 &HOLE XB=120.0,178.32,0.0,9.1,0.0,4.75 /
 &HOLE XB=120.0,130.32,9.1,12.57,0.0,4.75 /
 &HOLE XB=233.82,438.0,0.0,9.1,0.0,4.75 /
 &VENT XB=0.0,0.0,0.0,4.25,0.0,4.75, SURF_ID='OPEN',RGB = 0.0,1.0,0.0 /

 &VENT XB=0.0,0.0,4.85,9.1,0.0,4.75, SURF_ID='OPEN',RGB = 0.0,1.0,0.0 /

 &VENT XB=438.0,438.0,0.0,9.1,0.0,4.75, SURF_ID='OPEN',RGB = 0.0,1.0,0.0 /

 &VENT XB=131.0,137.0,16.5,19.5,4.75,4.75, SURF_ID='OPEN',RGB =
 0.0,1.0,0.0 /
 &VENT XB=131.0,137.0,9.6,12.65,4.75,4.75, SURF_ID='OPEN',RGB =
 0.0,1.0,0.0 /

```

&VENT XB=147.51,151.01,50.12,50.12,0.0,3.7,SURF_ID='OPEN',RGB =
0.0,1.0,0.0 /
&VENT XB=131.0,137.0,-0.5,-3.55,4.75,4.75, SURF_ID='OPEN',RGB =
0.0,1.0,0.0 /
&VENT XB=131.0,137.0,-7.0,-10.4,4.75,4.75, SURF_ID='OPEN',RGB =
0.0,1.0,0.0 /
&VENT XB=149.41,153.11,-43.75,-43.75,0.0,3.7, SURF_ID='OPEN',RGB =
0.0,1.0,0.0 /
&VENT XB=268.43,275.4,14.07,16.65,4.75,4.75, SURF_ID='OPEN',RGB =
0.0,1.0,0.0 /
&VENT XB=268.43,275.4,9.6,12.18,4.75,4.75, SURF_ID='OPEN',RGB =
0.0,1.0,0.0 /
&VENT XB=268.43,275.4,-0.5,-3.08,4.75,4.75, SURF_ID='OPEN',RGB =
0.0,1.0,0.0 /
&VENT XB=268.43,275.4,-4.97,-7.55,4.75,4.75, SURF_ID='OPEN',RGB =
0.0,1.0,0.0 /
&VENT XB=120.8,123.8,12.57,12.57,1.3,3.64,
SURF_ID='SHAFTLEFT',COLOR='GREEN'/
&VENT XB=125.63,128.63,12.57,12.57,1.3,3.64,
SURF_ID='SHAFTRIGHT',COLOR = 'GREEN'/

```

```

&REAC ID='WOOD'

```

```

FYI='Ritchie, et al., 5th IAFSS, C_3.4 H_6.2 O_2.5'
SOOT_YIELD = 0.01
NU_O2 = 3.7
NU_CO2 = 3.4
NU_H2O = 3.1
MW_FUEL = 87.
EPUMO2 = 11020. /

```

```

&SURF ID = 'STEEL'
RGB = 0.20,0.20,0.20
C_DELTA_RHO = 20.
DELTA = 0.5 /

```

```

&ISOF QUANTITY='TEMPERATURE',VALUE(1)=30.0,100.0 / Show 3D
contours of temperature at 30 C and 100 C

```

```

&PART ID='tracers',MASSLESS=.TRUE.

```

```

&SLCF PBY=10.0, QUANTITY='TEMPERATURE',VECTOR=.TRUE. /
&SLCF PBY=2.0, QUANTITY='TEMPERATURE',VECTOR=.TRUE. /
&SLCF PBY=6.0, QUANTITY='TEMPERATURE',VECTOR=.TRUE. / Along
train
&SLCF PBZ=2.5, QUANTITY='TEMPERATURE',VECTOR=.TRUE. / 2.5 m
temperature

```

```

&SLCF PBZ=3.0, QUANTITY='TEMPERATURE',VECTOR=.TRUE. /
&SLCF PBZ=3.5, QUANTITY='TEMPERATURE',VECTOR=.TRUE. /
&SLCF PBZ=4.0, QUANTITY='TEMPERATURE',VECTOR=.TRUE. /
&SLCF PBX=148.0, QUANTITY='TEMPERATURE',VECTOR=.TRUE. /
&SLCF PBX=195.0, QUANTITY='TEMPERATURE',VECTOR=.TRUE. /
&SLCF PBX=265.0, QUANTITY='TEMPERATURE',VECTOR=.TRUE. /
&SLCF PBY=10.0, QUANTITY='carbon monoxide' /
&SLCF PBY=2.0, QUANTITY='carbon monoxide' /
&SLCF PBY=6.0, QUANTITY='carbon monoxide' /
&SLCF PBZ=2.5, QUANTITY='carbon monoxide' /
&SLCF PBZ=3.0, QUANTITY='carbon monoxide' /
&SLCF PBZ=3.5, QUANTITY='carbon monoxide' /
&SLCF PBZ=4.0, QUANTITY='carbon monoxide' /
&SLCF PBX=148.0, QUANTITY='carbon monoxide' /
&SLCF PBX=195.0, QUANTITY='carbon monoxide' /
&SLCF PBX=265.0, QUANTITY='carbon monoxide' /
&SLCF PBY=10.0, QUANTITY='VELOCITY' /
&SLCF PBY=2.0, QUANTITY='VELOCITY' /
&SLCF PBY=6.0, QUANTITY='VELOCITY' /
&SLCF PBZ=2.5, QUANTITY='VELOCITY' /
&SLCF PBZ=3.0, QUANTITY='VELOCITY' /
&SLCF PBZ=3.5, QUANTITY='VELOCITY' /
&SLCF PBZ=4.0, QUANTITY='VELOCITY' /
&SLCF PBX=148.0, QUANTITY='VELOCITY' /
&SLCF PBX=195.0, QUANTITY='VELOCITY' /
&SLCF PBX=265.0, QUANTITY='VELOCITY' /
&SLCF PBY=10.0, QUANTITY='visibility' /
&SLCF PBY=2.0, QUANTITY='visibility' /
&SLCF PBY=6.0, QUANTITY='visibility' /
&SLCF PBZ=2.5, QUANTITY='visibility' /
&SLCF PBZ=3.0, QUANTITY='visibility' /
&SLCF PBZ=3.5, QUANTITY='visibility' /
&SLCF PBZ=4.0, QUANTITY='visibility' /
&SLCF PBX=148.0, QUANTITY='visibility' /
&SLCF PBX=195.0, QUANTITY='visibility' /
&SLCF PBX=265.0, QUANTITY='visibility' /
&THCP XB=193.07,199.57,5.21,7.61,0.0,0.0,
    QUANTITY='HRR',LABEL='whatever' /
&THCP XB=193.07,199.57,5.21,7.61,0.0,0.0, QUANTITY='VOLUME
FLOW',LABEL='smoke' /
&BNDF QUANTITY='GAUGE_HEAT_FLUX' /
&BNDF QUANTITY='BURNING_RATE' /
&BNDF QUANTITY='WALL_TEMPERATURE' /

```

B.3 KCK STATION FIRE SIMULATION RESULTS WITH FDS

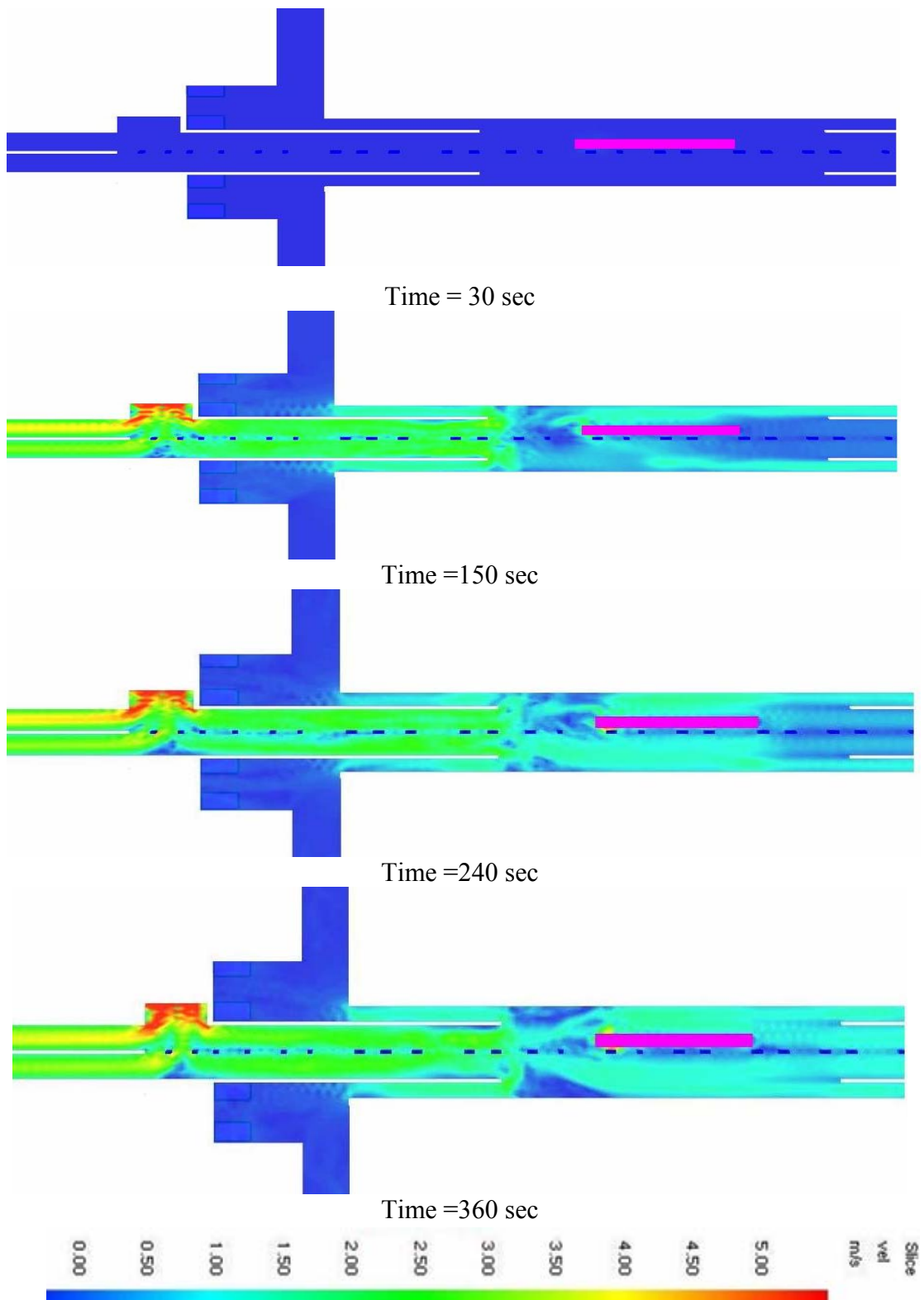


Figure B.1 Velocity distribution at Horizontal plane 2.5 m above floor level

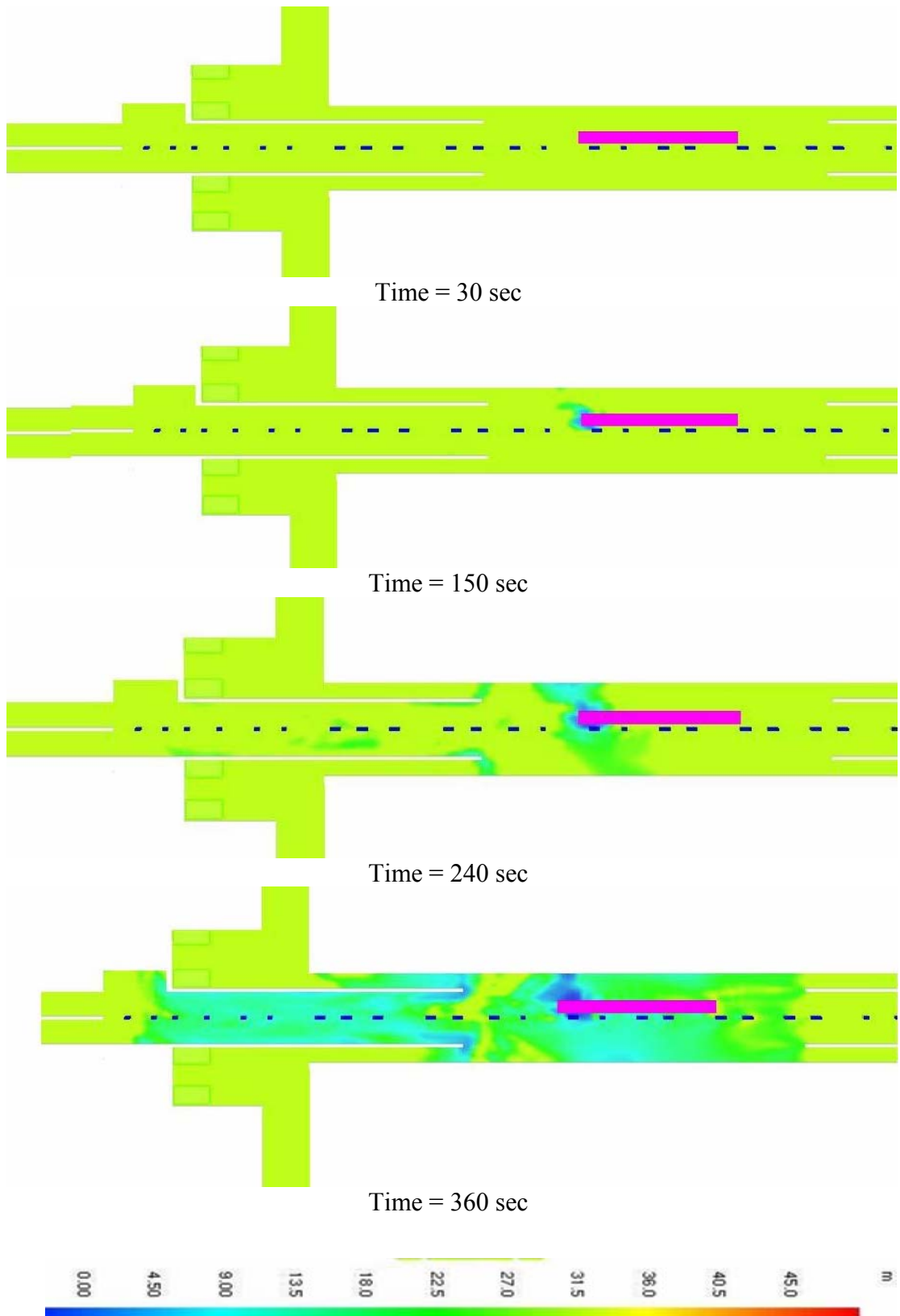


Figure B.2 Visibility distribution at Horizontal plane 2.5 m above floor level

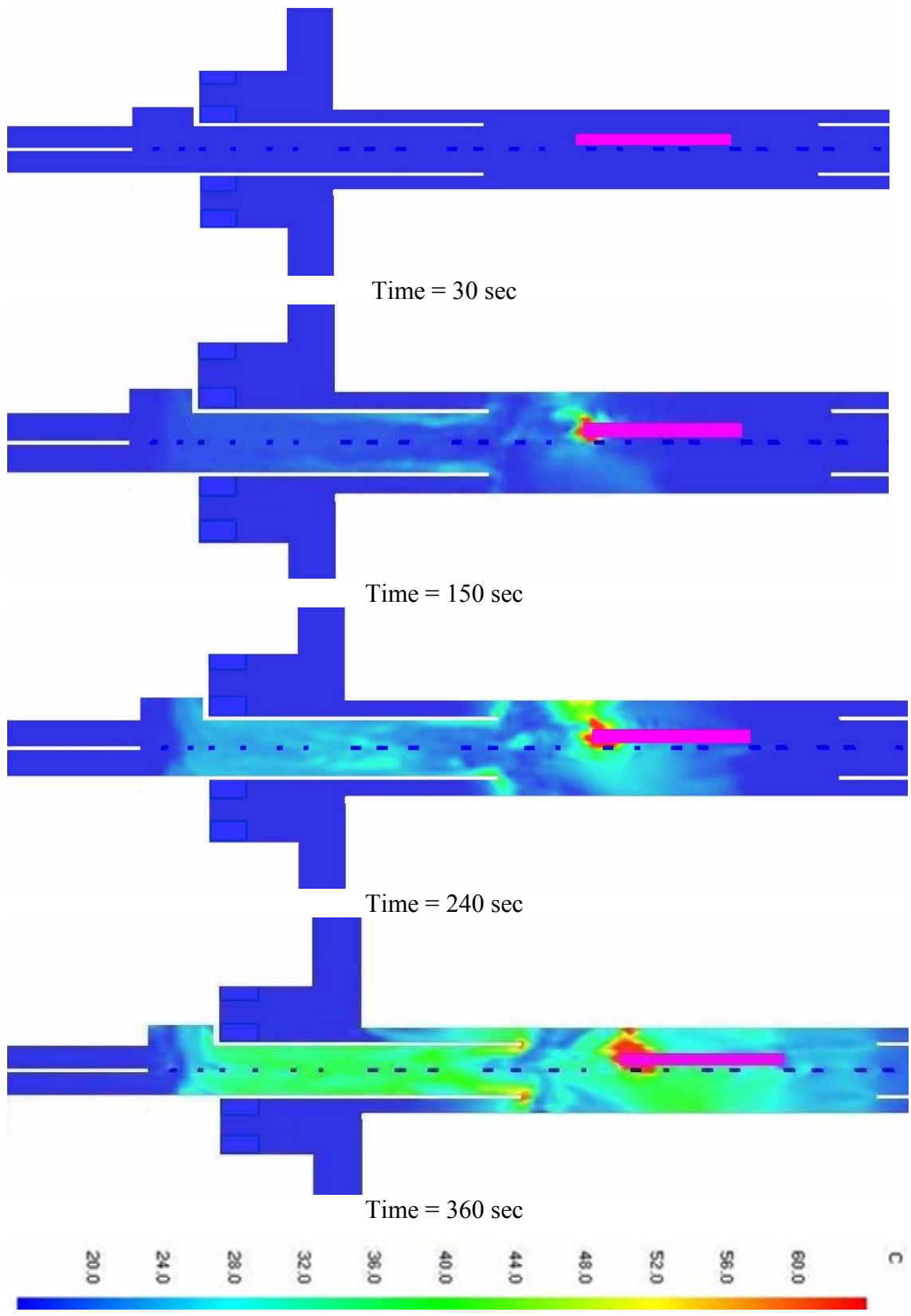


Figure B.3 Temperature Distribution at Horizontal plane 2.5 m above floor level (KCK Scenario-2)